MLF ANNUAL REPORT 2011

J-PARC/MLF

Preface to the Annual Report of the Materials and Life Science Experimental Facility for Year 2011

The year 2011 started with the devastating disaster in March. The facility and instruments were devastatingly damaged. The users were immediately evacuated from the facility to outside, where it was thought to be safe. It was then, when they heard the sea, near the site, roaring. It was Tsunami. Very fortunately, however, Tsunami didn't reach the J-PARC site since the shallow bottom of the seashore mitigated the strength of it.

Tokai is located only 120 km south of the Fukushima reactor. A week after the disaster, a high level radioactivity being decreased in the atmosphere, we formed scout teams in order to investigate damages in the facility. We found most surrounding ground and utilities around the main buildings were badly subsided or leaned. Biological front shield of instruments was shaken, largely shifted and even collapsing. The floor of annex building sank enormously, breaking neutron guides at the boundary between the buildings. MLF staffs were highly motivated to work week after week morning till night. By the end of June, we were able to speculate the target date to finish the restoration work to be the end of November. Although hard work went on for another six months, finally we successfully had a proton beam at the neutron target in December as we had speculatively scheduled. We have started facility operation for user program since January 2012, starting at a low power of 100kW. The power of accelerator was recovered to its previously highest power of 200kW by February. We have seen many users come back to the facility, enjoying their experiments.

The year 2011 was obviously the most regrettable year for all of us, but also astonishing year to see all the staffs devoting themselves for restoration and completely achieving their goal. Here, I would like to give my highest appreciation to them for their great efforts. Now we have been achieving 300kW in December, 2012, and are relaxed and looking forward to new challenges for the future.

Masatoshi Arai
Head of the Materials and Life Science Division (MLF)

This Annual Report – which describes the scientific, technical and organizational activities of the MLF during FY2011 (April 2011-March 2012) – is the first to be compiled jointly by J-PARC MLF and CROSS-Tokai*.

Consistent with its longstanding policy of promoting open access to major publicly-funded research facilities, in March 2011 the Japanese Government appointed CROSS-Tokai as the “Registered Institution for Facility Use Promotion” to administer and support user operations on the neutron Public Beamlines at J-PARC MLF.

This appointment was made under the terms of the so-called “Promotion of Public Utilization” legislation that aims to advance science and technology through effective promotion of the general use of specific world-leading large-scale research facilities. It brings J-PARC MLF into line with the SPring-8 synchrotron radiation and SACLA free-electron laser facility and the K-Computer facility where the legislation has already been successfully applied.

In practice, this will be achieved by attracting and facilitating use by researchers from around the world in a wide range of fields that spans from basic and applied research to industrial applications.

On 1 April 2011, CROSS-Tokai commenced activities associated with its role of promoting the use of the Public Beamlines at J-PARC MLF: the selection of research proposals, the support of user experiments and the selection and implementation of proposals to build Contract Beamlines put forward by other organizations.

Our first year of operation has been characterized by building: both as part of the earthquake recovery effort and also in establishing CROSS-Tokai as a fully functioning organization. I am delighted with the progress we have made and the team that has been assembled.

CROSS-Tokai is committed to delivering the highest standard of user services via an expert team of research and support staff. The ability of our team to facilitate excellence in scientific outcomes will be strengthened by the development of new user support mechanisms and an active, robust exchange of ideas with researchers both within and external to the organization.

On behalf of the team at CROSS-Tokai, it is my great pleasure to extend a warm welcome to researchers from around the world who wish to make use of the Public Beamlines at J-PARC MLF.

Yasuhiko Fujii
Director, CROSS-Tokai

* Research Center for Neutron Science and Technology, Comprehensive Research Organization for Science and Society
www.cross-tokai.jp

Contents

What's new at the MLF ?

Facility Report

Organization Chart

Organization Chart of J-PARC Center

- Director, J-PARC Center
  - Deputy Director, J-PARC Center
  - Deputy Director, J-PARC Center
  - Accelerator Division
  - MLF Division
    - Materials and Life Science Division
      - Neutron Source Section
      - Neutron Science Section
      - Neutron Instrumentation Section
      - Muon Science Section
  - Particle and Nuclear Physics Division
  - Transmutation Section
  - Cryogenics Section
  - Safety Division
  - Management Supporting Section
  - Information System Section
  - Public Relations Section
  - Administration Division
    - User Office Team

Organization Chart of CROSS

CROSS is "Registered Institution for Facility Use Promotion" for the public-access neutron beam facilities at J-PARC.

- President
  - CROSS Head Office
  - Director, CROSS-Tokai
    - Science Coordinators
    - Safety Division
    - Administration Division
    - Utilization Promotion Division
    - Neutron R&D Division

J-PARC MAP

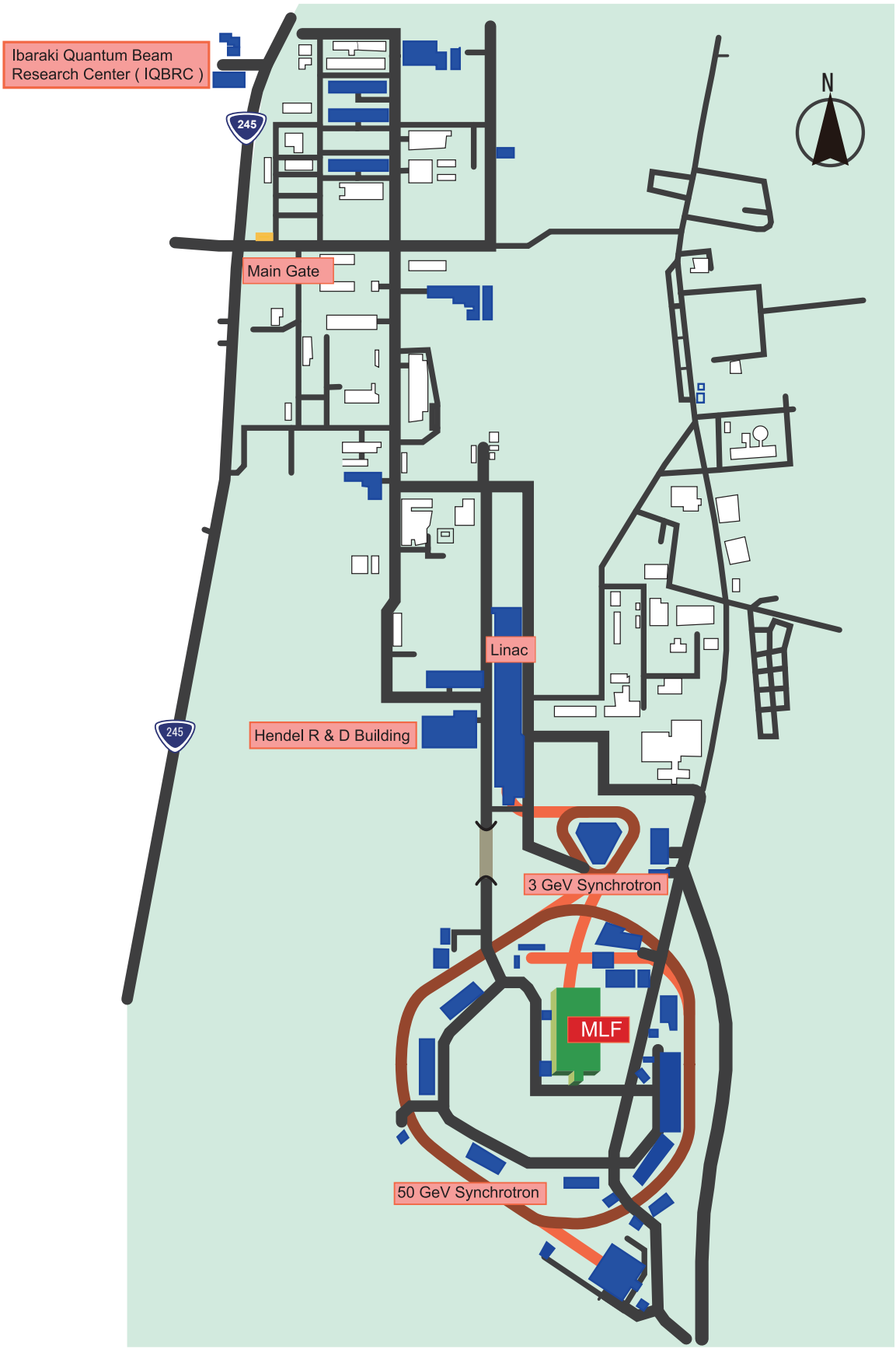
Ibaraki Quantum Beam
Research Center (IQBRC)
245
N
Main Gate
Linac
245
Hendel R & D Building
3 GeV Synchrotron
MLF
50 GeV Synchrotron

Muon Instruments

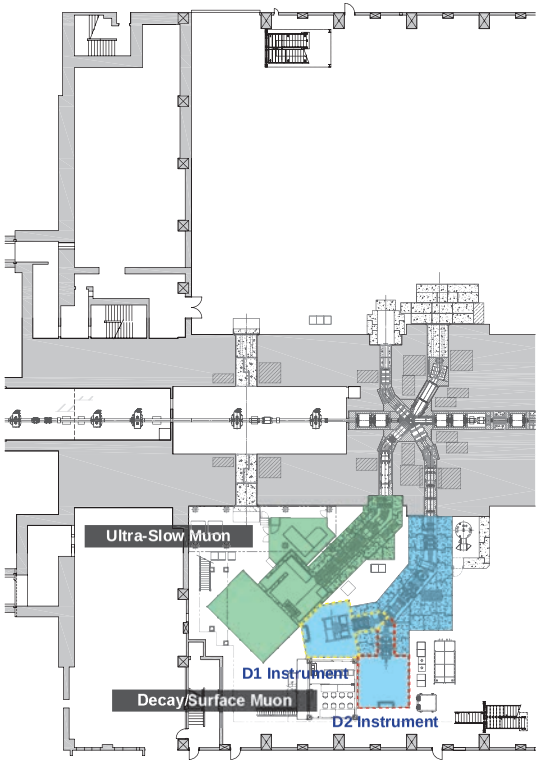

Neutron Instruments

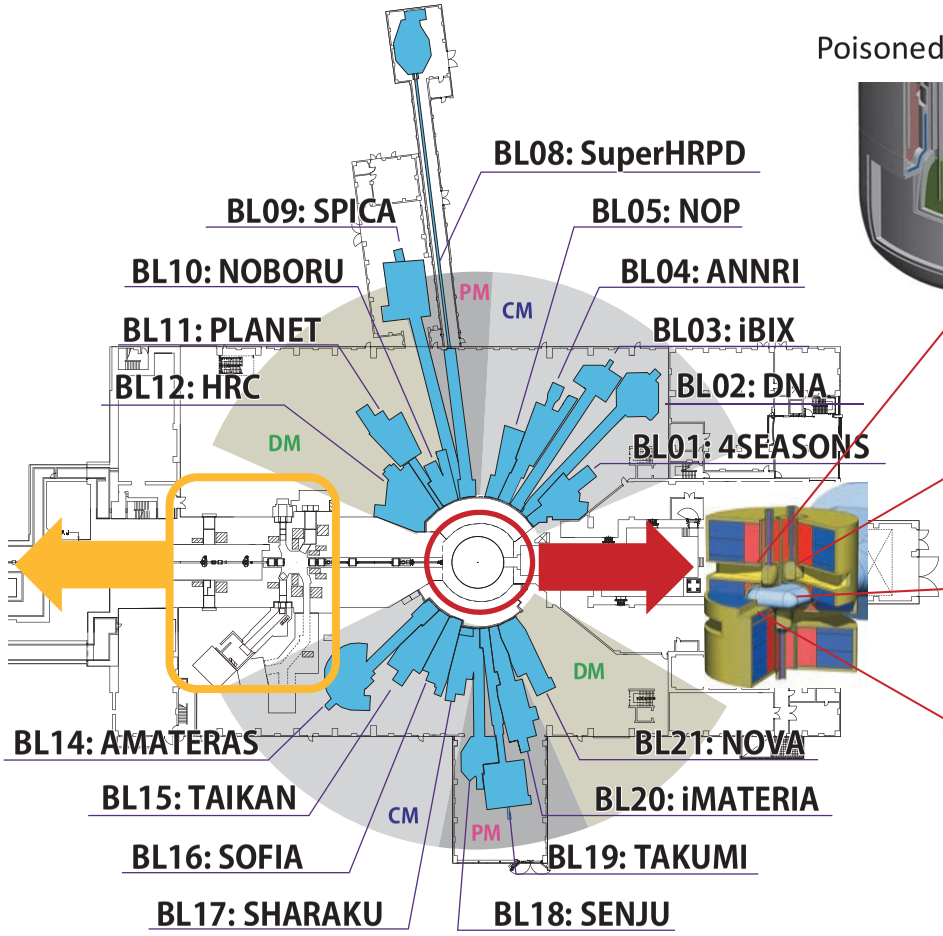

Neutron Source

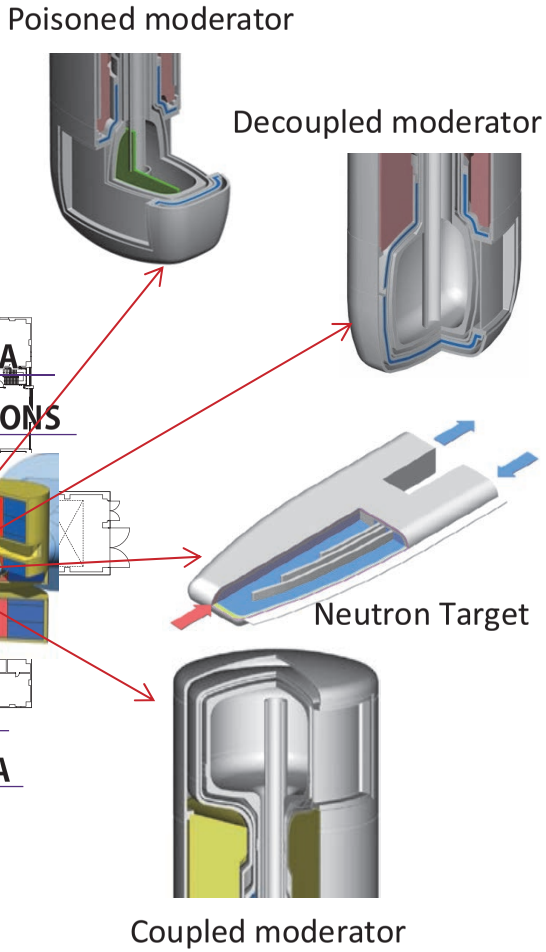

CM Coupled moderator DM Decoupled moderator PM Poisoned moderator

The MLF and the Great East Japan Earthquake – From Calamity to Revival

The MLF and the Great East Japan Earthquake – An Overview

The Earthquake and Tsunami

At 2:46 pm on the 11th of March 2011, eastern Japan was rocked by a massive magnitude 9.0 (M_w) earthquake. Centered on a location about 70 km east of the Oshika Peninsula off the coast of Miyagi Prefecture, the earthquake caused widespread damage and major disruption throughout eastern Japan. The tsunami waves triggered by the undersea megathrust quake wreaked devastation along the Tohoku Pacific coast.

Although the epicentre of the quake was a little over 250 km from Tokai, the impact of this enormous seismic event was extensive with serious damage to some buildings and infrastructure being sustained in the local area. J-PARC and the MLF were not spared from the effects of the disaster. Although J-PARC was protected from the 4.5 m tsunami that struck the Tokai coastline by an 8 m high sea wall that borders the site, it could not, however, escape the impact of the violent quake.

This overview provides a synopsis of events at and around the MLF starting from the time of the earthquake up until the restoration of the experimental program at J-PARC ten months later.

The MLF on the day of the earthquake

On the day of the earthquake, the MLF was in a scheduled shutdown and, consequently, the number of facility users on site was comparatively few. Being close to the end of the fiscal year, however, the facility was alive with activity; MLF staff and contractors were busily working on a variety of installation, testing and commissioning projects associated with the beamlines and supporting facilities.

The earthquake and immediate aftermath

The major shaking of the earthquake subsided after about 3 minutes, by which time 500 km of fault line along the Japan Trench had ruptured. Thousands of aftershocks would follow – many of them potentially damaging to already compromised structures.

The immediate priority was to safely evacuate the MLF building. The seriousness of the situation was instantly obvious to all and the evacuation was rapidly completed with staff and contractors calling out to their co-workers and making their way out of the building via both normal and emergency exits. The experimental hall had been plunged into darkness due to the loss of power and the evacuation was effected by the emergency lighting with power provided only by backup supplies.

People made their way to the initial evacuation assembly area: the carpark outside the MLF main entrance. The process of accounting for everyone who had been in the MLF at the time of the quake was commenced using the Personnel Entry Record that had been retrieved from the access control point during the evacuation.

Amid continuing aftershocks and before the head count could be completed, it became known that a tsunami alarm had been issued. Amidst confusion and uncertainty caused by inaccurate and differing media reports and realizing that the MLF evacuation assembly area was not high enough above sea-level to guarantee safety in the event of a major tsunami, the group who had evacuated from the MLF made their way to the relatively high ground of the HENDEL Building – about 0.5 km away – and once again began the process of confirming the safety of all who had been in the MLF at the time of the earthquake.

Meanwhile, similar events were taking place at the HENDEL Building where staff had sought shelter under their desks during the most violent shaking before fleeing the building as best they could. The building suffered significant structural damage; the 2nd floor passageway became impassable and at least one car parked outside was damaged by falling debris.

With no hand-written entry record and no way to print a hard copy, the head count at HENDEL was confused and time-consuming. This situation was compounded by the actions of some visitors who left the assembly area before the safety of all could be confirmed.

The disaster readiness of the facility was tested during the initial response period. Emergency equipment including torches, transceiver handsets, staff lists, radios and megaphones that had been in storage at the designated evacuation assembly areas were put into service as the site-wide response gathered pace.

By evening on the 11th of March, all staff, users and outside contractors had been accounted for. The situation was, however, quite desperate; there was no power or running water and telephone services that were not cut were hopelessly jammed. Roads were damaged and in some places impassable. There was no public transport and the expressway was closed. Even leaving the JAEA site by car was impossible as the exits and surrounding roads became grid-locked; many abandoned their vehicles after attempting to leave for several hours. An air of worry and despair hung over the facility as people tried desperately to make contact with loved-ones and find a way home.

Emergency supplies of water, food and blankets were available in the Tokai Dormitory where many – including foreign users – spent the night sleeping on the floor. Others left the site on foot in search of a way home or somewhere to spend the night. Many from the JAEA site bedded down on the first night at a local community center which had become an emergency shelter.

In and around Tokai

Compared to the devastation that the earthquake and tsunami had caused in regions further to the north, the Tokai area was relatively well off. Nevertheless, it would be days and weeks before essential utilities and transportation links were re-established.

In the early days after the earthquake, drinking water was in short supply and without any refrigeration, perishable food items soon spoiled. The luxuries of everyday life were soon forgotten as securing water for drinking and sanitation and energy for heating and cooking became the priorities. Queues formed outside the few stores that were able to open as residents attempted to purchase essential items.

The situation was exacerbated by the shortage of fuel for motor vehicles that developed in the initial aftermath. Cars and trucks queued for hours to purchase even a small quantity of fuel and many petrol stations simply ran out of supply and closed their doors. With the expressway cut and local roads jammed, it was taking more than 4 hours to travel between Tokai and Tsukuba – a journey that would normally take less than an hour. J-PARC operated a minibus shuttle service to move staff between the campuses.

The local electricity supply was restored on 14 March – 3 days after the earthquake – but it was not until 24 March that town water was completely restored. The expressway that links the Tokai area to Tsukuba and Tokyo was re-opened to the public on 21 March but the train service from Tokai Station did not resume until 7 April. By the end of March, the fuel shortage was largely over and movement by car was again possible: albeit restricted by damage to roads that would not be addressed for many months.

Initial Response and MLF Damage Assessment

The first priority was to confirm the safety of all staff and visitors. While dealing with their own personal situations, MLF management spared no effort to make contact with every member of staff either by phone or email. It was with great relief that the well being of all staff and visitors was confirmed. By 13 March, J-PARC had assisted all foreign users to evacuate to the relative safety of Tsukuba or to Narita Airport from where they could leave for their home countries.

On 17 March the first inspections to establish the degree of damage inside the MLF were carried out by torchlight and the coordinated process of damage assessment started on 22 March.

The first scout teams found that most of the ground surrounding the MLF building had significantly shifted and subsided by up to ~1.5 m causing serious damage to utilities infrastructure. Within the MLF itself, there was toppled equipment and electronics racks and unsecured items – including in some cases experimental samples – were strewn around the floor. It soon became clear, however, that the impact of the earthquake was far more serious than such superficial damage.

Figure 1. Ground subsidence around the MLF building ©KEK

At an early stage, it became apparent that the entire shielding structure of the MLF – nearly 2,500 tonnes of material – had been displaced. The massive blocks that comprise the radiation shielding for the target and beamlines were shifted, damaged and, in some cases, had even fallen over or collapsed. At several points around the experimental hall the violence of the earthquake had left shielding blocks sitting precariously over thoroughfares and equipment. As a result, access to the MLF had to be restricted because of the danger posed by the continuing aftershocks.

Though severely shaken by the earthquake, the MLF main building was largely protected by the deep foundation piles on which it sits. The annex buildings that house beamlines BL08, BL09 BL18 and BL19, however, are of surface concrete-slab design and subsequently susceptible to any shifting or subsidence of the ground beneath. As a result, these structures were displaced both laterally and vertically destroying neutron guides at the building boundaries with the MLF and causing severe damage to the beamlines and instruments.

Toward Recovery

Starting on Monday 28 March, the Beamline Recovery Meeting was convened every morning at 9 am. This gathering served as the focus point for ongoing damage assessment activities and information gathering and distribution. Over time, the daily meeting morphed into the nerve center for the management and coordination of recovery work.

In an announcement made on 20 May 2011, J-PARC Director Shoji Nagamiya laid out his ambitious plan to have the J-PARC accelerators operating again before year's end and to resume user operations by the end of January 2012. At the time, there was widespread disbelief among both J-PARC staff and outsiders that such a rapid recovery was possible.

Thus began the daunting task of restoring the MLF to operational status and resuming the strategic growth plan. In a truly team effort, the staff and management of the MLF demonstrated unflagging determination and industry towards their common goal. The work plan was structured such that restoration activity continued every day – very often in double shifts and on holidays and weekends. Detailed descriptions of the major recovery projects appear elsewhere in this report.

In anticipation of a successful on-schedule recovery, the MLF announced a Call for Proposals for the 2012A operations period in mid-November 2011. The user community showed similar confidence with 155 General Use applications being submitted by the deadline in December.

Return of the beam

True to his promise to restart the accelerators at J-PARC within calendar 2011, at noon on 9 December 2011, Shoji Nagamiya pressed the button that sent the first proton beam since the earthquake accelerating along the linac.

The Rapid-Cycling Synchrotron (RCS) followed soon after and on 22 December 2011, a 3 GeV proton beam was successfully transported via the 3NBT facility to the neutron production target. On the following day, the first neutron beam in the MLF since the earthquake was observed at *NOBORU* – the JSNS diagnostics and testing beamline. The measurements at *NOBORU* confirmed the intensity of the beam to be the same as before the forced shutdown.

On 17 January 2012, most of the beamlines that had been in operation prior to the earthquake (BL01, BL03, BL04, BL05, BL10, BL11, BL12, BL14, BL15, BL16, BL20 and BL21) were checked for radiation safety and received permission to resume operations. The last daily Beamline Recovery Meeting was held on the morning of the following day.

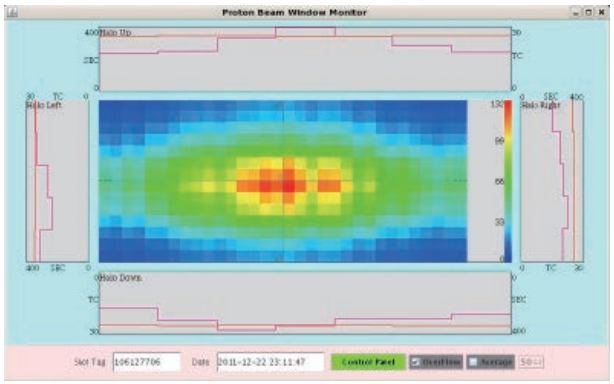

Figure 2. Profile of the proton beam delivered to the MLF neutron target during the first beam study after the earthquake

Beamlines that had been newly completed during the recovery shutdown (BL02, BL09, BL17 and BL18) were inspected and received permission to start commissioning operation at the end of January.

BL19 and BL08 that had been heavily damaged, returned to service in March. BL08 reported a similar beam intensity as during pre-earthquake operations while BL19 experienced a 30% increase in beam intensity thanks to a re-alignment during the recovery period.

After further checking and re-commissioning the 2011B MLF User Program began on 24 January 2012.

Appreciation to our Colleagues

In the wake of the 11 March 2011 disaster, J-PARC received expressions of concern and support from hundreds of our colleagues from both within Japan and overseas.

The MLF was similarly supported. We take this opportunity to express our sincere gratitude to all the facilities who generously offered beamtime and other material support to the MLF and our user community during the time that we were out of action. We were all very much moved by the heartfelt concern and the generosity of the assistance that was forthcoming.

We would like to express a big “Thank-you” to:

- SNS, Oak Ridge National Laboratory, USA
- LANSCE, Los Alamos National laboratory, USA
- Rutherford Appleton Laboratory, UK
- Centre for Molecular and Materials Science, TRIUMF, Canada
- Paul Scherrer Institute (PSI), Switzerland
- Australian Nuclear Science and Technology Organisation (ANSTO), Australia
- Korean Atomic Energy Research Institute (KAERI), South Korea
- SPring-8, RIKEN, Japan
- The Institut Laue-Langevin, France
- Kyoto University Research Reactor, Japan

Figure 3. Scenes of celebration in the MLF Control Room as the proton beam is accepted for the first time since the earthquake – 22 December 2011

Figure 4. J-PARC Director, Shoji Nagamiya, marks the return of the beam to the MLF with a traditional "Daruma no Me-ire" ceremony – 22 December 2011

The Road ahead…

It would be disingenuous to pretend that the physical and psychological impacts of the events of March 2011 do not still linger; there remains repair and recovery work to be done and the process of mental healing is ongoing.

Nevertheless, we are delighted to report that thanks to the tremendous effort of our staff and the support of our colleagues worldwide, J-PARC and the MLF have been restored to fully operational status and the science program has re-commenced. More than that, the staff have taken advantage of the shutdown and recovery period to upgrade facilities and install new equipment. Accordingly, the MLF has not just recovered but is in fact moving ahead. We are all pleased to be back on the path of developing J-PARC toward its full potential.

We look forward to reporting exciting research results and further progress in coming reports.

Earthquake Damages to the Utility Facilities and Subsidence of the MLF Building

Utility Facilities

The Great East Japan Earthquake on March 11, 2011 shook the J-PARC site furiously and the surrounding ground of the MLF building subsided enormously. All the pipes of the water supply, waste discharge and pressurized air were severely damaged and torn off just outside of the main building as shown in Figure 1.

Figure 1. Ground surrounding the MLF building subsided ~1 m (top) and the pipes of the water supply and water drain were torn off.

The electricity supply stopped soon after the earthquake. The emergency power generator was successfully started and the air circulation system kept the hot cell at negative pressure properly. [1]

The inspection started several days after the earthquake. First of all the electricity power lines were thoroughly examined and the electricity supply resumed by the end of March.

The recoveries of the water supply pipes and the waste discharge pipes took longer, since the surrounding ground had to be dug over to examine the damages and to fix them (Figure 2). The water supply was restored gradually till the end of August.

Figure 2. Restoration work for a drain pipe.

Level differences before and after the earthquake

Figure 3 compares the level differences of the MLF measuring points between before and after the earthquake. The levels inside the main MLF building were changed little, less than 10 mm. However, the extension buildings to the experimental halls subsided significantly by around 100 mm. Large steps appeared at the building joints. Consequently the shielding blocks leaned and the neutron guide tubes were broken in those areas.

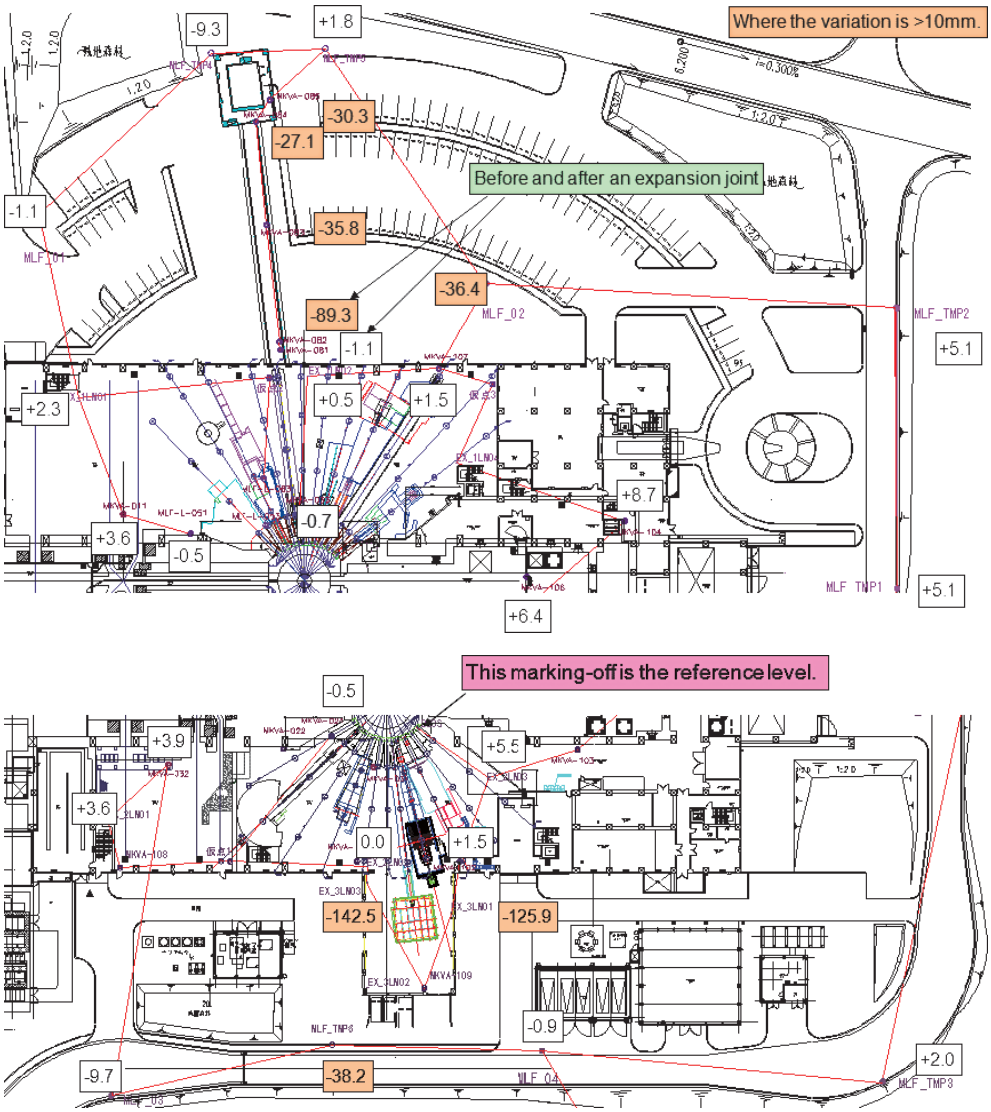

Figure 3. Level differences between before and after the earthquake (in mm).

Reference

[1] K. Sakai *et al.* "Influence of Great East Japan Earthquake on Neutron Source Station in J-PARC," JAEA-Technology 2011-039, 2012, in Japanese.

S. Sakamoto, and M. Harada
Neutron Source Section, Materials and Life Science Division, J-PARC Center

Influence of the Earthquake on the Mercury Target System

Structure of the devices related to the damages on the target system

The helium vessel is installed to keep the helium atmosphere at the center of the spallation neutron source, where the irradiation of the atmospheric gas by the strong radiation field should be prevented, as shown in Figure 1. The inner components such as the reflector, the moderators, and the radiation shield blocks are placed in the helium vessel, and the mercury target vessel is inserted into the helium vessel during the proton beam operation period. In order to isolate the helium atmosphere in the helium vessel from the air atmosphere in the maintenance area, the helium vessel seal system is mounted on the mercury target vessel. The helium vessel seal system consists of metal bellows, a base plate and a metal O ring as shown in Figure 2. When it is actuated, the interspace between the metal bellows is pressurized with helium gas to 0.9 MPa, then the metal O ring on the base plate is pushed onto the seal plane of the helium vessel. The total pushing force reaches 18 tons and the same counterforce is loaded onto the target trolley as well. Thus the target trolley is equipped with a clamp system as shown in Figure 3, which prevents the target trolley from moving away from the beam operation position.

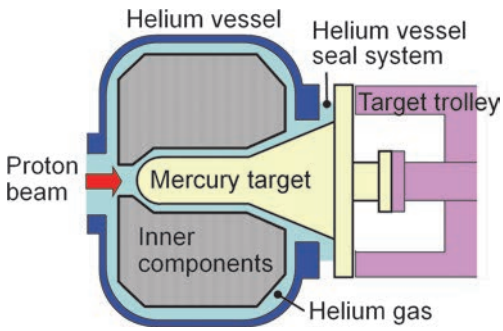

Figure 1. Helium boundary of the helium vessel.

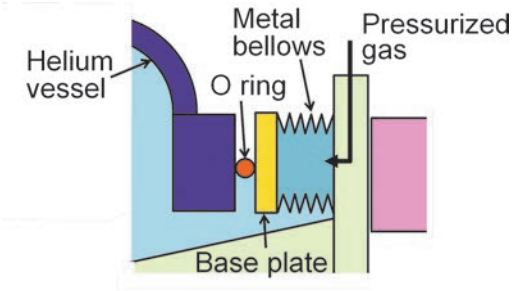

Figure 2. Detail of the helium vessel seal system.

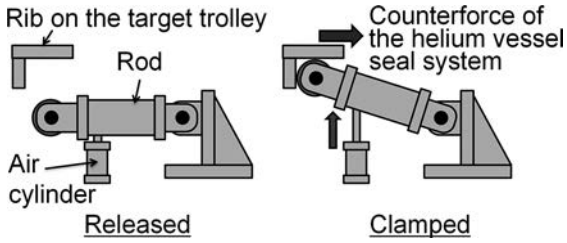

Figure 3. Clamp system of the target trolley.

The clamp system consists of a rod to receive the counterforce and an air cylinder to change the rod position. When the rod is moved upward by the air cylinder, the target trolley position is fastened by the rib contacting with the rod, and when the rod is moved downward, the clamp system is released. The pressurized air, which is fed to the air cylinder is supplied from the facility utility system.

Situation of the target system after the earthquake

The mercury boundary of the target system was not damaged by the earthquake. The mercury sensors, the thermocouples, the pressure sensors, and the electrical devices were also intact. Part of the lining plates of the radiation shielding blocks of the target trolley were stripped off and fell on the floor, but the influence of those plates was negligible. The only serious trouble was the damage to the helium vessel seal system.

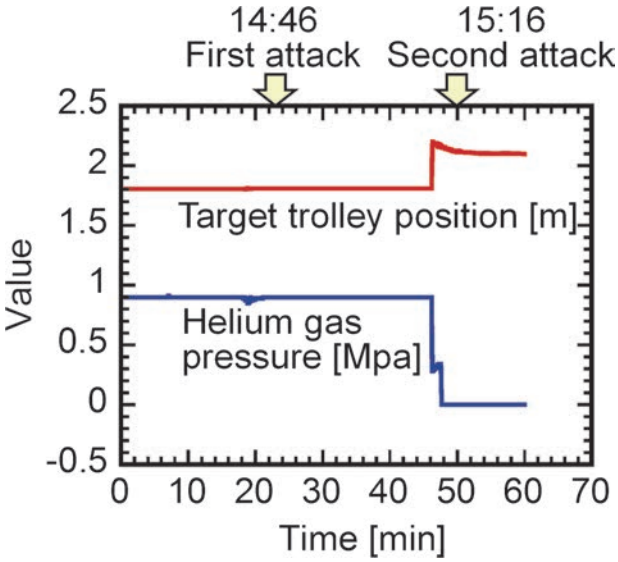

Figure 4. System data before and after the earthquake.

Figure 4 shows the target trolley position and the helium pressure supplied to the helium vessel seal system with the time before and after the earthquake. When the earthquake occurred, the target trolley was at the beam operation position and the clamp system was in a clamped position. At 14:46 when the first attack came, the target trolley moved several mm but it was kept at the same position by the clamp system, but when the second attack came at 15:16, the target trolley moved 380 mm away from the beam operation position. That was caused by the damage to the air supply line of the facility by the second attack, and the air pressure to raise the rod of the clamp system to the fastening position was lost. The target trolley was swayed by the earthquake, which detached the rod of the clamp system from the rib, then it was released by the dead weight of the rod and the target trolley was pushed with the counterforce of 18 tons. The bellows of the helium vessel seal system extended over the upper limit and fractured, which reduced the helium gas pressure. Because the helium vessel seal system is welded on the mercury target vessel, the target vessel became useless.

Replacement of the mercury target vessel

The target vessel replacement was the first large scale remote handling operation after the MLF received the first beam in May 2008. The operation was carried out from November 21 to 30 and it needed 7 days, except the seal performance test. Finally we could replace the used target vessel with a new one successfully, and the target system began its operation again.

K. Haga, T. Wakui, H. Kogawa, T. Naoe, K. Hanano, H. Kinoshita, M. Seki, and T. Suzuki
Neutron Source Section, Materials and Life Science Division, J-PARC Center

Cryogenic Hydrogen System

Introduction

The Great East Japan Earthquake occurred on March 11th. At the time, the cryogenic hydrogen system was operated for RUN#38. The cryogenic system was stopped by the interlock system without any problem. A helium buffer tank (50m^3), a cold evaporator (18m^3) and a cooling tower leaned toward the MLF building due to the ground sinking by about 0.7 m. Although the gas supply pipes that penetrated the building wall were bent into an S shape as shown in Fig.1, there was no hydrogen leak from them. Later in 2011, the cryogenic hydrogen system was restored and the proton beam operation resumed in December without any delay (Fig.2).

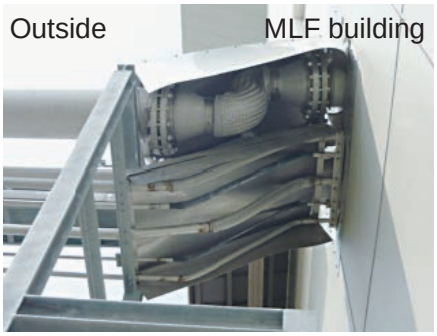

Figure 1. Deformed pipes due to ground sinkage.

Besides, a purification system for a helium refrigerator has been installed in order and its operational instability caused by impurities such as water has been resolved.

Restoration after the Great East Japan Earthquake

The electric supply to the MLF was restored in early April. We were able to start the investigation of the damage situation of the cryogenic hydrogen system in the radiation controlled area. It was confirmed that it had no damage, although the outside area was affected by the ground sinkage.

In July, the inclined tanks were temporally removed and the ground sinkage and their inclined foundation were restored as shown in Fig.3.

After September, we started reinstalling the tanks and restored the deformed pipes. The work was finished by mid-November (Fig.4).

In early December, we conducted an off-beam commissioning and managed to restore the cryogenic system to its former state. We successfully resumed the 120 kW proton beam operation as scheduled.

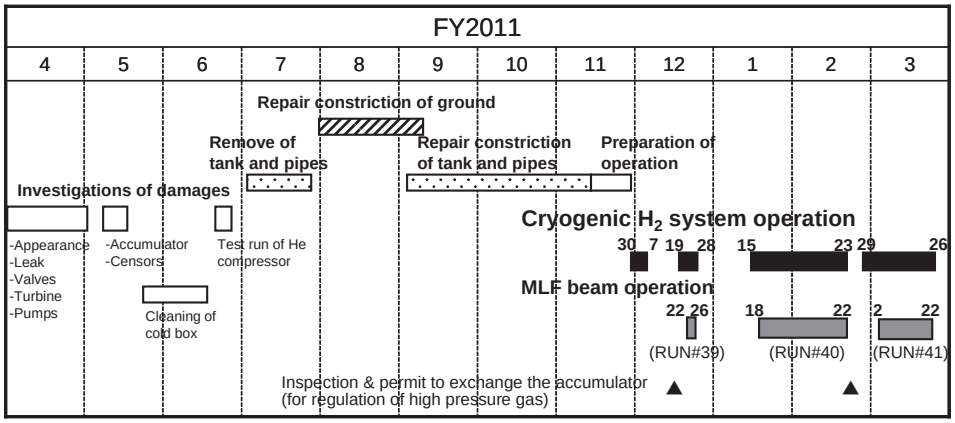

Figure 2. Events of the cryogenic hydrogen system in FY2011.

Figure 3. Temporarily removing the helium buffer tank.

(a) After the earthquake (Mar.)

(b) Foundation work (Aug.)

(c) Completion (Nov.)

Figure 4. Repair construction around the helium buffer tank.

Installation of a helium purifying system

So far, we had a problem with the unstable operation of the helium refrigerator, which was caused by impurities such as moisture [1]. In RUN#35, the pressure drop through a heat exchanger increased up to more than 100 kPa within one week after the cool-down operation as shown in Fig. 5. This is because impurities attached to its surface brought about deterioration of its cooling power. Accordingly, we installed a purification system for the helium refrigerator, which had a dryer, a cryogenic adsorber and a heater for regeneration (Fig.6).

Before the cryogenic operation, the purification in the helium refrigerator had been carried out for a week. We succeeded in stabilizing the operation of the helium refrigerator in one-month long-term proton beam operation (RUN#40) for the first time.

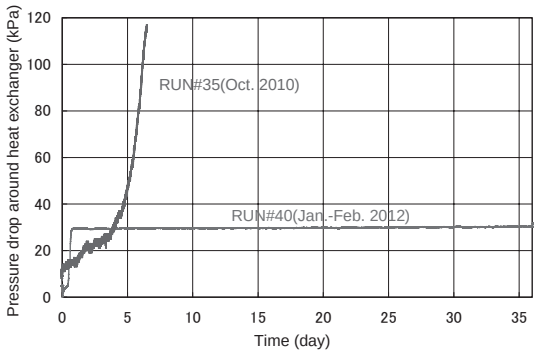

Figure 5. Transition of the pressure difference in RUN#35 and RUN#40.

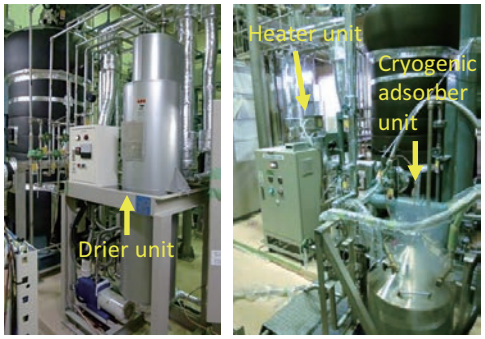

Figure 6. Helium purifying system.

References

[1] MLF Annual Report 2010, p.36-38 (2011).

T. Aso, H. Tatsumoto, S. Hasegawa, K. Ohtsu, T. Uehara, Y. Kawakami, and H. Sakurayama
Neutron Source Section, Materials and Life Science Division, J-PARC Center

Recovery of the Proton Beam Transport System from the Earthquake Damage

Due to the Great East Japan Earthquake on March 11th 2011, the beam transport system was terribly damaged. For instance, the air rushed into the vacuum system of the beam transport system. Several minutes later, due to the stop of helium supply to the pillow seals located around the muon production target, the vacuum seal performance was completely lost. Consequently, the air rushed into the vacuum system from the downstream section. In order to prevent the air from rushing into the vacuum system, fast closing valves (FCV1 and 2) were installed as shown in Fig 1. During the earthquake, the loss of compressed air supplied to the drive of the valve caused by the fact that the earthquake vibration broke the transfer tube located outside of the building, made the fast closing valve of FCV2 located at downstream inactive. Fortunately, the other fast closing valve of FCV1 continued to function normally, so we avoided the loss of vacuum. Without the functioning of FCV1, the accelerator could have suffered critical damage, which might have prolonged the recovery time. We learned the importance of redundancy. When assessing the damage to the vacuum system, our main concern was the possible damage to the pillow seals at the M2 tunnel and the proton beam window. However, the leak examination confirmed that the seals were functioning well.

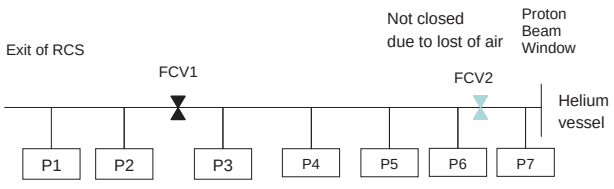

Figure 1. Schematic drawing of vacuum system of the beam transport system.

The building for the beam transport suffered serious damage. Around the expansion joint section, where the structure of the tunnel is isolated, terrible damage was found. The wall of the tunnel around the expansion joint collapsed significantly, as shown in Fig 2. Above the tunnel, the embankment soil on the expansion joint also collapsed significantly. Inside the tunnel, the suspension crane has also been damaged seriously. The bolts of the rail for placing the crane on the cell were cut due to the earthquake vibration as shown in Fig 3. The repairs of the construction structure damage, took longer even though the restoration works continued at end of September.

Figure 2. Collapsed wall by the Great East Japan Earthquake at the expansion joint in the tunnel.

Figure 3. Broken bolts for the rail of the suspension crane due to the vibration.

Due to the vibration of the earthquake, the magnet was displaced by several cm. An uneven

settlement was observed in the beam line. At the downstream section, depression of 12 mm was observed. Even with the presence of such large depression, the good flatness of the beam line was still preserved. In order to adjust the geometrical condition, the beam components were aligned in the tilting plane. After the tunnel was repaired, the alignment of the magnets started, and it must be completed with a short deadline of 3 months in order to comply with the schedule. The alignment work has continued even at midnight. We will begin beam operation with power of about 100 kW. It was expected the beam loss would increase because of the missalignment at the rapid cycling synchrotron (RCS), where realignment was not performed due to some difficulties.

Due to our devoted efforts, all restoration works on the beam transport system were finished in December 2011 as scheduled. The beam commissioning started again. With only one shot of the beam, we succeeded in delivering it. A memorable proton beam profile 1st shot of the beam profile on the target after repairing the damage is shown in Fig 4. Due to the distortion of the geometrical configuration existing before earthquake, the beam position without tuning of the magnet has shifted. After adjustment, the beam properties were measured. It was recognized that the observed beam emittance was similar to the one before the earthquake. Furthermore, during the beam study it was demonstrated that several shots of beam with equivalent beam power of 450 kW were introduced into the target without a significant beam loss. After the completion of the beam studies, we started beam operation for users and increased the power gradually. In March 2012, the beam power reached 200 kW, which was the same as the power before the earthquake. Finally we overcame the difficulties.

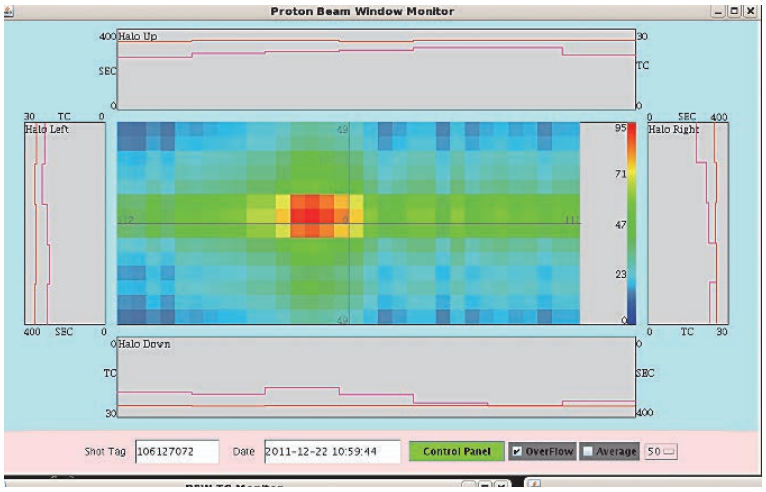

Figure 4. Observed beam profile on the mercury target as 1st shot after restoring.

S. Meigo[1], M. Ohi[1], K. Ikezaki[1], A. Akutsu[1], H. Fujimori[2,3], and S. Sakamoto[1]

[1]Neutron Source Section, Materials and Life Science Division, J-PARC Center; [2]Muon Science Section, Materials and Life Science Division, J-PARC Center; [3]Institute of Materials Structure Science, KEK

Restoration of the Shutter System

Introduction

On March 11, the primary shutters of beam line (BL-) 01, 03, 04, 05, 08, 10, 11, 12, 14, 15, 16, 19, 20 and 21 were being hung at the closed position, while the others were landed on a base. The earthquake did not damage the MLF shutter system [1] severely, however, the vacuum of the shutter inserts of BL-01, 03, 04, 05, 11, 14, 15, 16 and 19 was broken.

In April and May, the shutter inserts of BL-01, 02, 05, 12, 14, 15 and 16 were investigated and we identified the origin of the vacuum break. None of the aluminum vacuum ducts, which contain a neutron guide tube or a steel collimator as an inclusion, had any cracks or ruptures, but the bolts which fasten an aluminum window to a flange using a metal O-ring were loosened.

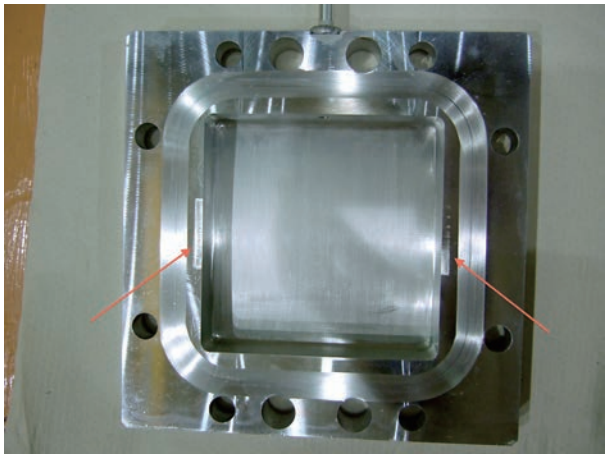

Figure 1. Picture of an inner side of an Al window. Scars are indicated by red arrows.

Analysis

This was the first occurrance of heavy air leakage in the shutter system. As shown in Fig. 1, we found impact scars on most of the leaked aluminum window facing on protrusions of the inclusion. This told us that the inclusion of each vacuum duct was shaken by the earthquake, and the protrusions struck the bolted aluminum window. This impact motion loosened the bolts fastening a metal O-ring of the flange. The shutter insert itself protruded little from the shutter block by a fixing bracket, however, bolts of the bracket were also damaged by the motion of the insert.

Review of the O-ring of the duct

The shutter inserts were more or less radioactivated and their sealing groove and surface were somewhat scratched after usage of the initial metal O-ring. Actually, the vacuum seal attempt by using a fresh metal O-ring was unsuccessful while a tentative rubber O-ring worked well. Then we reviewed the radiation hardness of the EPDM rubber O-ring. The absorbed dose of the EPDM rubber was calculated using the PHITS code with a geometry model shown in Fig. 3.

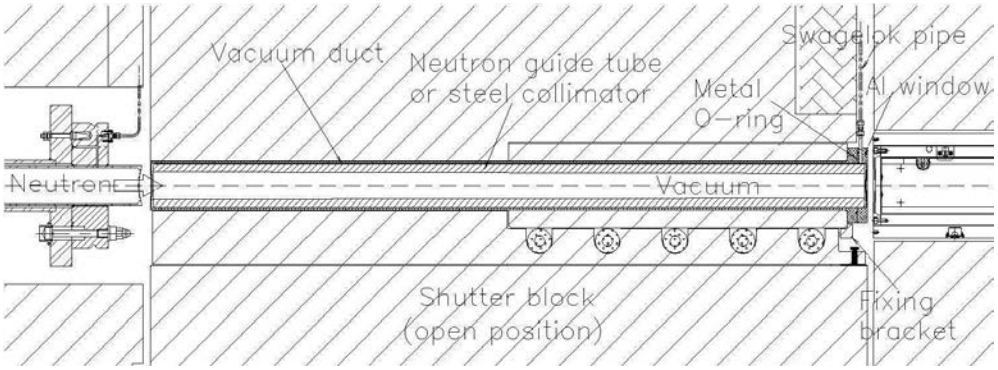

Figure 2. Cut view of a beam duct in a shutter block.

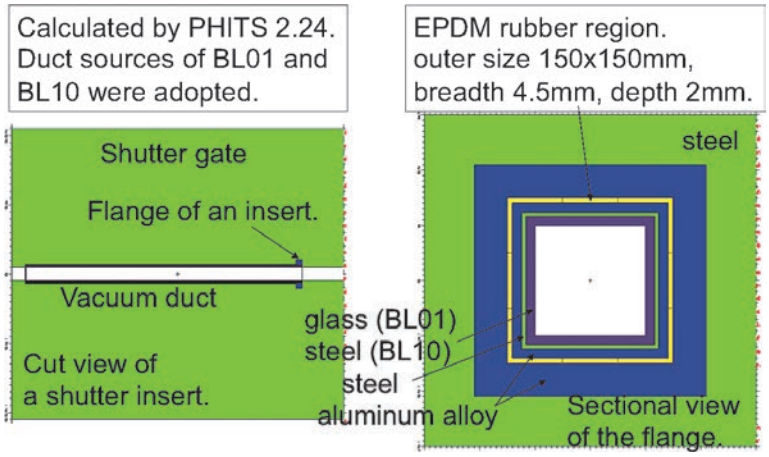

Figure 3. Structure model for the absorbed dose calculation of the EPDM rubber at O-ring position.

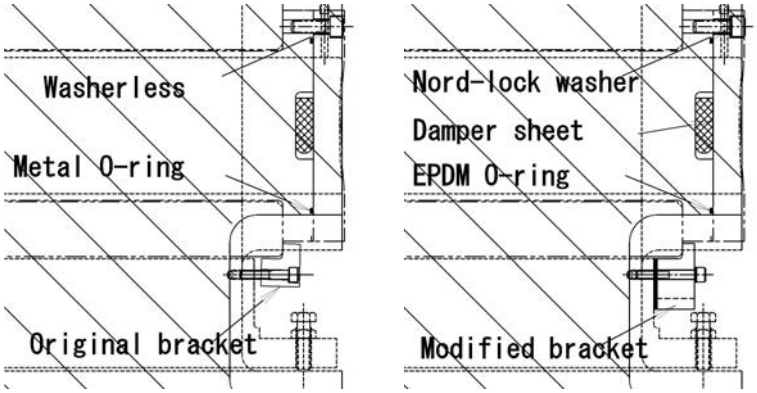

Figure 4. Improvements of the sealing and its surrounding parts.

Table 1. Estimated absorbed dose of the EPDM rubber after 1-year operation at 1 MW.

Source	Aperture size [mm]	Absorbed dose by 1 MW·y [MGy]
BL01	90 x 90	0.0468
BL10	100 x 100	0.0264

Following the calculation result and the advice of the J-PARC accelerator experiencer, we finally decided to replace the metal O-rings with radiation-resistant EPDM rubber ones (HAYAKAWA rubber 355 EB) which can hold its function over 10 MGy [2]. Additional improvements were applied as shown in Fig. 4. A hard-loosen type washer (Nord-lock washer) was added to the bolt, a dumber sheet was attached on the face of the protrusions, and a fixing bracket was modified to prevent bent motion on the bolts.

From August 1 to October 6, we handled shutter inserts of BL-01, 02, 03, 04, 08, 10, 11, 12, 14, 15, 16, 17, 18, 19, 20 and 21. New inserts for BL-05 and 09 were also installed in October. The restoration of the shutter system was completed in mid-November.

References

[1] JAEA-Technology 2011-035 (2011).
[2] JAEA-Technology 2011-039 (2011).

K. Oikawa, F. Maekawa, M. Harada, and H. Takada
Neutron Source Section, Materials and Life Science Division, J-PARC Center

Restoration of the Pre-Shielding for Neutron Beamlines

Introduction

The strong shaking caused by the gigantic earthquake of March 11 damaged significantly the pre-shielding of MLF. We restored a large quantity of pre-shielding blocks for the planned J-PARC re-start by the end of 2011 and resolved the problems caused by the earthquake in a short period of time.

Pre-shielding of the MLF neutron beamline

The pre-shielding is a beamline shielding of a part of the beamline of upper stream. The pre-shielding is a shielding block constituting a tunnel of 1 m in width 2 m in height between 7 m – 12 m from the center of neutron target/moderator of the neutron beam lines which are installed in 23 lines in MLF radially.

There are two kinds of shielding blocks, and one of them serves as a wall and pillar at the side block. Another upper block is used as the roof between the side blocks. The total number of the side shieldings is 280, and the upper shieldings are 248. The weight of each block varies from 3 to 7 tons. The total weight of the pre-shielding reaches 2772 ton.

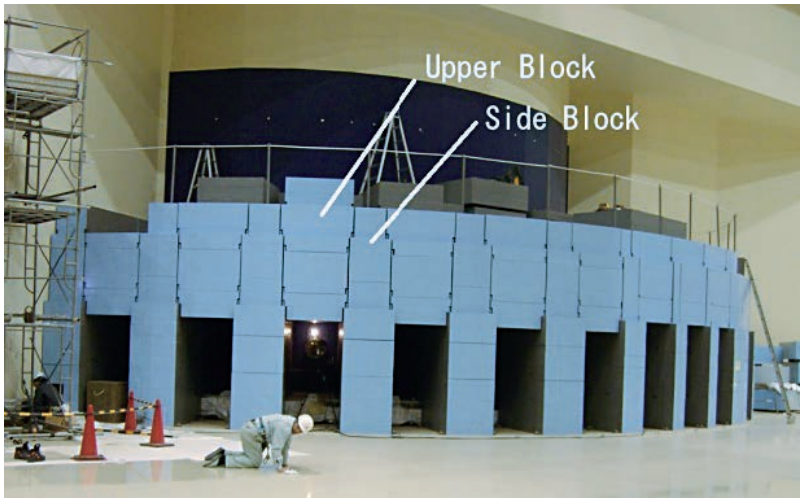

Figure 1. Pre-shielding of neutron beamline.

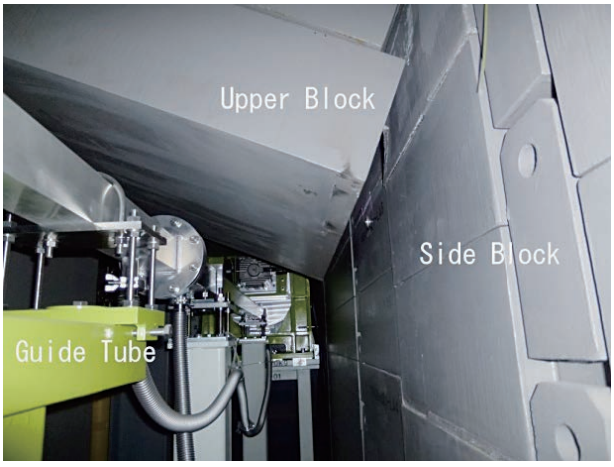

Figure 2. Upper block in a critical state.

The pre-shielding suffered the following consequences due to the strong shaking from the earthquake. 1) A side slip of the foot-block which fixes a side block to a floor with M24 bolts. 2) The all around gaps between the side blocks were moved. 3) A degree of leaning of the block due to the movement of the shim of first construction.

The movement of these side blocks caused the following problems, 1) The upper blocks were on the edge of falling (very dangerous state). The equipments in the beamline were nearly damaged. 2) The positions of the internal setting equipments (guide tubes, choppers) were moved due to the side block pushing out. They needed to be re-aligned. 3) Setting position disorder of the whole pre-shielding.

Reconstruction

We gave top priority to ensuring safety while the aftershocks continued, and it was impossible to enter under the upper block which was about to fall. We prepared an iron structure device, which we were able to insert from the side and carried out the work safely even though the block fell during the demolition work. After removing the dangerous situation, we started the repair work of the blocks which had slipped off. Almost all cover blocks were moved. We investigated the cause of that damage to the pre-shielding and decided to plan the restoration while taking measures.

As a result, the measures taken to deal with these issues are as follows. 1) Since the fit part of the stack is too big, a gap is easy to be accumulated by the multistage configuration of the blocks. Thus, we reduced the gap of the fit part by the special spacer, or through fixation by a plate on an addition. 2) Depending on a beam line, the upper block which is on the top may drop if the side block shifts. Thus, we prepared a bracket to prevent the block from dropping even if a gap caused by an earthquake occurrs.

The work consisted of dismantling a shielding block by a crane, performing threading processing on the site, and setting a shielding block to its correct position as needed while adjusting a gap by the spacer. Unlike the initial shielding block installation, the restoration construction was performed in conditions where the equipments such as the guide tubes, optical equipments, and choppers have already been installed. Therefore various problems occurred and we examined their relevance pushing forward the construction each time. For example, we could not lift the block which was outside of the operating range of the crane. Or we scraped off the welding of the positioning mechanism because of an obstacle to move it aside.

The pre-shielding restoration construction used exclusively the crane of the MLF experiment hall, and other crane work was not possible at the same time. For these reasons, we had to complete it as soon as possible it was the first priority because it became the basis for all repair work in the experimental hole of MLF. We carried out the repair work by both day and night shifts, and it continued for approximately three months. At last, after the pre-shielding repair work was completed, we started the restoration construction of the main body of the beam line. That was in mid-September, 2011.

W. Kambara, and Y. Yamauchi
Neutron Science Section, Materials and Life Science Division, J-PARC Center

Damages from the Earthquake and Recovery of MLF West-Side Extension Building, and BL18 (SENJU) and BL19 (TAKUMI)

Introduction

The extension building （21m long × 16m width × 10m height）in which BL18 (SENJU) and BL19 (TAKUMI) are stored is located at the west of the MLF main building（140m long × 70m width × 35m height）(Figure 1).

The west-side extension building sank about 14 cm by great east Japan earthquake on March 11, 2011. On the other hand, MLF main building did not have significant subsidence because it have deep foundation piles (up to about 20 m below ground). Then, BL18 and BL19 over both buildings suffered serious damage by the difference in level between the buildings (Figure 2). The beamlines; neutron guides, shields, etc. were greatly damaged with the level difference. This paper reports the damages and the restoration process of the extension building and beamlines of BL18 and BL19.

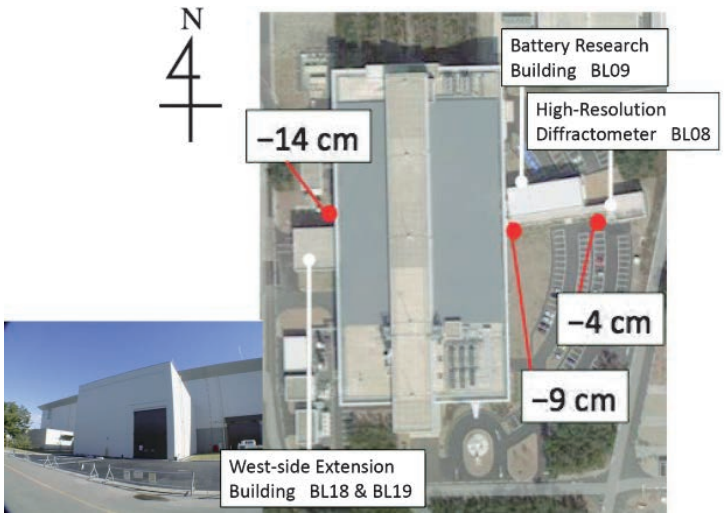

Figure 1. MLF main building and extension buildings with the quantities of subsidence.

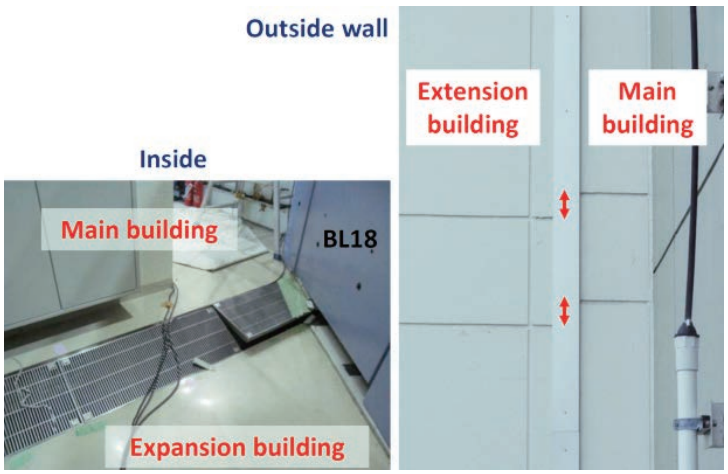

Figure 2. Inside floor and outside wall around MLF main and west-side extension buildings.

Recovery of west-side extension building

MLF and the construction department of JAEA decided to jack the west-side extension building up to the original floor-level together with ground improvement works from the viewpoint of cost and re-installation of BL18 and BL19. For jacking up and performing ground improvement, it is necessary to drill a large number of deep holes into the floor and to inject grout into the foundation soil through the holes. For that, we disassembled shields and all devices; guides, diffractometers, detectors, and wiring etc. of BL18 and BL19, and moved them to the outside of the extension building (Figure 3).

In that way, the jack up and the ground improvement of the extension building were carried out for about two months from the beginning of August, 2011 to the middle of September. The method of jacking the building up is as follows.

1) Inside the building, drilling deep holes into the ground through the floor and injecting low-viscosity grout gradually into the cavities of the ground through the holes using high-pressure jet grouting system (Figure 4). The grout is based on cement, silicate, or other materials, selected to suit particular ground conditions and improvement objectives. The grout fills in voids and cracks of the ground and permeates into soil pores to produce a solidified soil-grout mass.
2) From the outside, grouting the various types of grout into the ground at a deliberately controlled pressure and flow rate by same method as in 1) (Figure 4).
3) Mounting many hydraulic jacks under the building basic, and jacking the building up gradually a building (Figure 5).
4) The procedure of 1)-3) is repeated until the level of the building reaches to the original level and is stabilized at the level.

The jacking and the ground-improvement were difficult constructions because the ground around MLF building is sandy, but all the recovery construction of the extension building was completed on September 10, 2012. The floor level of the extension building was returned to the original level which is consistent to that of the MLF main building (Figure 6). After that, re-installation construction of BL18 and BL19 started in the extension building.

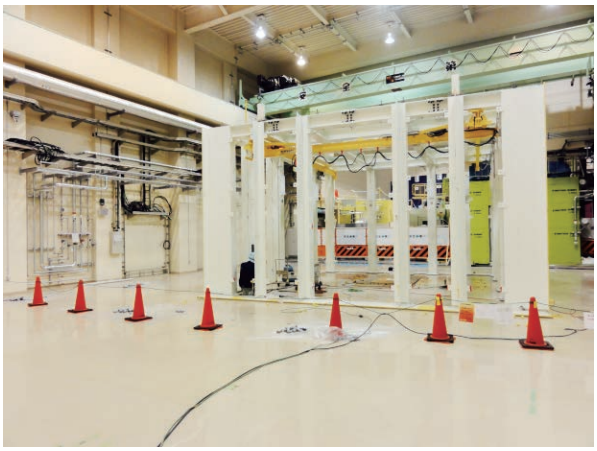

Figure 3. Floor of the west-side extension building after removal of shields and diffractometers of BL18 and BL19.

Figure 4. Grouting (injection of low-viscosity grout) for ground improvement at outside and inside the extension building.

Figure 5. Jacking the extension building up by many hydraulic jacks.

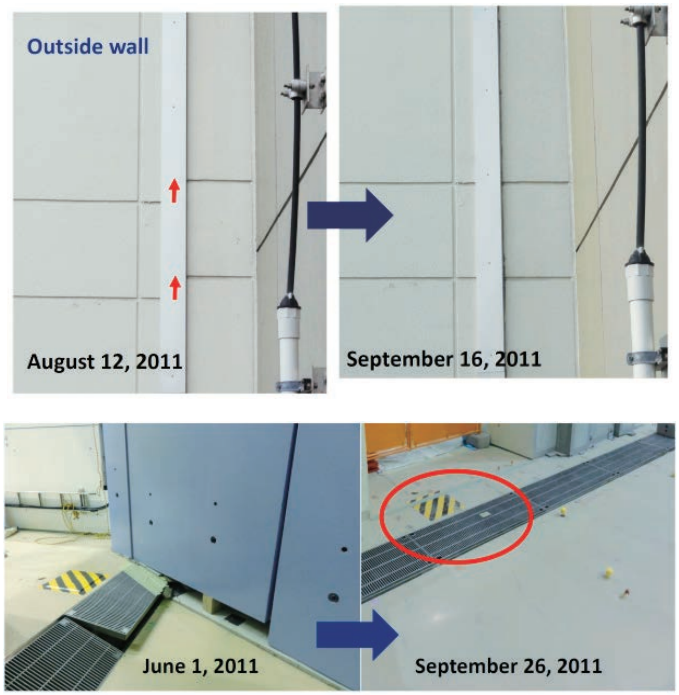

Figure 6. Restoration to the original position (upper) and to the original floor-level (bottom).

Recovery of BL18 (SENJU)

SENJU is a new TOF single-crystal neutron diffractometer designed for use in materials physics and chemistry research. Commissioning of SENJU had been scheduled to begin in April 2011 but was delayed due to severe damage to the instrument caused by the earthquake of 11 March 2011. Since the surrounding neutron shields of the diffractometer were in the boundary region between the MLF main building and the west-side extension building, many shields were destroyed partially and the shields were leaned very much (Figure 7).

The two-dimensional detectors in the shield remained intact fortunately (Figure 8). However, the detectors were migrated after the work to prevent the collapse of the shields (Figure 8), since the inside of the shield was in very dangerous condition. After that, all shields around diffractometer and the diffractometer were also removed to the outside storage area. Moreover, since the positions of the upstream iron collimator, neutron guide cases, supports and the upstream beamline shields were shifted, they were reinstalled to the original correct locations.

Figure 7. Outside view of neutron shields around the SENJU diffractometer (left) and the inside (right). The shields were partially damaged and tilted. The locking bolts of the shields were broken.

Figure 8. Two-dimensional detectors (left) and the reinforced inclined-shields (right) in the shield room of SENJU diffractometer.

The SENJU instrument team spent one year deconstructing the beamline, repairing damaged components, and rebuilding the instrument. On 5 March, 2012, the reconstruction of SENJU was completed and the first neutron beam was delivered to the sample position.

Recovery of BL19 (TAKUMI)

TKAUMI suffered significant damages by the Japan earthquake; the west-side extension building sank about 14 cm. The beam line shields at the joint part between the main building, and the expansion building were tilted and the neutron-guide parts (total about 4 m) including the supports inside the shields, were broken (Figure 9). Although the bolts, used to fix the detector-frames at alignment-position, were also broken, the detectors were saved fortunately.

To recover TAKUMI, all parts, including the spectrometer shields, were removed (Figure 3), after that the sunken extension building was jacked up to a former floor-level, the broken parts were repaired and/or repurchased, and all parts were reinstalled at the original location as they were at the time of the construction. In light of lessons learned from these earthquake damages, we devised to design of the shielding and the guide for releasing the stress; the beam line shield, the neutron guide, and their supports were separated at the boundary between the main and the extension buildings (Figure 10). The recovery of the main part of TAKUMI finished at the end of February 2012. TAKUMI started its re-commissioning on March 6th, 2012 and is now ready for various engineering experiments.

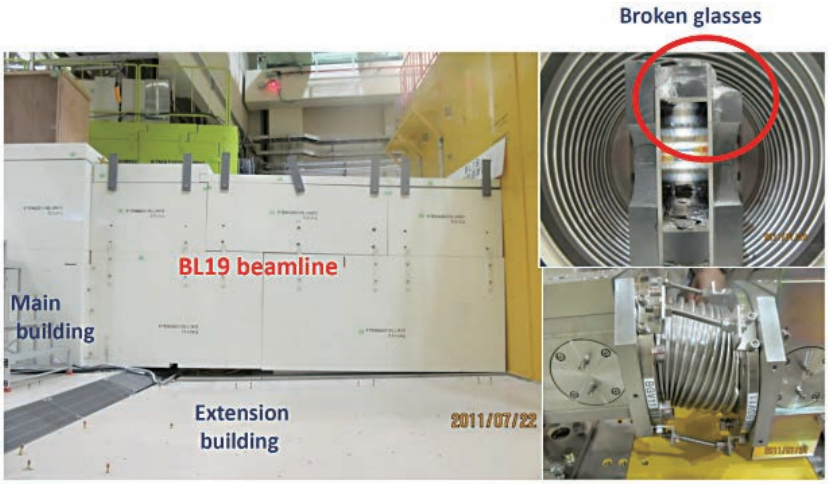

Figure 9. Overview of the inclined shields (left) and the broken glass of the neutron guide mirror (upper-right) and the tilted bellows of the neutron beamline (lower-right).

Figure 10. The lessons learned from the earthquake disaster. The separated beamline shields (left) and the separated neutron guides and the supports (right) around the boundary region between MLF main building and the extension building.

K. Suzuya[1], K. Aizawa[1], S. Harjo[1], K. Oikawa[1], and T. Ohhara[2]
[1]*Materials and Life Science Division, J-PARC Center;* [2]*Research Center for Neutron Science and Technology, CROSS-Tokai*

Recovery Works for BL08 SuperHRPD Beamline

The Great East Japan Earthquake

The Great East Japan Earthquake hit the east area of Japan at 14:46 JST of March 11, 2011. J-PARC experienced it at level 6 of the seismic intensity scale. When the annex buildings were planned to be constructed without concrete piles by the building teams of JAEA and KEK, we were informed that uneven settlement as large as 1 cm might occur at building boundaries with the MLF building with deeply driven piles. However, what actually occurred was that the annex buildings were dropped by 10 - 15 cm compared to the MLF building, and heavy iron blocks of the beamline shielding dropped which destroyed guide tubes. The BL08 annex building moved to the north by 3 cm and to the east by 5 cm (Fig. 1).

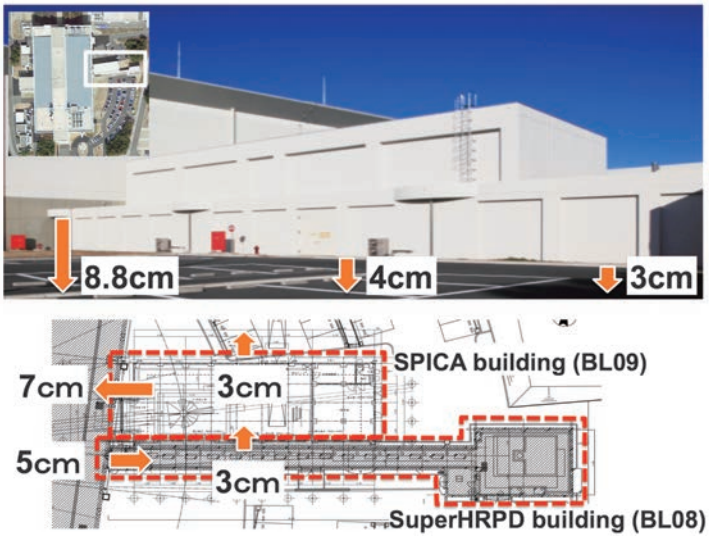

Figure 1. The displacement and subsidence of two KEK buildings.

The building had subsided by up to 8.8 cm near the Expansion Joint. The sample position of SuperHRPD moved to the north by 1.25 cm, to the east by 3.39 cm and subsided by 2.77 cm.

Restoration Work

After the restricted admissions due to the risk of collapse by aftershocks were relaxed, damage evaluation and temporary repairs were quickly carried out. In BL08, the iron shielding blocks at the expansion joint were immediately removed with caution. The instrument group agreed with the building team to, 1) carry out underground investigation quickly, 2) fill earthquake-origin void space with concrete if discovered, 3) re-install the beamline without restoring the subsidence and displacement of the BL08 building itself. The voids caused by the earthquake were finally discovered on November 7 - 9 between the MLF and BL09 buildings (Fig. 2), and were filled with concrete on December 5 - 12.

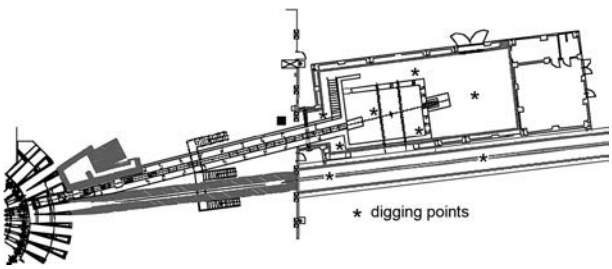

Figure 2. Underground surveying of BL08 and BL09. Asterisk (*) marks are digging points.

As described, since the beamline shielding dropped at the building boundary, several pieces of guide tubes were broken as shown in Fig. 3. Once all pieces of guide tubes were removed and cleaned up, many small scratches were found inside them.

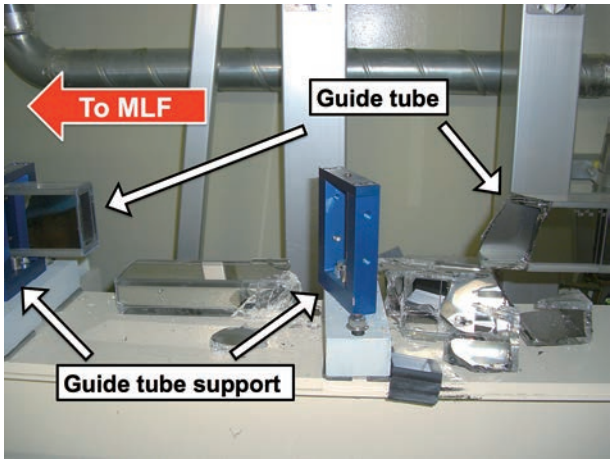

Figure 3. Part of the guide tubes was broken at the building boundary.

In the MLF building, part of the BL08 guide tubes were moved and/or rotated inside iron jackets. For instruments with straight beamlines inside the MLF building, re-alignment is not so difficult, but for BL08 with curved guides followed by straight guides at the annex building, re-alignment is more problematic because the direction of the straight guides is not known due to the displacement and subsidence of the annex building. We repeatedly surveyed the land and the building, and measured the shifts and subsidence of the beamline and the sample position (Sep. 12 - 16 and Nov. 21 - 26). We finally decided to leave it at the sample position and to align the guide tubes so as to bring the beamline to the sample position.

In the MLF building, since the beamline displacement was small, the guide tube support structure was simplified so that the guide tube re-installation and alignment could be performed easily. In the BL08 beamline building, the guide tube support mechanism was re-designed so that an adjustment as large as 10 cm along the vertical and horizontal directions was made possible. The iron shielding in the BL08 beamline building was raised by several centimeters instead of restoring the subsidence and displacement of the building itself. Furthermore, we adopted structures which were damage-proof against earthquakes, and/or structures in which breakage concentrates on a specific part.

After installing three disk choppers in November, we installed guide tubes in the MLF building on Dec. 12 - 22, and those in the beamline building on January 10 - February 3. The earthquake-proof glue was pasted to the glass guide tube connection in the beamline building on February 6 - 10, followed by drying (10 days) and a leak check. The shielding at the building boundary was re-designed and carefully re-installed on February 27 and 28, 2012. The beamline shielding in the MLF and the beamline buildings were installed on January 24 - 25 and March 5 - 21, respectively. All the temporary restoration was completed by the end of March 2012 and the operation was permitted on March 23 by the J-PARC radiation protection supervisor. However, one of the power supplies of the linac klystrons broken on March 22 was not repaired until April 8.

S. Torii[1,2], M. Yonemura[1,2], T. Muroya[1,2], Y. Noda[3], and T. Kamiyama[1,2]

[1]Neutron Science Section, Materials and Life Science Division, J-PARC Center; [2]Institute of Materials Structure Science, KEK; [3]Tohoku University

Recovery of ANNRI from Damages Caused by the Great East Japan Earthquake

At the time of the Great East Japan Earthquake on March 11, 2011, the Accurate Neutron-Nucleus Reaction Measurement Instrument (ANNRI) installed in BL04 suffered serious damages.

As shown in Fig.1, the gamma-ray shields made of heavy metals for the large Ge spectrometer leaned to the walls. One of the shields was stopped by breaking an air-conditioner, and the other by a signal cable rack installed along the walls. At the same time, several of the annular shaped BGO scintillators fell onto the floor, and their PMTs were damaged.

Furthermore, the ^{6}LiH neutron shields set in front of the cluster Ge detectors were also damaged by the stress of the detectors, and small amounts of ^{6}LiH powder were leaked. This made the recovery procedure very complicated. However, the team members of BL04 immediately made a plan to recover from the situation. The inclined gamma-ray shields were removed from the BL04 experimental area on April 11, 2011 and reinstalled on March 4, 2012 as shown in Fig. 2. The recovered ANNRI has been used again in the user program since Feb. 2012.

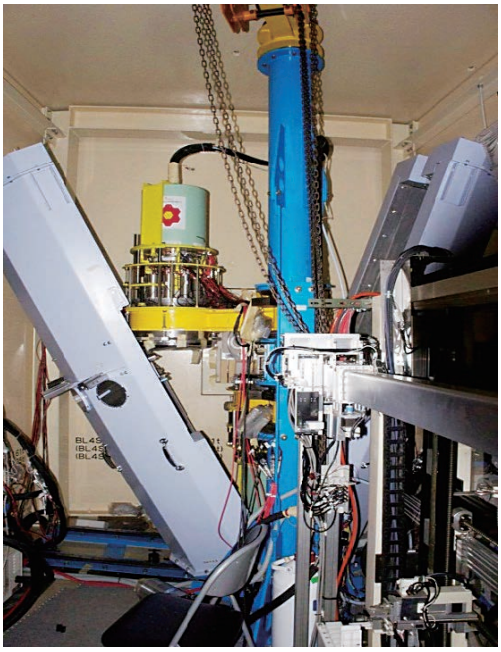

Figure 1. Inclined gamma-ray shields for the large Ge spectrometer.

Figure 2. Recovered gamma-ray shields for the large Ge spectrometer.

A. Kimura[1,2], K. Hirose[1,2], T. Kin[2,3], and H. Harada[1,2]

[1]Neutron Science Section, Materials and Life Science Division, J-PARC Center; [2]Nuclear Science and Engineering Directorate, Japan Atomic Energy Agency; [3]Present address, Kyushu University

Recovery from Earthquake Damage and Progress in the High Resolution Chopper Spectrometer (HRC)

The High Resolution Chopper Spectrometer (HRC) was installed at BL12 to study dynamics in condensed matters with high resolutions and high energy neutrons, and we confirmed that the HRC works well as designed. Due to the earthquake on March 11, 2011, 9 pieces of 2.8m PSDs were damaged and some shieldings were slipped on the HRC. We realigned the beamline, restored the shieldings, replaced the damaged PSDs with new ones, and confirmed the operations of the choppers, the vacuum system, and the electronics. After these recovery works, neutron scattering experiments were started in January 2012, also the first general user program was performed on the HRC.

On the HRC, 64 pieces of 2.8 m PSDs are mounted on each detector bank panel of 1.5×3 m^2 with a vacuum flange, and at present two panels with PSDs are held on the vacuum scattering chamber. Previously, to mount PSDs, it was necessary to remove the shielding blocks above the panels first, and then, remove the panels by using a crane at the experimental hall. At present, we mounted a rail just above each panel, and the panel can be removed from the chamber along the rail by using a hand chain hoist. By using this mechanism, we replaced the damaged PSDs with new ones in a much easier procedure without removing the shieldings.

During the recovery works, we also improved the performance of the HRC. A supermirror guide tube of 5.2 m in the down stream part of the primary flight path was installed, a greater intensity gain was obtained by a factor of 3 at E_i = 100 meV and a factor of 5 at E_i = 50 meV, for instance, in comparison with the previous set-up. A soller collimator system was installed just upstream of the sample, and the background noise was dramatically reduced. Software for an experimental control environment was developed to combine the measurements of neutron counts with the control of devices such as temperature controllers, goniometers, choppers, vacuum system, and so on. The regeneration process to release absorbed molecules in the cryopump, which is used for evacuating the vacuum scattering chamber, was optimized and a frequency of the evacuation process without the regeneration process was greatly improved. A cryomagnet to apply magnetic field of up to 14 Tesla to the sample was designed, manufactured and delivered. The commissioning work of the cryomagnet has been started.

S. Itoh[1,2], T. Yokoo[1,2], D. Kawana[1,2], S. Satoh[1,2], T. J. Sato[3], T. Masuda[4], and H. Yoshizawa[4]

[1]Neutron Science Section, Materials and Life Science Division, J-PARC Center; [2]Institute of Materials Structure Science, KEK; [3]Institute of Mutlidisciplinary Research for Advanced Materials, Tohoku University; [4]The Institute for Solid State Physics, The University of Tokyo

Return of the Neutron Beam

Neutron source

The first target damaged by the earthquake was replaced with a new target in November 2011. Figure 1 shows the first target with elongated seal bellows and the new target, which replaced it. The new target vessel, equipped with a bubbler in it for mitigating the pitting damage caused by pressure waves in mercury, had been fabricated as a spare target. That was the first time to replace the target vessel, i.e. the heavy and large radioactive component, by remote-handling system since the MLF began the beam operation. The target replacement was successfully completed in 7 days just the same way as the handling test under the cold condition. Unfortunately, the installation of the helium gas supply system, which supplies compressed helium gas to the bubbler, was not completed in time for the beam operation due to the trouble in the helium compressor. The mercury circulation operation of the target system started again in December 2011. The pressure drop of mercury in the target vessel increased due to the bubbler installation, but the flow test showed the operation property agreed well with the estimation.

The beam operation was resumed in late December 2011. The proton beams were transported from the accelerator to the mercury target and their beam orbits and profiles were tuned without any serious problems. The beam emittances were measured and no significant changes were found.

On December 22, the first proton beam after the earthquake was successfully delivered to the mercury target in the MLF. On December 23, a neutron beam was introduced for the first time to the NOBORU instrument (BL10) under a 1 Hz operation. A neutron beam profile was measured with an image plate (Fig. 2). The neutron flux intensity was measured with the gold foil activation method. A neutron TOF spectrum was measured with a He-3 monitor counter (Fig. 3). It was confirmed through these measurements that the earthquake did not affect significantly the neutron beam characteristics.

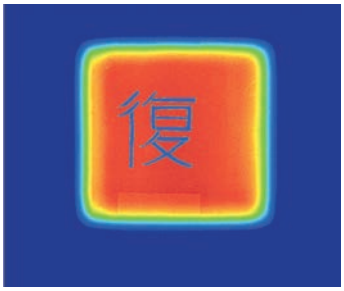

Figure 2. The first neutron beam in the MLF after the earthquake on which the kanji character “復” (fuku), meaning "recovery", emerged.

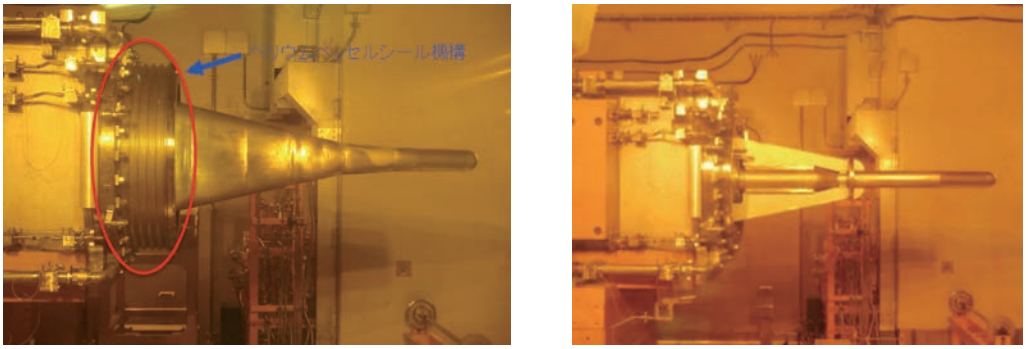

Figure 1. The first target vessel with plastically elongated seal bellows and the new replacement target vessel, which was redesigned to be compact and reduce the radioactive wastage.

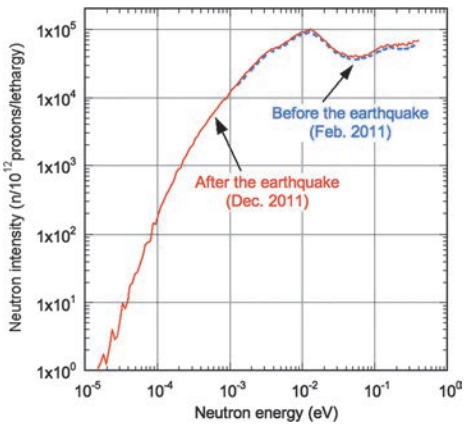

Figure 3. Neutron flux spectra before and after the earthquake.

Resuming the user operation

Neutron beam was supplied to the existing (operated before the earthquake) neutron instruments (BL01, BL03, BL04, BL05, BL10, BL11, BL12, BL14, BL15, BL16, BL20, BL21) from January 24 after finishing the radiation safety inspections on January 17. The inspections of the new instruments (BL02, BL09, BL17, BL18) were done on January 26 and February 1, and the permissions for operation were granted. Two instruments in the annex buildings, BL19 and BL08, were severely damaged and should wait to resume their operation until March 1 and 23, respectively.

36 neutron proposals out of 142 approved proposals (103 general-use and 46 project-use) in 2012A were performed at overseas neutron facilities (SNS, LANSCE, ISIS, ILL and HANARO), and 2 proposals were done at SPring-8. (See Table 1.) In 2012B, 19 neutron proposals out of 37 approved general-use proposals were carried out after resuming of the user program.

References

[1] M. Futakawa, Proc. ICANS XX, Bariloche, Rio Negro, Argentina (2012).

Table 1. Number of neutron proposals in 2011A transferred to other facilities.

	approved	SNS	LANSCE	ISIS	ILL	HANARO	SPring-8
BL01	13	3		1			
BL03	20	2					
BL05	1				1		
BL08	13	4				1	
BL10	14						
BL12	3	3					
BL14	12	3		1	1		
BL16	11	2	3	1			1
BL19	19	3					1
BL20	34	4	2				
BL21	2	1					

M. Futakawa[1], and H. Seto[1,2]
[1]*Materials and Life Science Division, J-PARC Center;* [2]*Institute of Materials Structure Science, KEK*

MUSE - Damage and Recovery from the Earthquake

Introduction

MUSE (MUon Science Establishment) suffered severe damages from the earthquake on March 11, 2011, the so-called 'Higashi-Nippon Dai-Shinsai'. Fortunately the damaged apparatus, ducts, and shields had been fixed on schedule. We were able to restart the user's run in February 2012.

Damages and their recovery

In particular, the damages on the boundaries of the building structure were serious, since severe settlements occurred there. The following sections shows the major damages suffered at MUSE.

2-1) The helium ducts, control cables, power cables, compressed air piping for the superconducting magnet and on-line refrigerator system were damaged for D-line, due to ground settlements, about 10 cm to 1.5 m outside the MLF building. Also a buffer tank for the He gas was tilted by 2-3 degrees. Because of the high-pressure gas regulations, we had to replace all the helium ducts at the boundary. Therefore we fixed the affected ducts as well as a support for the ducts and had a high pressure gas inspection in September, 2011. Finally, we managed to establish a stable operation of the superconducting solenoid magnet with the use of the on-line refrigerator in December, 2012, although we had to overcome some difficulties with components not working properly.

2-2) The M1 and M2 air circulation systems for the proton beam tunnels in the vicinity of the muon target were damaged. In particular, it was found necessary to remove and rebuild some water ducts and control cables, since the wall where they have been fixed, located at an expansion joint between MLF and the proton beam transport line from 3-GeV RCS (3NBT), was about to collapse. Finally, the wall and water ducts etc. in the vicinity of the expansion joint were fixed by November, 2011, which enabled us to run a stable operation of the air circulation systems.

2-3) The M2 tunnel consists of a target chamber, six quadrupole magnets, four steering magnets, two sets of profile monitor assemblies, 29 sets of pillow-seal assemblies, and seven sets of duct assemblies. When the electric supply was restored after the earthquake, it turned out that the vacuum pressure in the M2 line primary beam duct was air-pressure. We suspected that something wrong with the pillow-seals caused some leakage in the vacuum. Eventually, after conducting vacuum leak check for all the pillow-seals, we found out that the

Figure 1. Damaged helium ducts for the on-line refrigerator at the boundary of the MLF building.

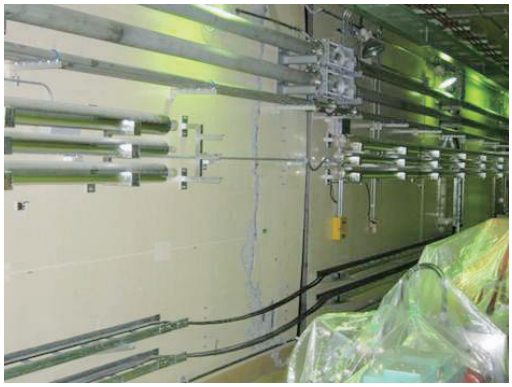

Figure 2. The damaged wall was about to fallen down at the expansion joint between 3NBT and MLF, as if water ducts for the M1 and M2 air circulation systems, were supporting the wall.

pillow-seals themselves were OK, but the tightness of a metal gate valve was not appropriate.

2-4) We have been adopting an edge-cooled non-rotating graphite target, so called 'fixed target' because of its ease of handling during maintenance. In this target, graphite is indirectly cooled by the copper frame, which surrounds the graphite. In order to reduce stress, a titanium buffer layer of 2 mm is placed between the graphite disk and the copper frame.

In order to inspect the soundness of the graphite target, just in case if damage to it was caused by the earthquake, the graphite target assembly was transported to the hot cell. There we investigated not only the dimensional change but also the heat conductivity by the way of remote handling. Consequently, it turned out that the graphite target was sound and could be operated for at least another year.

2-5) It was surprising that a lot of anchor bolts (M24) were split out from the concrete shielding blocks due to slipping off caused by the strong quake. Therefore several concrete shielding blocks themselves were broken or cracked. All of the damaged blocks were temporarily repaired with concrete maker until November, 2011.

Muon Beam Commissioning

Consequently, we managed to resume the operations of the D-line after recovering from almost all the damage by the end of December, 2011. It is our great pleasure to report we could deliver again surface and decay muons up to 60 MeV/c beam towards D1 and D2 during the commissioning beam time held on Jan. 17th, 2012, with an intensity equal to the one before 2011[1]. The regular users' runs were restarted from Feb. 2nd, 2012. Fig.3 shows a picture of MUSE members celebrating the muon beam recovery on Jan. 17th, 2012

Figure 3. MUSE members celebrating the muon beam recovery on Jan. 17th, 2012.

Y. Miyake[1,2]

[1]*Muon Science Section, Materials and Life Science Division, J-PARC Center;* [2]*Institute of Materials Structure Science, KEK*

Recovery from the Earthquake – Building and Concrete Shield for MUSE –

A tremor with an intensity of 6+ on the Japanese seismic scale, which corresponds to Mi9.0 on the Richter scale, befell J-PARC on the 11th of March, 2011. The seismograph in the Tokai nuclear reactor which is about 2 km north of MLF recorded a horizontal acceleration of about 0.4 G. Although the damage to the MLF building was not serious, many small cracks were formed in the wall, and the devices, designed to withstand only 0.25-G quake, were damaged seriously.

The pictures shown in Fig. 1 were taken just after the earth quake. The damaged devices were located mainly around the movable shields and around the expansion joint between the buildings. The damage to the expansion joint originated from the movement and settlement of the building. The utility lines such as power cables and cooling water pipes striding over the expansion joint were damaged, and were fixed or replaced. The cooling water had been kept in the lines since the day of the earthquake. Before the earthquake, MLF was operated for about two weeks, and the activated water remained in the magnet. Due to the radicals in the water, it was not good for cooling the water pipes, thus quick refreshment of the water was required. However, it took about half a year to fix the problem. After the recovery of the

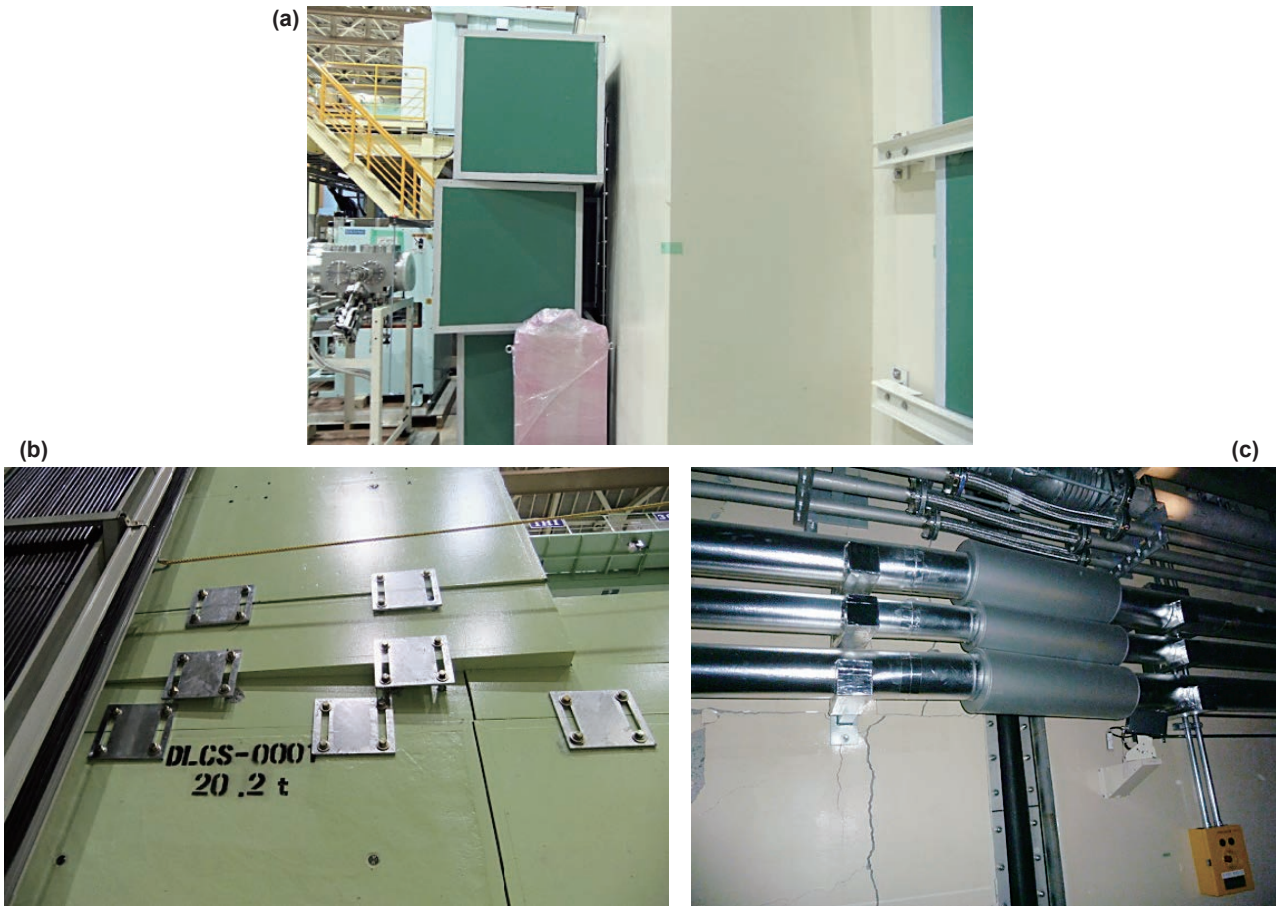

Figure 1. (a) The concrete shields of H line in experimental hall #1 and (b) that of D line in experimental hall #2, and (c) broken expansion joint between 3NBT and MLF.

cooling water system, the insulation resistance of the magnets in M2 tunnel was found to be reduced by the order of kΩ. Although this level of insulation resistance does not affect the magnet operation, we will take measures to address the issue in the next fiscal year.

The radiation shield blocks piled in the experimental hall were moved. Some of them were fixed on the building wall and floor by the metallic plate, and low shields were just piled with safety bars against overturning. The fixing plates and safety bars were broken at the anchors. About a quarter of the anchors for the D-line shield blocks were pulled out. The broken anchors were cast-in type, a.k.a. grip anchor. Their execution management is difficult, and by out-looking, it is not easy to judge that they have designed strength against 0.25-G quake. Because it is known that the quake of 0.4 G was coming, we fixed the fixing plates for the shield blocks to with stand about 0.4-G quake. We stopped using cast-in anchors, and replaced them with anchors fixed be resin, which can be controlled much easier during construction.

By the beginning of Decemeber 2011, we completed the fixing work and the muon facility was ready to operate. The recovery was quick because the beam line magnets were not damaged. We didn't need to realign them.

N. Kawamura[1,2], and Muon Sci. Sec., J-PARC

[1]*Muon Science Section, Materials and Life Science Division, J-PARC Center;* [2]*Institute of Materials Structure Science, KEK*

Recovery of Superconducting Solenoid from the Great East Japan Earthquake

A conventional superconducting muon channel, which can extract surface (positive) muons and decay positive/negative muons up to 120 MeV/c, is successfully operating at the MLF experimental hall II. The 6 m long superconducting solenoid magnet consists of twelve units of 0.5 m coil. The magnet coil is forced-indirectly cooled by supercritical helium gas (4.8K at 0.80 MPaG) supplied from the on-line helium refrigeration system. The maximum magnetic field was designed to be up to 5T (currently 730A) at the operational temperature of 6 K. The present magnetic field for normal operation for surface/decay muon extraction is 0.308 T (45A)/2.33 T (340A), respectively

For the long-term stable operation, the on-line helium refrigeration system is employed. The cooling power of the on-line helium refrigeration system is 35 W at 4.5K and 200W at 80K, and it can also produce 8 l/h of liquid helium. The whole system is monitored and controlled by a VME controller combined with a personal computer with dedicated software based on the LabVIEW System, and it cools

Figure 1. Photograph of the broken He piping for the refrigerator, located just outside of MLF building before (above) and after the repair (below)

down automatically. The typical cooling period from room temperature to operation temperature (~5 K) is about 3 days. The long-term (typically 1 month) operation is now established under quite stable conditions.

To avoid any serious damage to the superconducting solenoid and the helium refrigeration system, a VME based interlock system has been installed. The system can detect any anomaly in the voltage and the temperature of the solenoid and the power lead; the trip signals from the helium refrigeration system and the electric power supply are also included. Once any emergency status is detected, the electric power supply immediately stops the current supply and the refrigeration system changes to self-operation mode. In addition to these interlock systems, this part can also record automatically the temperatures and pressures of the superconducting coils, the helium refrigeration system and the power leads. All recorded data are also monitored and stored at the MLF control room, by using MELSEC-NET.

In FY 2010, the solenoid and on-line refrigeration system was operated smoothly for more than 5000 hrs, up to the gigantic earthquake on March 11th 2011. At that time, the system was operating, however, it stopped safely and there was no He gas release. The damage due to the ground sinkage was rather serious, especially the He piping from the outside compressor building was warped as shown in Fig.1. Therefore, we replaced three He pipes – the high pressure, the low pressure from the compressor and the buffer pass. At this time a 1m long flexible pipe was adopted instead of the 0.5m pipe to avoid damage from the gradual sinking.

The other components like solenoid, cold box and transfer tubes were fortunately not damaged. And also the whole cabling and interlock system was checked to be O.K. under room and also operational temperature conditions. We checked the leakage and pressure resistance for all components. The recovery was completed by the end of November 2011.

K. Shimomura[1,2], Y. Nemoto[1,2], A. Koda[1,2], K. Nishiyama[1,2], and Y. Miyake[1,2]
[1]*Muon Science Section, Materials and Life Science Division, J-PARC Center;* [2]*Institute of Materials Structure Science, KEK*

Measurement for Deformation of Muon Target by the Great East Japan Earthquake and Measurement for Thermal Diffusivity of Proton Irradiated Graphite

Because J-PARC was heavily affected by the Great East Japan Earthquake, serious deformation of the muon target rod could be predicted. Therefore the precise position of the muon target rod was measured in a remote handling room, *Hot cell* in August and September of 2011. Simultaneously, the 3-GeV proton irradiation effect on the thermal diffusivity of graphite was measured for the used target, because it is known that when the crystal structure of the graphite material is broken, the thermal diffusivity decreases by proton beam irradiation [1].

A muon target is integrated into a target rod. Then the target rod is attached to a plug shield through 4 screws. This assembled component is called muon target assembly. When the muon target assembly had been installed in the proton beam line, the muon target could be positioned with 0.5-mm precision against the beam line. The position is determined through three pairs of guide pins, male pins inside the chamber on the beam line and female pins on a plug shield. Consequently, the deformation of the target rod can be measured when the position of the muon target is measured against the female pins on the plug shield. Then a plug stand was positioned in *Hot cell*; three male pins with the same dimensions as the ones inside the chamber were equipped on the plug stand. Two laser displacement meters were set on a 3-dimensional motion stage, which was attached to the plug stand. Figure 1 shows the measuring devices attached to the plug stand. The positions of the used target and the un-irradiated target (spare target) were compared with the position of a mock target with the dimensions of the original design. Figure 2 demonstrates the results of the measurement. The differences of the positions on the used target and the un-irradiated target from the mock target were less than 0.5mm. The conclusion was that the deformation of the muon target rods was small enough, so they could be used again.

Simultaneously, a modified Thermal Imaging Scope, TSI (Bethel Co. Ltd. [2]) was set on a motion stage to measure the thermal diffusivity of the graphite. In this method, the material is heated by a periodic heating laser diode. The propagation of a thermal wave around the heated spot is measured with a two-dimensional infrared thermometer. The thermal diffusivity can be locally evaluated through the delay of propagation or the amplitude gradient, which depends on the distance between the laser-heated spots. The proton beam profile had complied

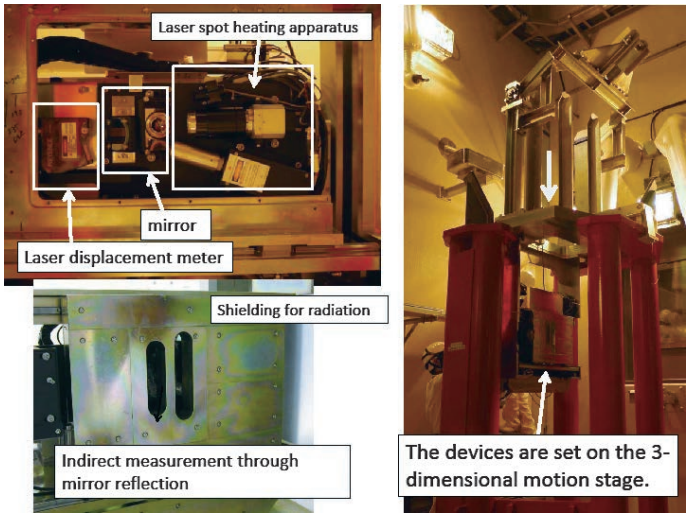

Figure 1. The picture of the measuring devices attached to the plug stand.

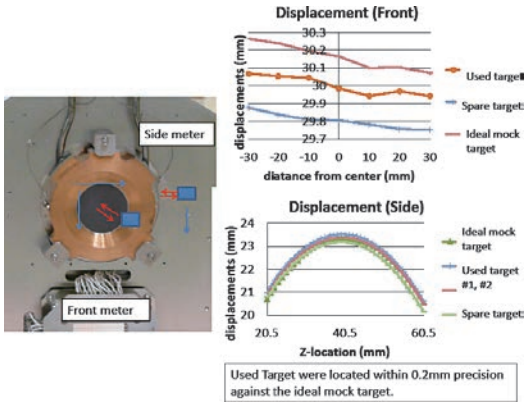

Figure 2. The result of the measurement for the positions of the used target and the spare target against the position of the mock target.

with a Gaussian distribution. The standard deviation of the distribution was approximately 4 mm on the horizontal direction and 3 mm on the vertical direction. Figure 3 demonstrates the integrated intensity of the 3-GeV proton beam. The integrated irradiation dose by the protons was evaluated through a Monte-Carlo simulation code, PHITS. The distribution of the dose followed the beam profile and complied with a Gaussian distribution as well. The maximum dose was 0.25 dpa at the center of the beam spot. The target temperature during the proton irradiation can be evaluated from thermal conductivities, which had been obtained in neutron irradiation, and it is supposed to be 470 K. The thermal diffusivities along a vertical line and a horizontal line going through the center of the muon target were measured every 1 mm. Furthermore, the thermal diffusivities on an area of 20 mm horizontally by 16 mm vertically were measured every 2 mm. Figure 4 demonstrates the thermal diffusivities along a vertical line and a horizontal line going through the center of the muon target. If decrement of the thermal diffusivity was proportional to the irradiation-dose, the decrement would also comply with a Gaussian distribution. However the thermal diffusivity on the center was higher than the one in the vicinity of the center. It can be considered as an annealing effect that smaller decrement of

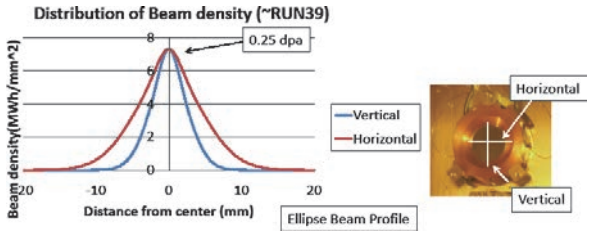

Figure 3. The integrated intensity of 3-GeV proton beam

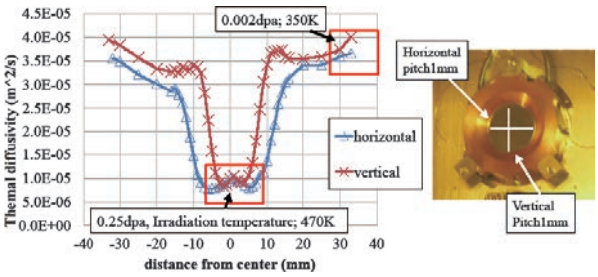

Figure 4. The thermal diffusivities along a vertical line and a horizontal line going through the center of the muon target.

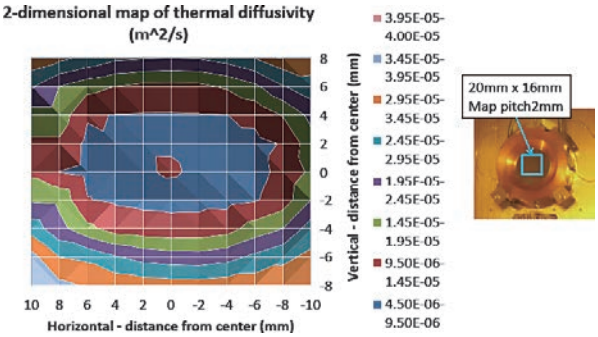

Figure 5. The distribution of the thermal diffusivities on the area of 20 mm horizontally by 16 mm vertically.

thermal diffusivity will occur under protons-irradiation at higher temperature. Figure 5 demonstrates the distribution of the thermal diffusivities on the area of 20 mm horizontally by 16 mm vertically. From these results, an ellipse-shaped distribution, which is similar to the beam profile, could be observed.

References

[1] H. Matsuo, graphite1991 [No.150] 290-302.
[2] http://www.bethel.co.jp/eng/index.html

S. Makimura[1,2], N. Kawamura[1,2], K.M. Kojima[1,2], A. Koda[1,2], A. Kurosawa[3], R. Shimizu[3], P. Strasser[1,2], J. Nakamura[1,2], and Y. Miyake[1,2]

[1]Muon Science Section, Materials and Life Science Division, J-PARC Center; [2]Institute of Materials Structure Science, KEK; [3]Nippon Advanced Technology Co. Ltd. (NAT)

Materials and Life Science Experimental Facility
Summary of 11 March 2011 Earthquake Damage and Recovery Action

	Damage	Recovery Action
Infrastructure and Utilities		
Electricity	• Total power loss to site • Displacement of high-voltage transformers (5 units)	• UPS and backup generators functioned as designed providing emergency power • Site power restored on 14 March • Low-voltage power to beamlines restored by the end of March • Transformers replaced/repaired and re-positioned…
Water supply and drainage	• Site water supply cut • Extensive damage to supply and drainage pipes caused by displacement and subsidence • Re-circulated cooling water knocked out – damage to heat exchange units	• Full water supply in the Tokai area resumed on 24 March • Re-circulated water restored for limited hours by end of May
Telecommunications	• Landline telephone system cut (On site and external mobile services working) • Web/email servers down	• Landline telephone system restored • KEK email server restored on 14 March. • JAEA email server restored on 22 March and JLAN on 23 March
Buildings and associated structures	• MLF building largely undamaged • Ground around the MLF building had subsided by ~1.5 m in places • Hendel Building sustained moderate damage to windows and shutters. The 2nd Floor corridor was impassable due to fallen debris • Large void space discovered under the floor of the MLF building in Nov 2011	• Remedial work on Hendel Building carried out immediately – full repairs ongoing • Under-floor voids of MLF building partially filled with concrete in Dec 2011 – some still remain and ground continues to settle
Roads and pathways	• Vehicle access to the MLF impossible due to subsidence of access roadway • Site-wide cracking, buckling and subsidence of roads and pathways	• Access routes required for recovery work repaired as top priority • Non-essential repair work will be carried out in the future
Facilities and Instruments		
Neutron target and moderators	• Target assembly displaced by 30 cm • Bellows attached to target vessel extended and destroyed • Air and water supply lines bent and broken • Components of the cryogenic hydrogen system outside the building shifted and damaged • Hydrogen supply lines damaged at the entry point to the MLF building	• Ventilation and air conditioning systems checked for damage and restarted during April 2011 • Broken air supply lines cut out for a temporary fix and normal operation restored in mid-May 2011. • Water lines re-connected to allow operation and full restoration completed in August • Target assembly removed and replaced
3NBT	• Entire tunnel displaced as foundation earthworks subsided by 20 cm • Sections of tunnel internal wall collapsed • Crane in tunnel severely damaged • Electromagnets and supporting structures undamaged but complete re-alignment required • Vacuum and cooling water plumbing damaged/ destroyed in some sections	• Electromagnets and supporting structures undamaged but complete re-alignment and re-conditioning required • Vacuum and cooling water systems repaired and replaced as needed • Full checks of all components carried out
Shutters	• 9 beamlines suffered loss of shutter vacuum (01, 03, 04, 05, 11, 14, 15, 16 & 19)	• Shutters and vacuum restored by the end of Sept 2012
Muon target	• No observable damage to edge-cooled graphite (fixed) target	• Target assembly removed to hot cell to be checked for changes in structural integrity and/or thermal conductivity • Found to be in operating condition and re-installed

	Damage	Recovery Action
Superconducting solenoid	• He leakage from the entire system – internal He pressure found to be 1 atm • Suspected internal damage	• Shielding removed and the solenoid disassembled for inspection • Some bolts found to be loose but the integrity of system confirmed • Re-assembled and re-installed
Refrigeration system	• Ground subsidence by 10 cm – 1.5 m outside MLF building caused damage to helium ducts, control and power cables and compressed air lines for superconducting magnet and on-line refrigerator system on the D-line • He buffer tank tilted 2-3 degrees	• All He ducts at the building boundary replaced and other damaged components repaired • Inspection of system in Sept 2011 • Stable operation of superconducting solenoid magnet achieved in Dec 2011
West Extension Building	• Entire structure displaced 4 cm to the north • Floor subsided by 14 cm at the expansion joint with the main MLF building • 1/500 slope from east to west	• All shielding and beamline/instrument components removed • The entire building jacked up to the original level and under-filled with supporting concrete over a 3-month period. Completed in August 2011.
Long (BL08) Building	• Entire structure moved to the north by 3 cm and the east by 5 cm • Floor subsided by 9 cm at expansion joint with MLF main building and 2.8 cm at 90 m point	• Decided not to re-position building but re-install beamline in new location • Under-floor voids created by earthquake filled with concrete
Shielding	• Over 2400 tonnes of shielding in more than 500 blocks displaced and in some cases damaged • Some overhead shielding on beamlines partially collapsed • Many shielding blocks tilted over • Positions of some choppers, guides and instruments shifted by the movement of shielding	• Almost all shielding blocks re-positioned • Brackets installed to improve stability in the event of another quake • Work completed in 3 months working in double shifts
BL01 *4SEASONS*	• Beam center was shifted by about 6 mm from the design position - probably due to misalignment of the guide tube • Crack in a concrete shielding block (Block size = 1530 mm x 842 mm x 365 mm)	• Confirmed that the shift in beam center would not severely affect most measurements • Re-alignment of guide tube will require major effort ⇒ postponed until next long shutdown • Replaced the damaged block with a new one in Nov 2011
BL02 *DNA*	• Concrete shielding blocks damaged • Surface of super mirror glass for neutron guide tube chipped after the assembly was dropped by workers when the earthquake struck	• Guide tube repaired with touch-up paint
BL03 *iBIX*	• Some shifting of equipment and 19-inch rack toppled over • No major damage	• 25 m guide tube alignment checked and neutron flux simulations performed No significant change to flux
BL04 *ANNRI*	• Lead shields around the spectrometers collapsed • LiH neutron shields damaged • Coaxial Ge and BGO detectors – part of the spectrometer – were damaged	• Lead and LiH shielding repaired and re-positioned • BGO detectors repaired • Coaxial Ge detectors will be repaired by the end of March 2013
BL05 *NOP*	• Supermirror guide inside shutter duct cracked • Control cables for beamline collimators crushed	• Super mirror guide replaced • Cables replaced
BL08 *S-HRPD*	• Guide tubes destroyed by collapsed shielding • Sample position subsided by 2.8 cm and shifted laterally by 1.25 cm (north) and 3.39 cm (east)	• Guide tubes in MLF building re-position and/or rotated • Repeated surveying required to determine recovery strategy (Sept and Nov 2011) • Determined to re-align beamline to the “new” sample position • Guide tube supports re-designed with greater adjustment range and re-installed • Disk choppers re-installed in Nov 2011 and guide tubes in Dec 2011 - Feb 2012 • Building boundary shielding re-designed and re-installed late Feb 2012 • Beamline shielding re-installed Mar 2012 • Temporary restoration completed and operations commenced end of Mar 2012

	Damage	Recovery Action
BL10 *NOBORU*	• Shielding blocks displaced by several mm • Beamline components on the shielding blocks were similarly displaced (downstream slits, filter exchanger, rotary collimator and vacuum duct)	• Beamline components re-aligned • Re-alignment completed at the end of March 2012
BL12 *HRC*	• ^{3}He detector bank damaged – 9 tubes lost • Shielding blocks displaced by several cm • Fermi chopper toppled over	• Tubes replaced and detector restored in December 2011 • Shielding blocks and beamline components re-aligned in July 2011
BL14 *AMATERAS*	• 20+ concrete shielding blocks damaged • Sample mount flange damaged after falling	• Concrete shielding repaired with mortar • Damaged flange repaired by internal engineering staff
BL15 *TAIKAN*	• Damage to shielding interlock due to ~50 cm displacement of movable shield	• Damaged interlock replaced • Stopper installed to secure movable shield to the main shield when closed
BL16 *SOFIA*	• A hatch made of concrete blocks was displaced causing the breakage of an interlock key. • Equipment for controlling sample environment (Langmuir trough) damaged.	• The hatch was re-positioned and fixed in place by a stopper • The damaged equipment was replaced with newly-purchased items
BL17 *SHARAKU*	• Displacement of beamline components • Several Shielding blocks damaged	• All beamline components dismantled and realigned • Damaged shielding blocks re-fabricated and re-installed
BL18 *SENJU*	• Displacement of the entire instrument • Shielding blocks on the boundary between the 2nd and 3rd Experimental Halls tilted and some severely damaged • Due to horizontal shift of the 3rd Experimental Hall fiducial marks unusable	• All beamline components dismantled and removed • Damaged shielding blocks were re-fabricated • All beamline components in the 3rd Hall reconstructed • New fiducial points in the 3rd Hall surveyed and marked out • Supermirror neutron guides removed and re-aligned • Instrument reconstructed
BL19 *TAKUMI*	• Shielding at the boundary between the MLF and satellite buildings tilted over due to subsidence • 4 m sections of guide including the support structures inside the shielding destroyed • Bolts holding detector frames snapped and the frames hit the sample table	• Shielding, guides and spectrometer dismantled and removed. • Building jacked up and reset • Damaged components repaired or replaced and re-installed • Beamline and instrument largely restored by end Feb 2012 • Re-commissioning began 6 Mar 2012
BL20 *iMATERIA*	• Front-end shielding collapsed • Beam dump and vacuum exhaust equipment tilted over due to subsidence of the 3rd Expt. Hall	• Guide tube removed to create work space • Shielding re-positioned with added reinforcement • Guide tube re-installed and re-aligned • Beam dump and vacuum exhaust components removed and re-installed after building restoration completed
BL21 *NOVA*	• Almost undamaged • Displacement of shielding blocks • Interlock pin of the shielding ceiling hatch broken	• Shielding blocks re-positioned • Interlock pin replaced and a fixing pin attached to prevent movement in any future tremors

Science Highlights

Pulsed Neutrons Light up the Hydrogen-Bond Network and the pH Sensitivity in Human Transthyretin

Introduction

Transthyretin (TTR) is a tetrameric human plasma protein (molecular mass 55 kDa) composed of identical 127-residue subunits, each having a β-sheet structure. TTR plays a major role in the transport of thyroxine and retinol, the latter via the TTR-retinol binding protein complex. TTR composes the amyloid fibrils found in patients afflicted with either familial amyloidotic polyneuropathy (FAP) or senile systemic amyloidosis (SSA).

The presented evidence indicates that it relies on dissociation of the tetramer, which is facilitated under mild denaturing conditions, followed by misfolding and misassembly of dissociated forms to generate amyloid fibrils. Remarkably, it has been found that *in vitro* an acidic medium promotes TTR fibrillogenesis, and that the extent of amyloid fibril formation is enhanced for amyloidogenic mutant TTR. In order to investigate the structural explanation for the pH-dependent effects and structural stability of TTR, time-of-flight neutron protein crystallography was performed using BL 03 (iBIX). In this article, the hydrogen-bond network and pH sensitivity of human transthyretin related to the amyloidosis are described [1].

Neutron diffraction experiments at BL 03 (iBIX).

The large deuterated crystals were prepared by sitting drop vapor-diffusion method at pD 7.4 (Fig. 1a). Neutron diffraction data were collected at BL 03 (iBIX). To complete the data, 41 data sets were collected using wavelength ranging from 2.7 to 6.7 Å. The exposure times were 22 hours for each set at 120 kW J-PARC accelerator and 12 hours at 220 kW. The neutron crystal structure of TTR were determined at 2.0 Å resolution with an R_{factor} of 23.4%. The protonation states and the direction of the water molecules were determined by difference Fourier density at the position of deuterium atoms in which the target residue was omitted (Fig. 2).

Hydrogen-bond network and pH sensitivity

The neutron crystal structure at pD 7.4 revealed the detailed hydrogen-bond network depending on the protonation states of H88 (Fig. 2). This hydrogen-bond network is composed of T75, W79, H88, S112, P113, T118-B and four water molecules. The W79, H88, S112 and P113 residues were located at the dimer-dimer interface (subunit A and D), while the H88 and T118-B were located at the monomer-monomer interface (subunit A and B). At neutral pD (pD 7.4), neutron scattering length density map clearly showed that H88 was single protonated. These results suggest that the full protonation of H88 by the acidic pH probably breaks this hydrogen-bond network and destabilizes both the tetramer and the dimer.

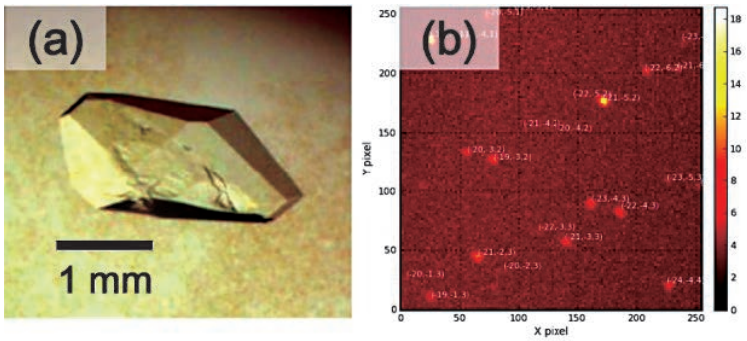

Figure 1. (a) TTR crystal grown up to 2.5 mm^3. (b) TOF neutron diffraction image showing from 3.16 to 5.03 Å resolution range.

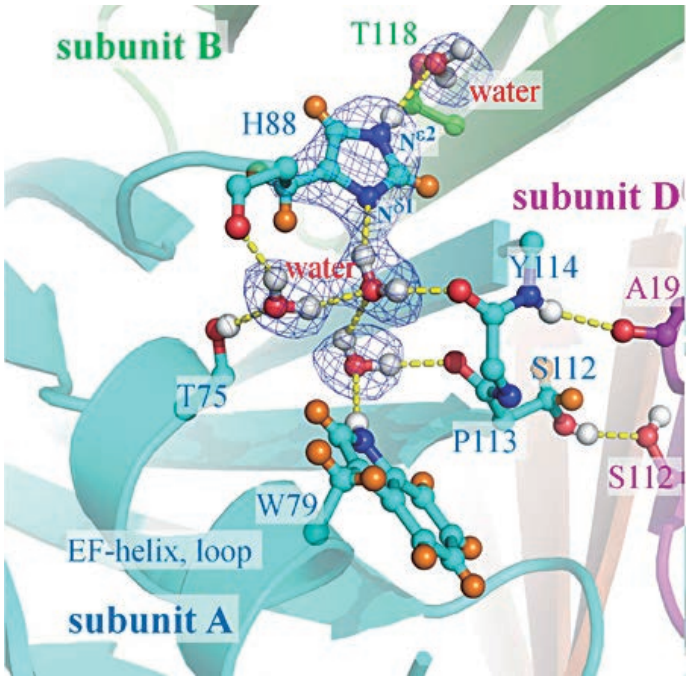

Figure 2. The $|F_o|$-$|F_c|$ difference neutron scattering length density map calculated omitting H88 and water molecules. The dashed yellow lines indicate the hydrogen bonds.

Furthermore, the structural comparison with X-ray crystal structure at pH 4.0 (PDB code 3D7P) revealed that the hydrogen-bond network involving H88 disappeared at pH 4.0. The structural destabilization caused by the lowered pH can be accounted for by the full protonation of H88. This is the first crucial piece of information on the way to elucidate the atomic details of amyloid fibril formation.

Conclusion

In conclusion, the neutron structure of TTR provides the first picture of the hydrogen-bond networks and protonation states in human TTR. Our structural analysis reveals a wealth of information about the hydrogen bonds at the subunit-subunit interface and the pH sensitivity in TTR. This information can be utilized to study the molecular stabilities and pH sensitivities in amyloidogenic TTR variants. The neutron crystal structure including hydrogen atoms could be useful for *in-silico* drug screening in terms of calculation of the accurate binding free energy. In addition, the present study demonstrates that neutron protein crystallography is a powerful method for studying hydrogen bonds and pH sensitivities in proteins.

References

[1] T. Yokoyama *et al.*, J. Struct. Biol. **177** (2012) 283.

T. Yokoyama[1], M. Mizuguchi[1], Y. Nabeshima[1], K. Kusaka[2], I. Tanaka[2], and N. Niimura[2]
[1]Facluty of Pharmaceutical Sciences, University of Toyama; [2]Frontier Research Center for Applied Atomic Sciences, Ibaraki University

Spin wave Measurements over the Full Brillouin Zone of Multiferroic $BiFeO_3$

Multiferroic materials, where the magnetic order and ferroelectric polarization coexist, are one of the most sought-after topics in the condensed matter physics [1]. The current intense interest on such materials is driven not only by the intellectual desire but also by its immense potential for future applications.

$BiFeO_3$ is arguably one of the most interesting multiferroic compounds with both ferroelectric and magnetic transitions above room temperature: with an antiferromagnetic transition temperature at T_N=650 K and a ferroelectric transition temperature at T_C=1100 K [2,3], exhibiting very large polarization value, ~100 μC/m^2 [4]. In addition, an incommensurate structure is formed with an extremely long period of 620 Å when it undergoes an antiferromagnetic ordering at 650 K [3], Despite the numerous reports of the unusual phenomena found in $BiFeO_3$, the underlying microscopic spin Hamiltonian is not well established yet.

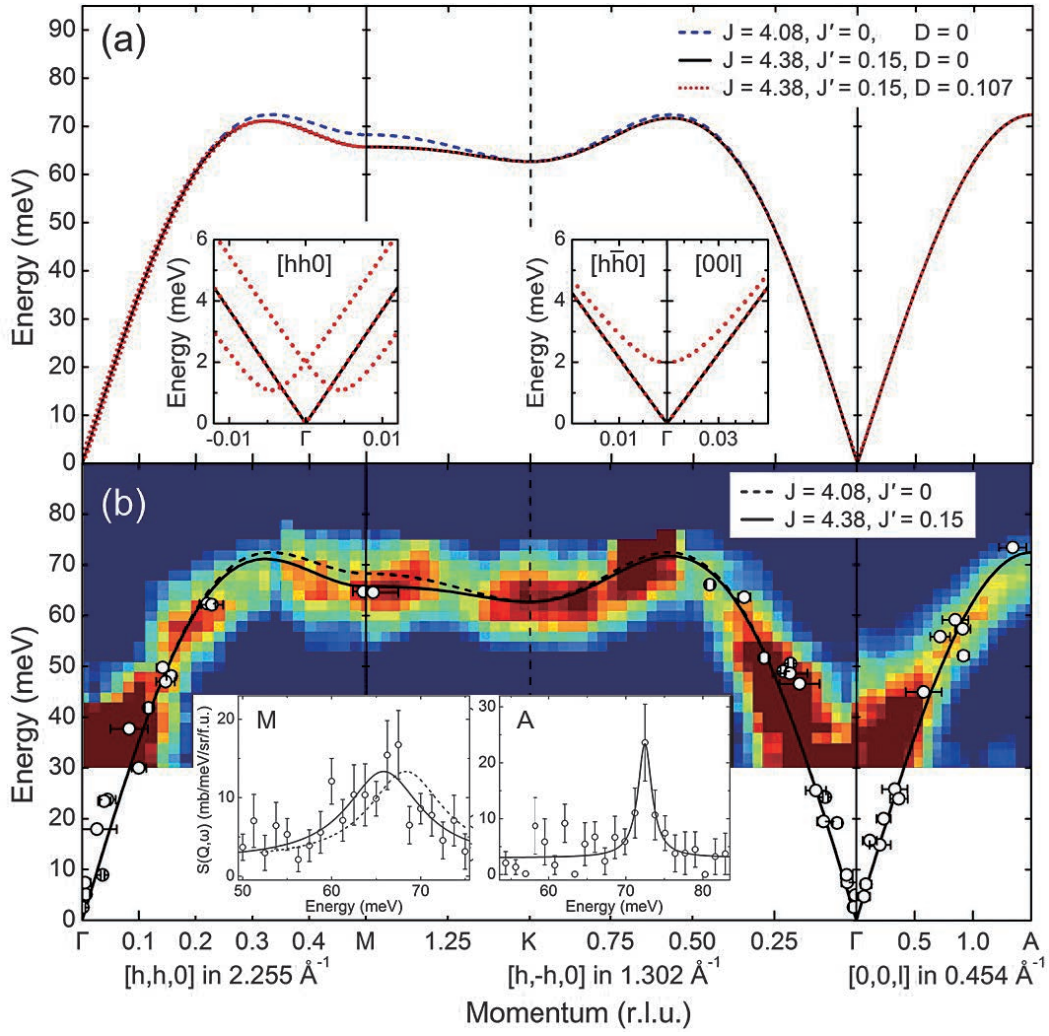

Figure 1. (a) Theoretical spin waves calculated with three different Hamiltonians. (b) Experimental spin waves measured at AMATERAS of J-PARC (circles) and MERLIN of ISIS (contour plot) together with the theoretical spin waves (solid line) calculated with *J*=4.38 and *J'*=0.15 meV.

We have grown several high quality single crystals and aligned ten crystals with a total mass of 1.9 g. Using these samples, we have carried out inelastic neutron scattering experiments with two time-of-flight spectrometers: one is AMATERAS at the J-PARC, Japan and another MERLIN at the ISIS, UK.

We started with a minimal Heisenberg Hamiltonian only with the nearest neighbor (NN) interaction, and then extended it to explain the measured dispersion curve by including the next nearest neighbor (NNN) interaction and a Dzyaloshinskii-Moriya-like term as the following model Hamiltonian:

$$H = J\sum_{NN}\mathbf{S}_i\cdot\mathbf{S}_j + J'\sum_{NNN}\mathbf{S}_i\cdot\mathbf{S}_j - \mathbf{D}\cdot\sum_i\mathbf{S}_i\times\mathbf{S}_{i+\delta},$$

for the magnetic unit cell of the G-type structure. The third term describes a Dzyaloshinskii-Moriya-like interaction with $i+\delta$ representing the next nearest neighbor of site i along the [1 1 0] direction: $\mathbf{D}$ is parallel to the chiral vector [1 -1 0]. By carefully examining the data, we succeeded, for the first time, in measuring the full spin waves of $BiFeO_3$ and determined the two most important exchange parameters, which are the nearest and next nearest neighbor interactions: J=4.38 and J'=0.15 meV, respectively [5]. Surprisingly enough, a simple spin Hamiltonian with these two exchange interactions explains the measured spin waves. We further estimated an effective Dzyaloshinskii-Moriya interaction: D=0.107 meV for the incommensurate magnetic structure. Our results provide the microscopic parameters for the spin waves of $BiFeO_3$, the key to a deeper understanding of the physical properties.

References

[1] S.-W. Cheong and M. Mostovoy, Nature Mater. **6** (2007) 13.

[2] J. R. Teague *et al.*, Solid State Commun. **8** (1970) 1073.

[3] I. Sosnowska *et al.*, J. Phys. C **15** (1982) 4835.

[4] J. Wang *et al.*, Science **299** (2003) 1719.

[5] J. Jeong *et al.*, Phys. Rev. Lett. **108** (2012) 077202.

J. Jeong[1], E.A. Goremychkin[2], T. Guidi[2], K. Nakajima[3], G.S. Jeon[4], S. Kim[5], S. Furukawa[6], Y.B. Kim[6], S. Lee[7], V. Kiryukhin[8], S-W. Cheong[8], and Je-Geun Park[1,9]

[1]*FPRD Department of Physics & Astronomy, Center for Strongly Correlated Materials Research, Seoul National University;* [2]*ISIS Facility, STFC Rutherford Appleton Laboratory;* [3]*Neutron Science Section, Materials and Life Science Division, J-PARC Center;* [4]*Department of Physics, Ewha Womans University;* [5]*Neutron Science Division, Korea Atomic Energy Research Institute;* [6]*Department of Physics, University of Toronto;* [7]*Neutron Science Division, Korea Atomic Energy Research Institute;* [8]*Rutgers Center for Emergent Materials and Department of Physics and Astronomy, Rutgers University;* [9]*Center for Korean J-PARC Users, Seoul National University*

Characterization of Swollen Brush Structure in a Solvent by SOFIA Reflectometer

Introduction

Polymer brushes are surface- tethered polymers on a solid surface with sufficiently high grafting density, which are applicable in colloid stabilization, wettability, antifouling, adhesion, and tribology. In particular, the polyelectrolyte brushes participate in the water lubrication of biological surfaces like articular cartilages of mammalian joints. Therefore, it is an essential study to characterize the thickness of swollen or collapsed brush structure and the segment density profile at solid/ liquid interfaces [1]. Neutron reflectivity (NR) measurement is quite useful for in situ determination of static structures at the solid/ liquid interface in the nanometer length scales.

SOFt Interface Analyzer (SOFIA) reflectometer in MLF is a horizontal type neutron reflectometer constructed by the collaboration of JST ERATO Takahara Soft Interfaces Project and KEK-IMSS [2,3]. We conducted NR measurement at D_2O/ polyelectrolyte brush interface by SOFIA to obtain the depth-profile of swollen brush structure [4].

Experiments

A hydrophilic poly[{2-(methacryloyl- oxy)ethyl}trimethylammonium chloride] (PMTAC) brush [5] was prepared by surface-initiated atom transfer radical polymerization from alkyl bromide-grafted silicon disk with 3-inch diameter and 10-mm thickness. The number of the average molecular weight of PMTAC was 110,000 g/mol. The incident neutrons were irradiated through the Si disk and reflected at the D_2O/ Si substrate interface as shown in Figure 1.

Results

Figure 2(a) shows the NR curves of the PMTAC brush interfaces in air and D_2O, and (b) the corresponding neutron scattering length density (SLD) profiles along with the distance from the Si substrate surface. Although the SLD of PMTAC was relatively low as 0.75×10^{-4} nm^{-2} due to non-deuterated polymer, the thickness of the brush film under atmosphere conditions (50% relative humidity at 298 K) was determined to be 29.0 nm from the periodic fringes.

On the other hand, NR of PMTAC brush in D_2O showed indistinguishable fringes, however, the specular reflection was measured down to 10^{-6} in reflectivity and up to 2.0 nm^{-1} in q using white neutrons with a wavelength range of 0.20 – 0.88 nm. The SLD profile of the PMTAC brush in D_2O was a smooth upward curve from 4.1×10^{-4} nm^{-2} at Si substrate surface to 6.38×10^{-4} nm^{-2} along with the distance from the substrate. SLD curve of the brush approached SLD_{D2O} at ca. 50 nm from the surface. The gradient profile indicated that the polymer chains in D_2O were stretched up to ca. 50 nm and relatively extended in the direction normal for the substrate.

However, the NR profile showed the specular reflection at q = 0.8 - 2.0 nm^{-1}, which indicated the presence of dense layer with 2-nm thick on Si substrate surface. PMTAC chains near the Si surface might be confined strongly to form the dense layer [6]. We assumed that the PMTAC brush adopted a two-region structure consisting with some thin and dense surface region and a brush region that

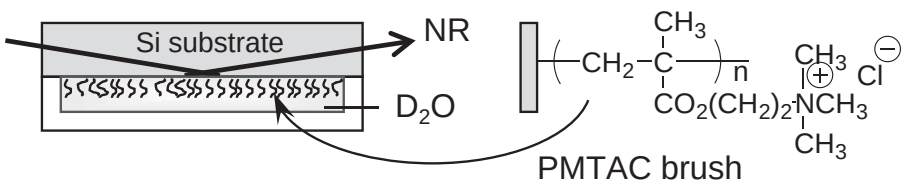

Figure 1. Schematic view of NR measurement of D_2O/ brush interface and chemical structure of PMTAC brush.

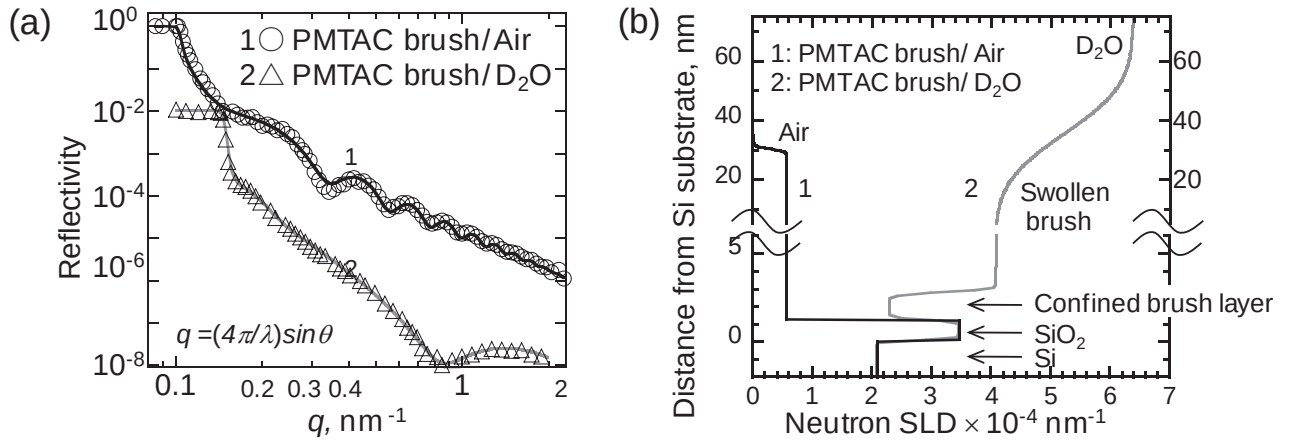

Figure 2. (a) NR curves of PMTAC brush interfaces in air (open circles) and D_2O (open triangles), and (b) the corresponding neutron SLD profiles along with the distance from the silicon surface.

stretches away from the substrate.

Owing to the high flux and low background noise even at high *q* range of the SOFIA reflectometer, a migrated thin layer with nano-meter thickness at solid/liquid interface was clearly observed. These findings will contribute to the understanding of unique behaviors, such as adhesion and frictions, of polyelectrolyte brushes in aqueous solution with various ionic strengths.

References

[1] M. Kobayashi *et al*., Soft Matter **3** (2007) 740.

[2] K. Mitamura *et al*., J. Phys. Conf. Ser. **272** (2011) 012017.

[3] N. L. Yamada *et al*., Euro. Phys. J. Plus **126** (2011) 108.

[4] K. Mitamura *et al*., Polym. J. in-press.

[5] M. Kobayashi *et al*., Macromolecules **43** (2010) 8409.

[6] I. E. Dunlop *et al*., Langmuir **28** (2012) 3187.

M. Kobayashi[1], H. Arita[2], N.L. Yamada[3,4], H. Jinnai[1,5,6], and A. Takahara[1,2,5,6]

[1]JST ERATO Takahara Soft Interfaces Project; [2]Graduate School of Engineering, Kyushu University; [3]Neutron Science Section, Materials and Life Science Division, J-PARC Center; [4]Institute of Materials Structure Science, KEK; [5]Institute for Materials Chemistry and Engineering, Kyushu University; [6]WPI-I2CNER, Kyushu University

Neutron Diffraction in 40 T Pulsed High Magnetic Fields at MLF J-PARC

Introduction

In high magnetic fields, various exotic states are induced. Magnetic order parameters and key characteristics of such phases can be examined precisely by neutron diffraction. A magnetic field of 20 T is the maximum of superconducting magnet for neutron diffraction and thus pulsed magnets are needed to access the field above this limit. Here, we report the achievement of the world's highest pulsed magnetic field for neutron diffraction and its application to a multi-ferroic compound.

Capacitor Bank and Magnet

Pulsed magnetic fields are generated by the capacitor bank method. The system consists of a 50 T pulsed magnet, a 250 kJ capacitor bank and a cryostat. Figure 1 shows the capacitor bank set at the BL10-Noboru spectrometer. The volume of the bank is about 11 m^3. The energy stored in the capacitor is discharged into the coil synchronizing with the neutron pulses.

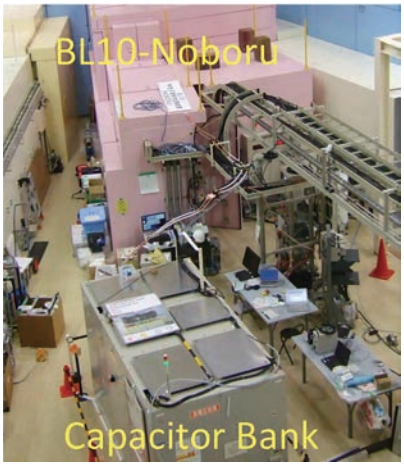

Figure 1. 250 kJ Capacitor bank set at MLF.

The solenoid magnet designed in collaboration with Kindo group at ISSP is shown in Fig. 2. High strength Ag-Cu alloy wire is used as a conductor. The outer side is supported by a ring made of Mar-aging steel. The magnet is set in horizontal direction and is cooled by liquid nitrogen. A temperature as low as 1.6 K is possible to reach by using a specially designed cryostat. The open aperture of the magnet in cryostat is 24 degrees.

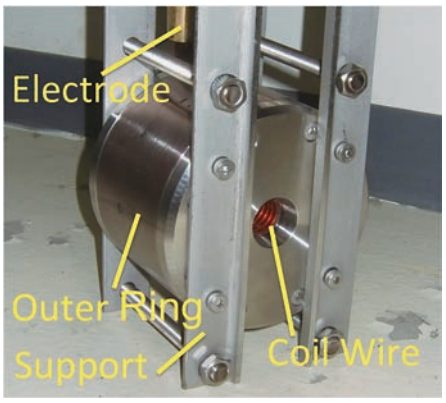

Figure 2. 50 T solenoid coil.

Figure 3 shows the waveform of the generated pulsed field. A pulse width is about 5 msec in symmetric mode and is about 10 msec in damping mode with a crowbar circuit.

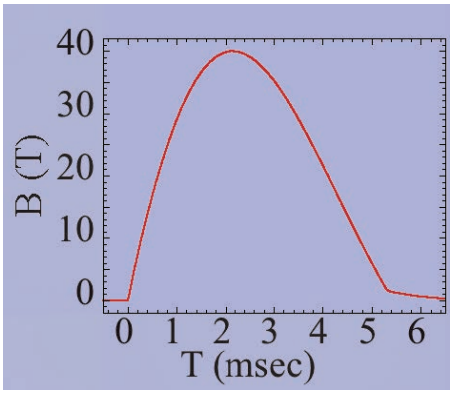

Figure 3. Waveform of a pulsed field.

Example of Laue Method Diffraction

In case of a pulsed white neutron source, the Laue method can be used to scan a wide range in reciprocal space [1]. As shown in Fig. 4, the time dependence of the diffraction pattern is measured by using a white

neutron beam. Note that the wavelength and the magnetic field intensity are related to each other by the time of flight (TOF). Hence, each pattern is taken at certain magnetic field intensity. In the pulsed magnetic field, the magnetic field dependence of the Laue pattern is measured as the time dependent "Laue movie".

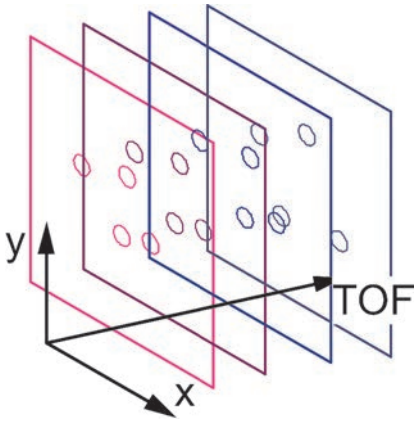

Figure 4. Schematic view of the Laue method. X and y show the axis of an area detector.

Figure 5 shows the two-dimensional pattern spanning with TOF and the vertical scattering angle. These data are captured by a single position sensitive detector set along the vertical direction with a fixed horizontal scattering angle. Several Bragg peaks are measured simultaneously in the time-dependent magnetic field. Note that the field is time dependent along the TOF axis and constant along the scattering angle.

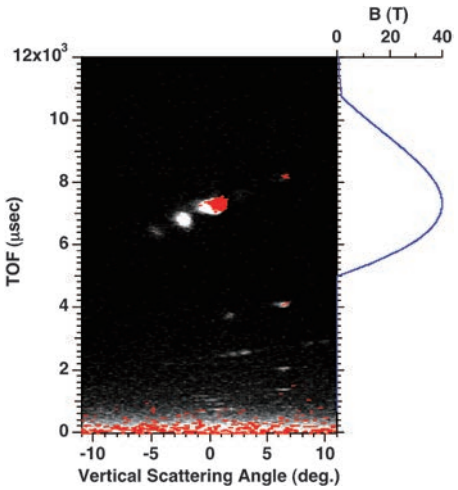

Figure 5. Two dimensional plot of data taken for multi-ferric $TbMnO_3$. The white and red are the data at zero field and at 40 T magnetic field maximum.

It has been discovered that some of the peaks disappear in high magnetic fields and some show shifts in positions. Such multi-peak scan is the advantage of using a pulse neutron source. The present result shows that a neutron diffraction experiment becomes possible for real samples at 40 T because of the strong instantaneous intensity of the J-PARC neutron beam.

References

[1] Nojiri *et al.* Phys. Rev. Lett. **106** (2011) 237202.

H. Nojiri[1], Y. Narumi[1], S. Yoshii[1], T. Morioka[1], M. Baker[1], M. Harada[2], K. Oikawa[2], F. Maekawa[2], and K. Nakajima[3]

[1]Institute of Materials Research, Tohoku University; [2]Neutron Source Section, Materials and Life Science Division, J-PARC Center; [3]Neutron Science Section, Materials and Life Science Division, J-PARC Center

Magnetic Excitation Spectra of Superconducting $Ca_{10}Pt_4As_8(Fe_{1-x}Pt_xAs)_{10}$ (x~0.20)

The multiband nature of Fe-based superconductors is a significant characteristic that differentiates them from high–T_c Cu oxides. Keeping that in mind, we have been working to see whether the superconductivity in Fe pnictides has a new pairing mechanism related to this multiband nature (or to the orbital degrees of freedom).

Up to now, a number of papers have been published suggesting that the magnetic mechanism similar to that of Cu-oxides is primarily important for the occurrence of the superconductivity of Fe-based systems, and that the so-called $S_{\pm}$ symmetry with the sign reversal of the order parameters Δ between two disconnected Fermi surfaces around Γ [=(0, 0)] and (0.5, 0) ($\equiv Q_M$) points in the reciprocal space is realized [we use the 2-D unit cell of FeAs square lattice with one Fe atom within a cell, where the Q_x axis in the reciprocal space is defined along the Fe-Fe direction]. On the other hand, if the orbital fluctuation mechanism, which may arise from the orbital degrees of freedom is important, we do not expect the sign reversal (S_{++} symmetry).

To investigate which of the symmetries $S_{\pm}$ and S_{++} is realized, we have paid attention to three kinds of physical quantities sensitive to the sign reversal, that is, effects of nonmagnetic impurities on T_c, magnetic excitation spectra and NMR $1/T_1$ have been carefully studied on $LnFeAsO_{1-x}F_x$ or so-called Ln1111 system (Ln=La and Nd).

One remarkable result we found at the very early stage of the study is that the T_c-suppression rates are much smaller than those expected from the pair breaking effect of nonmagnetic impurities in systems with the $S_{\pm}$ symmetry of Δ [1]. It suggests the existence of a new pairing mechanism [1, 2], because it is strongly against the magnetic mechanism and because the ordinary phonon mechanism cannot realize the maximum T_c value of ~55 K observed for $NdFeAsO_{1-x}F_x$.

Measurements of magnetic excitation spectra $\chi''(\boldsymbol{q}, \omega)$ by neutron inelastic scattering can present a different method to distinguish the symmetries of $S_{\pm}$ and S_{++}: According to the simple calculation [3], the spectra $\chi''(\boldsymbol{Q}_M, \omega)$ of systems with $S_{\pm}$ symmetry of Δ exhibit a sharp resonance peak at ω equal to or slightly *smaller* than $|\Delta_\Gamma|+|\Delta_M|$ in the superconducting state, where Δ_Γ and Δ_M are the Δ values on Fermi surfaces around Γ point and around $\boldsymbol{Q}_M$, while such a peak does not appear for the S_{++} symmetry. Experimentally, there are many publications which report observations of the "resonance-like" peak in $\chi''(\boldsymbol{q}, \omega)$. However, the peaks do not seem to be as sharp as those expected for the $S_{\pm}$ symmetry of Δ. Moreover, if the observations are the evidence for the $S_{\pm}$ symmetry, they contradict the small rates of T_c-suppression by nonmagnetic impurities. On this point, Onari *et al*. [4] pointed out, by considering a different mechanism from that of ref. 3, that even for the S_{++} symmetry, the peak in $\chi''(\boldsymbol{Q}_M, \omega)$ with larger energy broadening than that of ref. 3 can be expected in the region slightly *larger* than $|\Delta_\Gamma|+|\Delta_M|$. Therefore, it was highly desirable to carry out careful study of $\chi''(\boldsymbol{Q}_M, \omega)$ to judge whether the change of the spectral shape induced by the superconductivity really indicates the $S_{\pm}$ symmetry of Δ.

Here, the measurements have been carried out with the spectrometer 4SEASONS (BL-01) installed at J-PARC on a single crystal (~4.5 g) of $Ca_{10}Pt_4As_8(Fe_{1-x}Pt_xAs)_{10}$ (x~0.20) with T_c~30 K, where the crystal was set on the Al sample holder with the *c* axis parallel to the incident neutron beam and cooled down by using the He exchange gas. The incident neutron energy of 40.4 meV was mainly used. The energy resolution was ~1.7 meV at the neutron transfer energy ΔE~10 meV. Readers can find other details in refs. 2 and 5. In arguing the data, we paid attention to the shape of the "resonance-like" peak in the Q-ω space.

In Fig. 1, the map of the magnetic scattering intensity $S(\boldsymbol{Q}, \omega)=(n+1)\chi''(\boldsymbol{Q}, \omega)$ collected through the ΔE window of 11 meV<$\Delta E(=\omega)$<14 meV at T=4

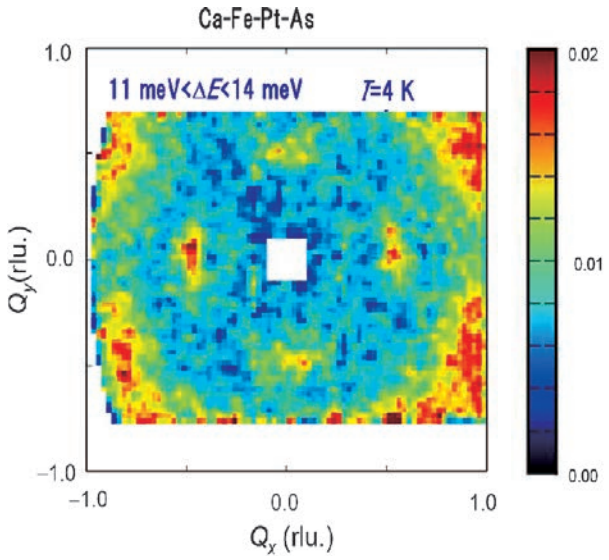

Figure 1. Intensity map of the magnetic scattering in the a^*-b^* plane of $Ca_{10}Pt_4As_8(Fe_{1-x}Pt_xAs)_{10}$ (x~0.20).

K is shown in the (Q_x-Q_y) plane of $-1.0<Q_x, Q_y<1.0$, where n is the Bose factor. We can see the intensity peaks at (Q_x, Q_y)=(0.5, 0) and other equivalent points as reported commonly to many other Fe-based superconductors. [Although in the actual measurement, the Q_z value depends on ΔE for each (Q_x, Q_y) point, we do not show it explicitly for the present quasi two dimensional system.] The peak widths along the Q_x- and Q_y-directions are different from each other, as reported for Ba122 and Ca122 systems. We do not see any other meaningful peak structure in this figure.

Figure 2 shows the neutron scattering intensities collected with the window of 10 meV<ΔE <14 meV by the Q_x scan through Q=($\pm$0.5, 0) at various fixed T values. The Q_y windows are shown in the figure. (Data taken with different Q_y windows are so scaled as to show the intensities per unit value of Q_y width, δQ_y.) In Fig. 3. the spectra $\chi''(\boldsymbol{Q}_M, \omega)$ are shown against ΔE above the backgrounds (dotted line; It was found to be T- and ΔE -insensitive in the region ΔE >5 meV) at several fixed T values.

After showing the above data as examples of data series collected with various window-widths, $\delta\boldsymbol{Q}$ and $\delta\Delta E$, we note here the following. (1) Both the Q_x- and ΔE-widths do not depend on the window widths or resolutions, that is, they are intrinsic values. We stress here, in particular, that the energy width of the peak of the $\chi''(\boldsymbol{Q}_M, \Delta E)$ curve is much larger even at $T<<T_c$ than the resolution width shown by the horizontal bar in Fig. 3. We argue this point again below. (2) The Q_x-width and peak intensity at Q_M do not exhibit significant anomalous behavior at T_c. (3) The peak energy of the $\chi''(\Delta E)$- ΔE curve is ~12 meV. Although it should be compared with the value of $|\Delta_\Gamma|+|\Delta_M|$, it is not easy to find reliable gap values at this moment.

Concerning the Q_x- and ΔE-widths of the peak of $\chi''(\boldsymbol{Q}_M, \Delta E)$, we presume the following: Let us consider systems with nonmagnetic impurities. Because it can be considered to have a Hamiltonian with time-reversal symmetry, Cooper pairs in such

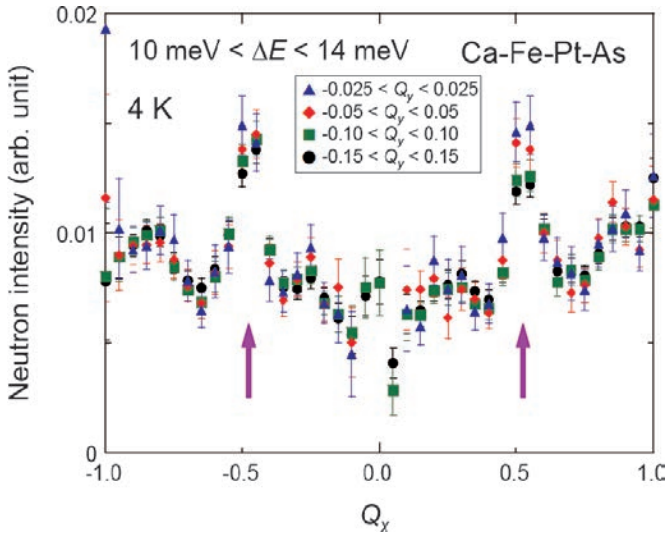

Figure 2. Neutron counts obtained at 4 K by the Q_x scan. The Q_y regions of the data collection are shown in the figure. 10 meV<ΔE<14 meV.

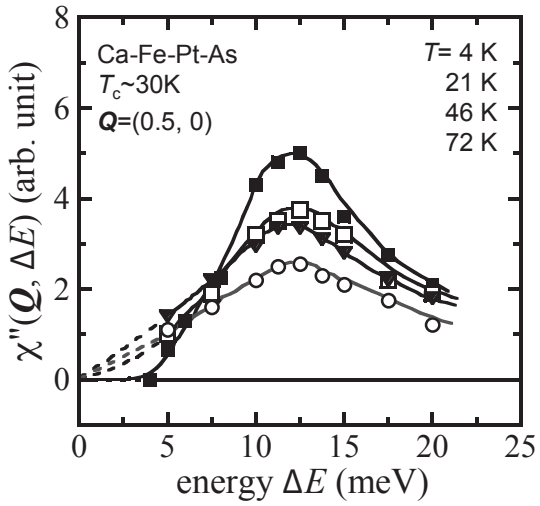

Figure 3. $\chi''(\boldsymbol{Q}, \omega)$ observed at $Q=Q_M$ (=0.5, 0) are plotted against ΔE (=ω) at several T values.

systems consist of two quasi particles which have same eigen energies (consider the Anderson theorem). However, these quasi particles are not in the momentum eigen states. Therefore, the spectra $\chi''(\boldsymbol{Q}, \Delta E)$ automatically have the broadening in the momentum space, but do not in the energy space, unless the localization effects become significant. It suggests that the peak should be sharp if the symmetry is $S_{\pm}$, which does not agree with the observation. The present arguments are consistent with the nonexistence of the pair breaking effects by nonmagnetic impurities and seem to support the S_{++} symmetry.

References

[1] M. Sato, Y. Kobayashi, S. C. Lee, H. Takahashi, E. Satomi, and Y. Miura, J. Phys. Soc. Jpn. **79** (2010) 014710.

[2] M Sato, and Y Kobayashi, Solid State Commun. Special Issue on Iron pnictides **152** (2012) 688..

[3] T. A. Maier and Scalapino: Phys. Rev B **78** (2008) 020514.

[4] S. Onari, H. Kontani, and M. Sato: Phys. Rev. B **81** (2010) 060504 (R).

[5] M. Sato, T. Kawamata, Y. Kobayashi, Y. Yasui, T. Iida, S. Suzuki, M. Itoh, T. Moyoshi, K. Motoya, R. Kajimoto, K. Nakamura, Y. Inamura, and M. Arai: J. Phys. Soc. Jpn. **80** (2011) 093709.

M. Sato[1,2,3], T. Kawamata[2,3], Y. Kobayashi[2,3], Y. Yasui[2,3], T. Iida[2], K. Suzuki[2], M. Itoh[2,3], T. Moyoshi[2], K. Motoya[2,3], R. Kajimoto[1], M. Nakamura[4], Y.Inamura[4], and M. Arai[3,5]

[1]CROSS-Tokai; [2]Department of Physics, Nagoya University; [3]JST TRIP; [4]Neutron Science Section, Materials and Life Science Division, J-PARC Center; [5]Materials and Life Science Division, J-PARC Center

A New Solid Electrolyte $Li_{10}GeP_2S_{12}$ for Li-Ion Batteries

From the point of view of improving the safety of the lithium-ion batteries, the non-flammable solid electrolytes have the promising potential to replace the currently used liquid organic electrolytes. Although the advantages of solid electrolytes are widely acknowledged, their low ionic conductivities prevent them from being used in practical applications.

In the search for new materials for solid electrolytes over the past few decades, crystalline, glassy and polymer systems were studied. Despite these efforts, the lithium nitride Li_3N, discovered in 1970s, still has the highest ionic conductivity of 6 x 10^{-3} $\Omega^{-1}cm^{-1}$. Unfortunately, however, its low electrochemical decomposition potential prevents it from being used in practical applications. Other systems currently investigated as potential battery electrolytes are crystalline materials ($La_{0.5}Li_{0.5}TiO_3$, $Li_{3.25}Ge_{0.25}P_{0.75}S_4$) and glassy materials ($Li_7P_3S_{11}$, Li_2S-SiS_2-Li_3PO_4); all these materials exhibit ionic conductivities of the order of 10^{-3} $\Omega^{-1}cm^{-1}$, which is lower than that of Li_3N. Polymer electrolytes are complexes of lithium salt and high-molecular-weight polymers, but they have low conductivities of $\sim 10^{-5}$ $\Omega^{-1}cm^{-1}$. None of these materials has conductivities comparable to those of the currently used liquid organic electrolytes of the order of 10^{-2} $\Omega^{-1}cm^{-1}$.

Recently a new lithium superionic conductor $Li_{10}GeP_2S_{12}$ exhibiting an extremely high lithium ion conductivity of 1.2 x 10^{-2} $\Omega^{-1}cm^{-1}$ was discovered by researchers of Tokyo Institute of Technology and Toyota Motor Corporation, and its crystal structure was determined in cooperation with the researchers of KEK. The structure analysis was carried out using the high-resolution neutron powder diffractometer SuperHRPD installed at J-PARC. The crystal structure is shown in Fig. 1a. The structure is tetragonal (space group $P4_2/nmc$) with lattice parameters of $a = b = 8.7177$ Å and $c = 12.6345$ Å. The structure is a three-dimensional framework structure consisting of $(Ge_{0.5}P_{0.5})S_4$ tetrahedra, PS_4 tetrahedra, LiS_6 octahedra and LiS_4 tetrahedra. Figure 1b shows a framework structure composed of $(Ge_{0.5}P_{0.5})S_4$ tetrahedra, LiS_6 octahedra and PS_4 tetrahedra. Figure 1c shows one-dimensional (1D) chains of LiS_4 tetrahedra along the *c* axis. Lithium ions at the 16*h* and 8*f* sites in LiS_4 tetrahedra (Fig.1c) are considered to participate in ionic conduction and form the 1D conduction pathways. These 16h and 8f sites were found to be occupied by 69 and 64% of Li, respectively; the result indicates partial distribution of lithium ions on the conduction pathway, which is a common characteristic of the superionic conductors.

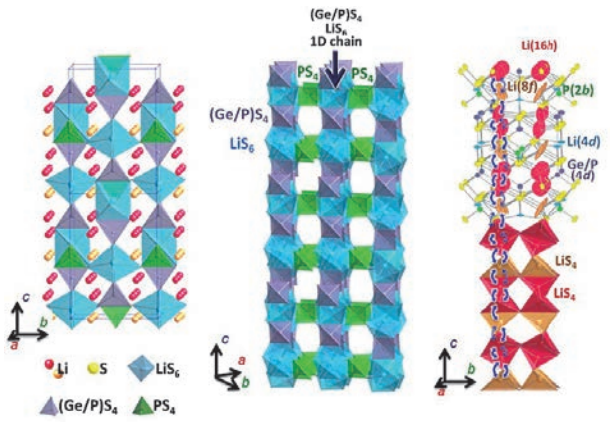

Figure 1. (a) Crystal structure of $Li_{10}GeP_2S_{10}$. (b) Framework structure of $(Ge_{0.5}P_{0.5})S_4$ tetrahedra, LiS_6 octahedra and PS_4 tetrahedra. (c) 1D conduction pathways of lithium ions along the *c* axis. The zigzag conduction pathways are indicated.

N. Kamaya[1], K. Homma[1], Y. Yamakawa[1], M. Hirayama[1], R. Kanno[1], M. Yonemura[2,3], T. Kamiyama[2,3], Y. Kato[4], S. Hama[4], K. Kawamoto[4], and A. Mitsui[5]

[1]Department of Electronic Chemistry,Tokyo Institute of Technology; [2]Neutron Science Section, Materials and Life Science Division, J-PARC Center; [3]Institute of Materials Structure Science, KEK; [4]Toyota Motor Corporation, Battery Research Division; [5]Toyota Motor Corporation, Material Engineering Management Division

Quantum Renormalization Effect in One-Dimensional Heisenberg Antiferromagnets

One-dimensional (1D) antiferromagnetism is one of the most mature areas in condensed matter research, in particular, the quantum nature for S = 1/2, where S is the spin quantum number of magnetic ions, is well understood. The ground state of a 1D Heisenberg antiferromagnet (1DHAF) with S = 1/2 is the degenerate singlet spin state (Bethe state), rather than the antiferromagnetic Néel state. The lowest spin excitations from the Bethe state are renormalized from the classical spin-wave state excited from the Néel state, where the lowest spin excitation energy can be described by $E(q) = 4SRJ|\sin q|$ with the exchange constant J, and the enhancement of excitation energies compared to those of a classical system is defined by the quantum renormalization factor R; $R = \pi/2$ for S = 1/2.

More generally, quantum effects that depend on the value of S require further investigations. The Haldane conjecture, which suggests a spin gap for integer S but no gap for half integer S, is conspicuous as an important milestone. It is well known that a 1DHAF with S = 5/2 behaves classically. However, the spin dynamics between S = 1 and 5/2 has not been confirmed, as there is a lack of consistent experimental data.

To detect the S-dependent quantum renormalization effect, inelastic pulsed neutron scattering experiments were performed at KENS and ISIS using the 1DHAFs $CsVCl_3$ (S = 3/2), $CsVBr_3$ (S = 3/2), and $CsCrCl_3$ (S = 2), as well as $CsNiCl_3$ (S = 1) as a reference system. At present, we improved the result by confirming $E(q)$ for $CsVCl_3$ on the High Resolution Chopper Spectrometer (HRC) at MLF, also by newly analyzing data for the other materials [1].

Fig. 1 shows excitation spectrum for $CsVCl_3$ measured on the HRC, where spin excitations were well observed in the entire Brillouin zone up to the zone boundary energy and $E(q)$ could be determined as peak positions of spin excitations. $E(q)$ for 1DHAFs determined in this study are summarized in Fig. 2. To discuss the quantum renormalization effect quantitatively, the value of J should be determined, because $E(q)$ provides the product RJ. The evaluation of R was successful for S = 1/2 and 1, because quantum theories describing $\chi(T)$, the temperature (T) dependence of the magnetic susceptibility, exist for both S = 1/2 and 1 as a function of J. On the other hand, no rigorous theory exists for S = 3/2 and 2. We measured the dynamical structure factor of the spin excitations $S(q,E)$ to determine $E(q)$. The

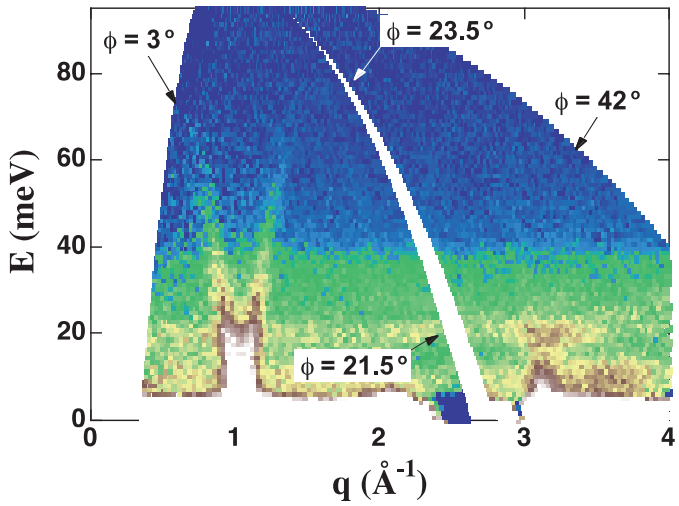

Figure 1. Excitations in $CsVCl_3$ observed on the HRC at T = 20 K with E_i = 100 meV

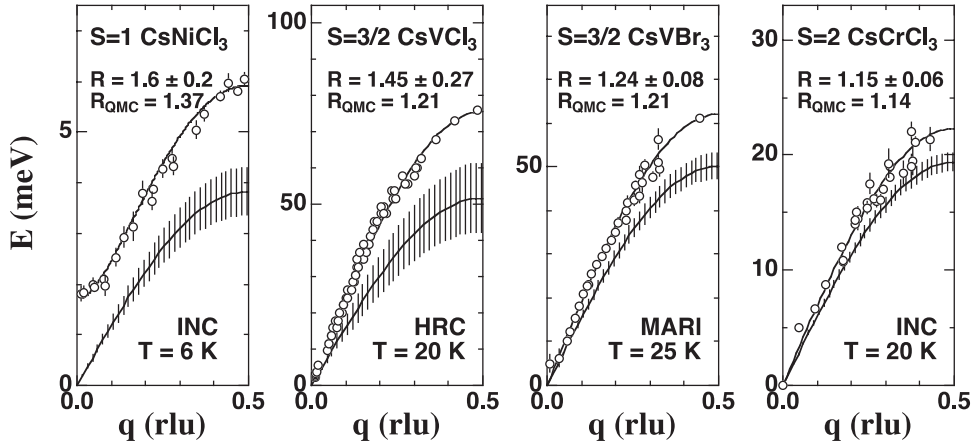

Figure 2. Dispersion relations of the lowest spin excitations at low temperatures in 1DHAFs. The solid lines on the data points (marks) are fitted dispersion curves. The sine curves with bars are the dispersion relations of classical spin waves.

static spin correlation function $S(q)$ was deduced by integrating $S(q,E)$ over E, following which $\kappa(T)$, the T dependence of the inverse magnetic correlation length, was obtained as a width of $S(q)$. The value of J can be determined from $\kappa(T)$, because $\kappa(T)$ is described as a function of J for any S by the quantum theory.

In Fig. 2, the sine curves with bars are the classical dispersion relations estimated by J, which was determined from $\kappa(T)$, and the bars represent the experimental uncertainties from the determination of J. The values of R, which is the ratio of $E(q)$ at the zone boundary (q = 0.5 rlu) to the classical spin wave energy, were in good agreement with the quantum renormalization factors predicted by quantum Monte Carlo calculations. We could determine the quantum renormalization factors by only inelastic pulsed neutron scattering experiments.

References

[1] S. Itoh, T. Yokoo, S. Yano, D. Kawana, H. Tanaka and Y. Endoh, J. Phys. Soc. Jpn. **81** (2012) 084706.

S. Itoh[1,2], T. Yokoo[1,2], S. Yano[3], D. Kawana[2], H. Tanaka[4], and Y. Endoh[2]

[1]Neutron Science Section, Materials and Life Science Division, J-PARC Center; [2]Institute of Materials Structure Science, KEK; [3]Aoyama Gakuin University; [4]Tokyo Institute of Technology

Facility Research and Development Highlights

Effect of the Si Interlayer on the Magnetic and Mechanical Properties of Fe/Ge Polarizing Multilayer Mirrors

Introduction

The neutron polarizing supermirror is one of the most important optical devices for polarizing neutron beams. Polarizing supermirrors need to display high polarizing efficiencies at low external magnetic fields to meet a variety of research demands. As shown by Hino et al. the strength of the external magnetic field required to achieve efficient neutron polarization (H_{pol}) can be suppressed by the use of an Fe/Si/Ge/Si multilayer, which is obtained by adding a thin Si interlayer into the Fe/Ge multilayer. In this study, we investigated the magnetic and mechanical properties of Fe/Si, Fe/Ge, and Fe/Si/Ge/Si multilayers to elucidate the mechanism that controls H_{pol} for a polarizing supermirror [1].

Experimental

Polarized neutron reflectivity measurement was performed on a SUIREN reflectometer installed at the research reactor, JRR-3, in the JAEA. The polarized neutron reflectivity profiles were measured during re-magnetization of the Fe/Si/Ge/Si supermirror with m=2.8 after it had been saturated in a field of 10 kOe opposing the guide field of the neutron beam to evaluate H_{pol}. The measured reflectivity profiles are shown in Fig. 1. The flipping ratio of the Fe/Si/Ge/Si supermirror is increased to a value of more than 30 within the momentum transfer range 0.3 < q_z < 0.61 nm^{-1} under an external field strength of 4.0 kOe, at which the Fe/Si/Ge/Si supermirror is magnetized to saturation. H_{pol} for the Fe/Si/Ge/Si supermirror was evaluated to be 200 Oe since the flipping ratio coincides with that at saturation. The same measurement was performed for the Fe/Si and Fe/Ge supermirrors. The result is summarized in Table 1. This result shows that H_{pol} for a neutron polarizing supermirror with m=2.8 is effectively reduced to 200 Oe by the addition of a Si interlayer to the Fe/Ge multilayer. The ratio of the magnetization under H_{pol} to that at saturation was estimated to be in the range of 97.5%–98.5%. In subsequent discussions, we assume that the ratio of the magnetization under H_{pol} to that at saturation is 98%.

Table 1. Estimated H_{pol} and external field at saturation H_s.

	H_s (Oe)	H_{pol} (Oe)
Fe/Si	2000	600
Fe/Ge	7000	400
Fe/Si/Ge/Si	4000	200

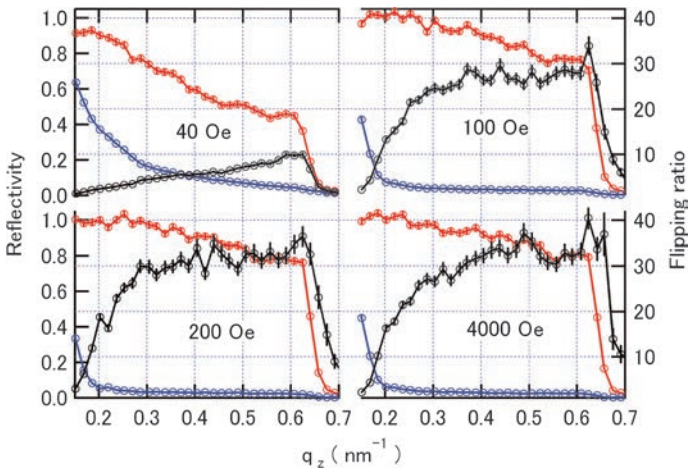

Figure 1. Polarized neutron reflectivity profiles for Fe/Si/Ge/Si supermirror with m=2.8.

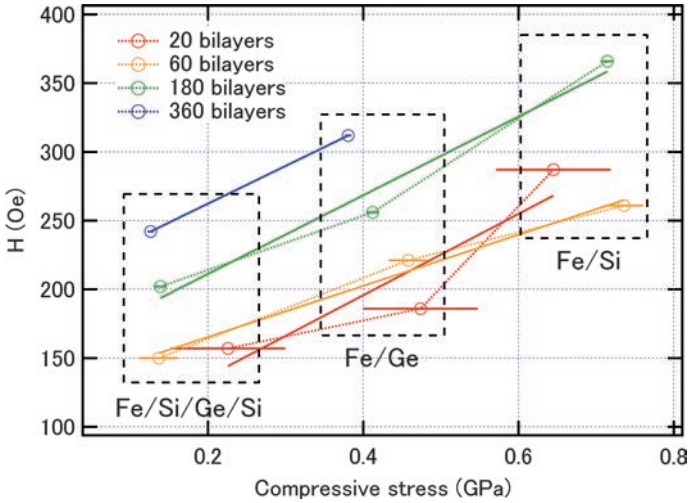

Figure 2. Dependence of estimated H_{pol} on compressive stress for Fe/Si, Fe/Ge, and Fe/Si/Ge/Si multilayers.

Fe/Si, Fe/Ge, and Fe/Si/Ge/Si multilayers with a multilayer period of 12 nm were fabricated to examine the dependence of H_{pol} on the film stress. This multilayer period was chosen because it is representative of the sequence occurring in a supermirror with m=2.8. Hysteresis measurement was performed to evaluate H_{pol} on a SQUID magnetometer. Stress measurement was performed on a laser scanning displacement meter. Stress in the layers was determined from the radii of curvatures of the Si substrates before and after deposition. The dependence of the estimated H_{pol} on compressive stress is plotted in Fig. 2. When we fix the number of periods and the multilayer period, H_{pol} is clearly seen to be linearly dependent on the compressive stress. These measurements and analyses show that, within the parameter ranges explored in this study, a reduction in the compressive stress effectively reduces H_{pol} for a polarizing supermirror.

Conclusions

The polarized neutron reflectivity measurement showed that H_{pol} is effectively reduced to a value of 200 Oe for a neutron polarizing supermirror with m=2.8 by adding a Si interlayer to the Fe/Ge multilayer. Magnetization and stress measurements for Fe/Si, Fe/Ge, and Fe/Si/Ge/Si multilayers showed that the technique of adding Si interlayers to the Fe/Ge multilayer is effective in reducing compressive stress and that H_{pol} is found to be proportional to the compressive stress. This study confirmed that a reduction compressive stress is very important for a high-performance neutron polarizing supermirror.

References

[1] R. Maruyama *et al.*, J. Appl. Phys. **111** (2012) 063904.

R. Maruyama[1], D. Yamazaki[1], S. Okayasu[2], M. Takeda[3,4], N. Zettsu[5], M. Nagano[5], K. Yamamura[5], H. Hayashida[6], and K. Soyama[6]

[1]Neutron Instrumentation Section, Materials and Life Science Division, J-PARC Center; [2]Advanced Science Research Center, JAEA; [3]Neutron Science Section, Materials and Life Science Division, J-PARC Center; [4]Quantum Beam Science Directorate, JAEA; [5]Graduate School of Engineering, Osaka University; [6]Neutron Instrumentation Section, Materials and Life Science Division, J-PARC Center

Multiwire-type Two-dimensional Neutron Detector with Individual Readout and Optical Signal Transmission System

Introduction

We are currently developing a position-sensitive neutron detection system that can read out individual signal lines and consists of a two-dimensional detector element [1−2]. In the neutron scattering experimental facilities, there are some difficulties as compared to a small experimental laboratory environment, for example, a long distance from a sample irradiation area to a data acquisition room, massive and inconvenient neutron shieldings, complicated background noises arisen from many sample environments, etc. We consider an optical fiber to be a promising candidate for a signal transmission device because the optical fiber has good properties such as an excellent optical transmission capability of less than a few dB/km, wide optical signal bands, a light weight, and no sensitivity to electromagnetic forces. Therefore, we have developed a neutron detector system that uses optical signal transmission devices to ensure that the system can be operated and meet the challenges to its performances in these facilities.

Developed Detector System

A developed neutron detector system consists of a 256 channel multiwire detector element (x: 128 lines, y: 128 lines) equipped into a pressure vessel, amplifier-shaper-discriminator (ASD) boards, optical signal transmission devices, position encoders with field-programmable gate arrays (FPGAs), and a fast data acquisition device. The photograph of the developed system is shown in figure 1.

The pitches of each axis are 1 mm and the conversion gap is 15 mm. The charge signals collected by the detector element were amplified, shaped, and discriminated by ASD application-specific integrated circuits (ASICs). The nominal settings of the ASD-ASICs had an amplification factor of 3.1 V/pC and a decay time of 90 ns. Digital signals from the ASD-ASIC were transmitted to the position encoders via optical fibers as optical signals converted by specially-fabricated E/O-O/E converters. The specially-fabricated optical devices used FPGAs with 106 MHz clocks and 1.06 Gbps optical transceivers. A developed 1-unit VME module equipped with an O/E converter and a position encoder is shown in figure 2. Multimode optical fibers and transmission light at 850 nm were used for transmitting the optical signals.

Figure 3 shows a typical pulse shape at anodes

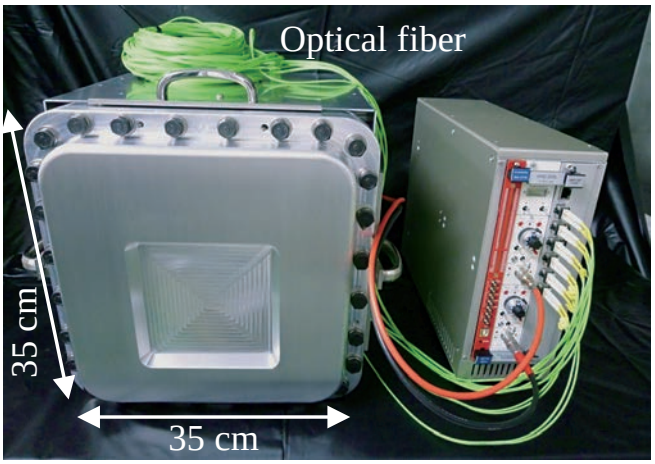

Figure 1. Photograph of a developed two-dimensional neutron detector system.

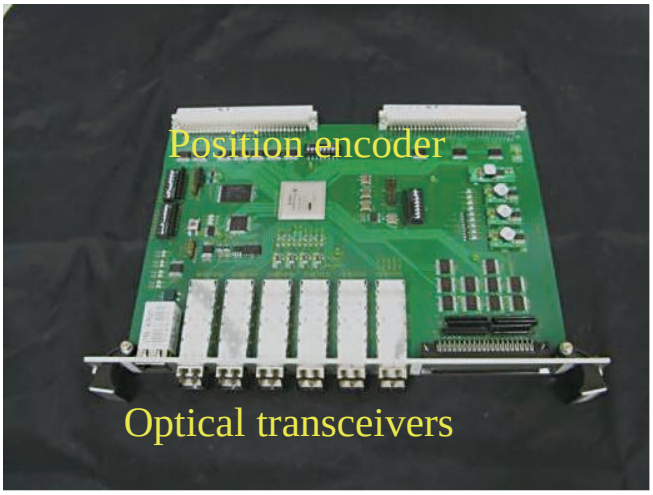

Figure 2. Specially-fabricated 1-unit VME module.

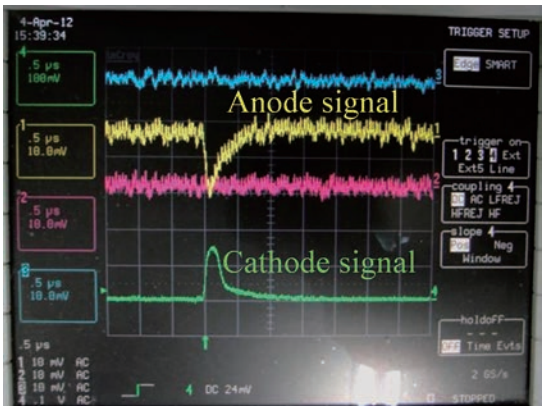

Figure 3. Output pulse shapes from ASD-ASIC.

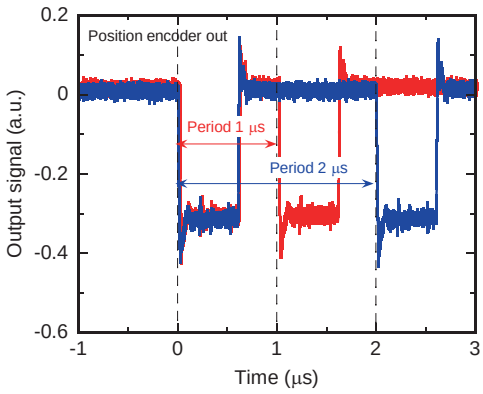

Figure 4. Output signal from position encoder. Double pulse with time interval of 1 and 2 μs.

and a cathode line after modification by the preamplifier in the ASD-ASIC under neutron irradiation measured using a 1.5 GHz oscilloscope (Lecroy, LC684DM). A signal-pulse peak of neutrons can be clearly observed with a fast temporal response; the FWHM of the response time was 180 ns. To evaluate the time response of our whole signal processing system, double pulses with various time durations were entered into the system. Figure 4 shows the output signals from the position encoder when the double pulse with a time interval of 1 and 2 μs is input. It was found that our system can separate signal pulses with a time interval of 1 μs.

References

[1] H. Yamagishi, K. Toh, T. Nakamura, K. Sakasai and K. Soyama, J. Instrum. **6** (2011) C12025.

[2] K. Toh, T. Nakamura, K. Sakasai, K. Soyama and H. Yamagishi, J. Instrum. **7** (2012) C01025.

K. Toh[1], T. Nakamura[1], K. Sakasai[1], K. Soyama[1], and H. Yamagishi[2]

[1]*Neutron Instrumentation Section, Materials and Life Science Division, J-PARC Center;* [2]*Nippon Advanced Technology Co. Ltd. (NAT)*

Damage Inspection of the 1st Mercury Target Vessel of JSNS

Introduction

The mercury target vessel of the JSNS, which is made of SS316L, is damaged by the proton and neutron irradiation during operation. Furthermore, the beam window portion where directly affected by the proton beams is also damaged by pressure wave inducing cavitation, because the proton beam injection produces the pressure waves in mercury due to heat deposition. The cavitation damage, which is correlated with the beam power and operation time, has a considerable effect on the lifetime of the target vessel. Damage inspection of the target vessel is important to determine the lifetime of the vessel. The 1st mercury target vessel was operated up to 475 MWh since 2008, and achieved 200 kW operation at the maximum. Because a part of the vessel was damaged due to the Great East Japan Earthquake in 11th March it was necessary to replace the target with a new one. Before replacing the target vessel, we cut out the disk from the spent target vessel to observe the damage which affects the lifetime reduction and to provide the test specimen for the post irradiation examination to evaluate the changes in mechanical properties caused by irradiation.

Cutout from target vessel

Figure 1 shows photographs of the cutout procedure. The beam window portion of the target vessel was cut out with a hole-saw. A cutout disk specimen with a diameter of 50 mm was taken out from the saw, and cleaned using ultrasonic bath to remove the mercury. All processes were conducted by the remote handling.

Damage inspection

Inside of the target vessel was inspected by putting a scope camera into the cutout hole of the beam window potion to observe flow inducing erosion and cavitation damage. Figure 2 shows the images of the flow guide and the beam window portion. Flow-inducing erosion around the flow guide edge where flow velocity exceeds 1 m/s was not observed in the captured image. Around the cutout hole at the beam window part, the damage cluster induced by cavitation is recognized. However, the clear cavitation damage was not observed except for the damage cluster part.

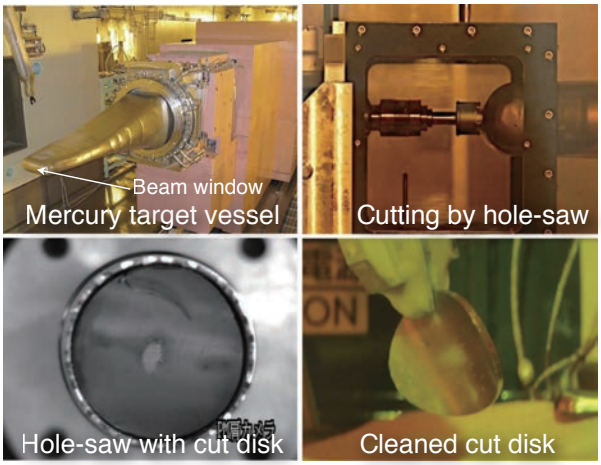

Figure 1. Photographs of cutting procedure.

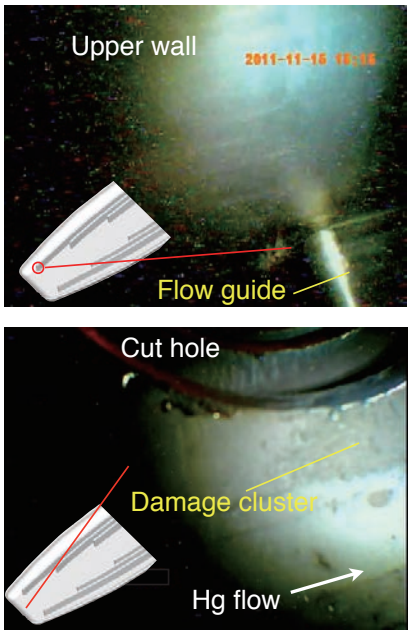

Figure 2. Captured images of the flow guide and the beam window portion inside the target vessel.

The cleaned cut disk was particularly observed in order to measure the eroded depth due to the cavitation. Macroscopic observation was performed using a high resolution video camera. Figure 3(a) shows captured images of the cutout disk. Cavitation damage clusters are recognized at the center and around both sides at 15 mm from the center. This damage distribution may be related to the pressure distribution. Detailed consideration is undergoing through the numerical simulation. Near the damage clusters, isolate pits were observed. The isolate pits seem to be delaminate a part of modification layer which had been treated to harden the beam window potion aiming for the cavitation damage reduction. In the damage cluster at the center, deep damage, so called localized pit, was recognized.

Furthermore, the cutout disk surface was replicated to observe the surface profile using a laser microscope. Figure 3(b) shows the microscopic image of the localized pit. A crack was observed at the edge of the localized pit. It may have been caused by the repetition of the cavitation impact. The depth of the localized pit in the figure is about 120 μm. In consideration of a homogeneous erosion on the damage clusters, we concluded that the maximum eroded depth of the beam window is 250 μm.

Summary

We have succeeded in the damage inspection of the 1st mercury target vessel with the help of many people. Useful data to determine the lifetime of the target vessel, i.e. the beam power and operation time dependencies on the eroded depth, was obtained.

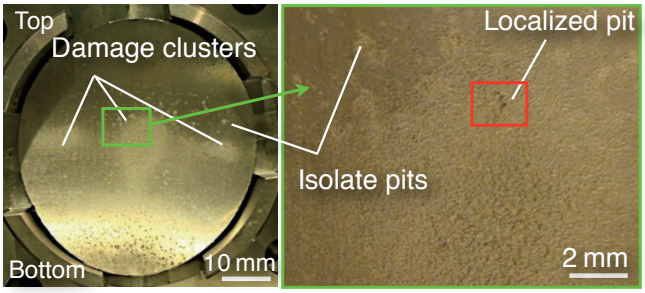

(a) Macroscopic image

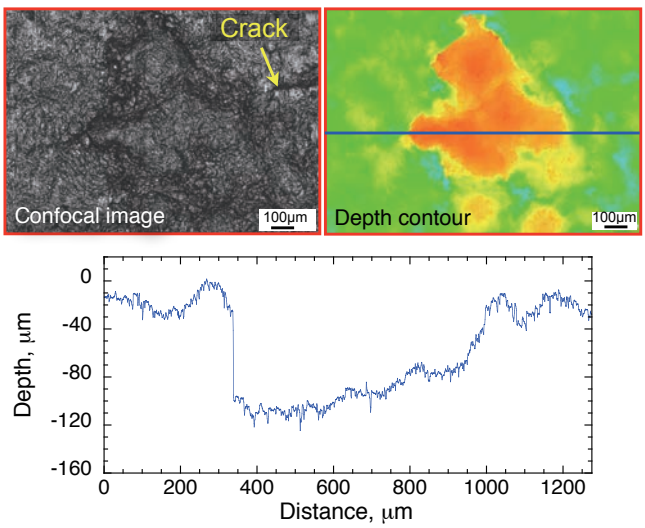

(b) Microscopic image of localized pit

Figure 3. Images of cutout disk surface.

T. Naoe, M. Teshigawara, T. Wakui, and H. Kinoshita
Neutron Source Section, Materials and Life Science Division, J-PARC Center

Radiological license update and inspection

An application for radiological license update was submitted in September 2011, and the test use was approved in November 2011. The followings items were newly approved in the application:

- Installation of a neutron beam line of BL09
- Partial change of the shield configuration to prepare it for installation of the ultra-slow-muon beam line

The government inspection for the update was carried out on February 6 and 7, 2012. The inspections for the previous applications approved in November 2010 and February 2011* as test use were conducted at the same time because those were postponed due to the disaster on March 11, 2011. The final approval for the whole inspections was issued on February 14, 2012.

Development of "UHAM"; Radioactivity monitoring system for the mercury system

The test operation of the monitoring system of the mercury target failure using radioactivity detection was started in October 2009, and continued until just before the 3.11 disaster. The monitor was called "HAM", which means "Helium-layer Activity Monitor"†. We could confirm, by the test operation, that the "HAM" system had enough sensitivity to catch the primary failure by detecting a tiny leak of radioactive products from the inner vessel [1]. The practical operation of the "HAM" system started when the beam operation was restored in December 2011.

In order to monitor the health of the whole mercury circulation system from the viewpoints of radioactivity confinement, a total monitoring system called "UHAM" was designed and constructed; the "HAM" system was unified with the total system. The conceptual diagram of the "UHAM" system is shown in Figure 1. The operation of the total system was started in March 2012.

* The previous applications included the intensity power-up from 250 to 320 kW, installation of the neutron beam lines, etc. The details are indicated in MLF Annual Report 2010.

† The mercury target has double walls; there is an intermediate layer containing helium gas between the walls. By the "HAM" system, the helium gas in the intermediate layer are continuously sampled and checked with gamma-ray spectroscopy analysis.

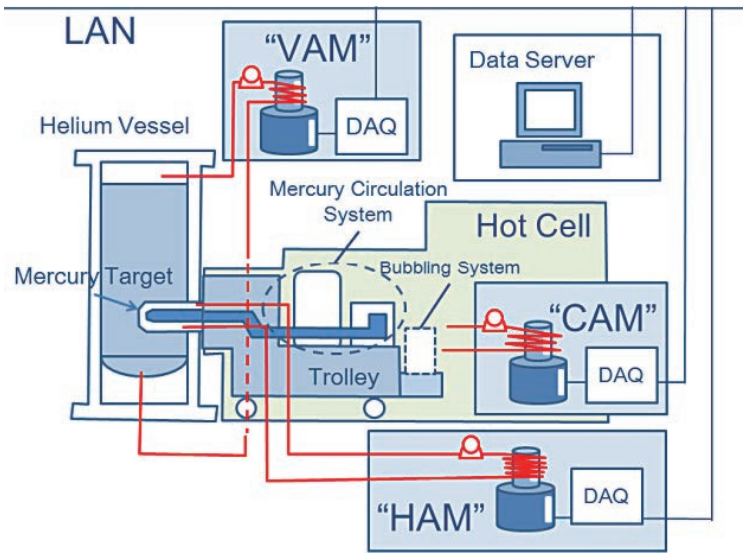

Figure 1. A conceptual drawing of the whole diagram of "UHAM" system.

The “UHAM” system consists of “HAM”, “CAM” and “VAM”. The “CAM” is a gas monitor of the hot cell in which the mercury circulation system has been installed, and “VAM” is that of the helium vessel enclosing cold-neutron production devises such as hydrogen moderators and beryllium reflectors.

As preparation for the future 1-MW operation, we are planning to upgrade the mercury system as follows:

- Mercury-bubbling operation will be started for mitigation of cavitation damage.
- The target design will be modified to minimize the exchange part for waste reduction.

However, these upgrades may increase the risk of radioactivity leakage. The “CAM” and “VAM” are necessary to take rapid measures by detecting the radioactivity leakage as early as possible.

Issue on Tritium behavior

In November 2011, the first attempt of the target-vessel exchange was successfully conducted. However, during the exchange process, a significant tritium release was observed, and the total amount of released tritium was much higher than our estimate which we evaluated based on the tritium-analysis measurement of helium gas injected in the mercury circulation system. The following is just one possible explanation of this phenomenon

- Considerable amount of tritium was adhered in the structural material of the mercury circulation system during the beam operation.
- Adhered tritium was released by the effect of isotope exchange with water-vapor of air.

For the preparation of the next target exchange, an analytical understanding of the tritium behavior is essential in order to prevent uncontrolled release of tritium. In any case, by purging the mercury circulation system, a large volume of radioactive gas will be produced. This forced us to change the scenario of the radioactive-gas process. Therefore we decided to adopt an “active” process instead of the “passive” process which means just keeping the gas for a year.

As a new device for the “active” process, a “cold-charcoal trap” will be adopted. The test apparatus will be made in the beginning of the fiscal year of 2012, and it will be tested in the summer. The full device will be installed by the end of the next fiscal year.

References

[1] Y. Kasugai, K. Otsu and T. Kai, “Monitoring System of Mercury Target Failure Using Radioactivity Measurement”, Proceedings of the 19th Meeting of the International Collaboration Advanced Neutron Source (ICANS-XIX), March 8-12, 2010, Grindelwald, Switzerland.

Y. Kasugai, M. Ooi, M. Harada, K. Ohtsu, H. Kinoshita, M. Seki, and T. Kai
Neutron Source Section, Materials and Life Science Division, J-PARC Center

Time-Transient Measurement of Hydrogen Absorption Process by NOVA

Introduction

In-situ H_2/D_2 gas atmosphere measurement is important to understand the mechanism of hydrogen absorption and desorption process in materials. On NOVA, a sample environment to control hydrogen composition in a sample by controlling the sample temperature and the hydrogen pressure has been equipped. This environment is able to measure Pressure-Composition isotherm (PCT) curve and the sample environment is called as PCT environment. Highest H_2/D_2 gas pressure is 10 MPa with controlling the sample temperature from 50 K to 473K. The layout of the PCT environment is depicted in Figure 1.

PCT and in-situ measurements

Measurement of PCT curve of $LaNi_5$, which is well-known hydrogen storage material, was performed with D_2 gas successfully on the beam position of NOVA as shown in Figure 2. By increasing the D_2 gas pressure, the content of D_2 (D/M) in $LaNi_5$ increases. From lower to higher D/M, three regions appears: solid-solution region (< 0.2 D/M), two-phase (solid-solution and hydride) region (0.2 ≤ D/M < 1.0) and hydride region (≥ ~1.0 D/M). At each hydrogen contents pointed by numbers enclosed in parentheses in Figure 2, neutron diffractions were measured as shown in Figure 3. According to the hydrogen absorption and desorption, diffractions from solid solution, two-phase region, hydride, two-phase region and solid solution were measured.

Time transient measurement

By utilizing event-mode DAQ recording system (DAQ-middleware), time-transient measurement is easily performed. Figure 4 shows the demonstrated result of measurement of hydrogen absorption process of $LaNi_5$. The sample was kept in vacuum by

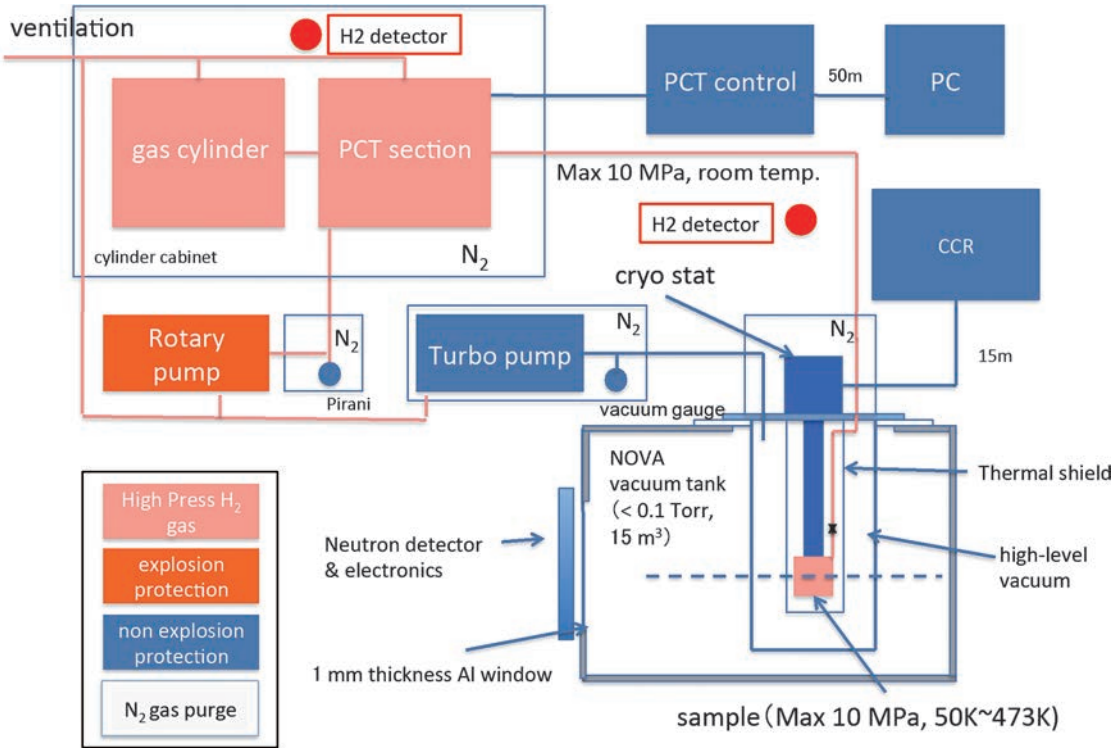

Figure 1. Sample environment Pressure-Composition isotherm (PCT) measurement on NOVA.

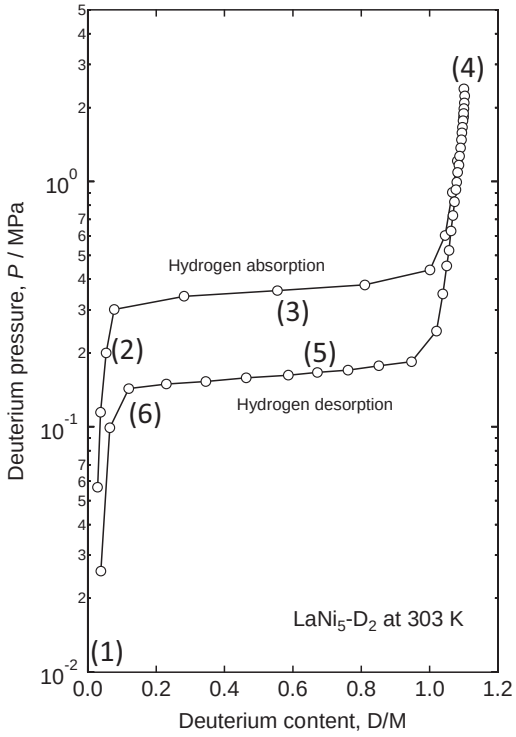

Figure 2. PCT curve $LaNi_5$ measured the PCT sample environment of NOVA.

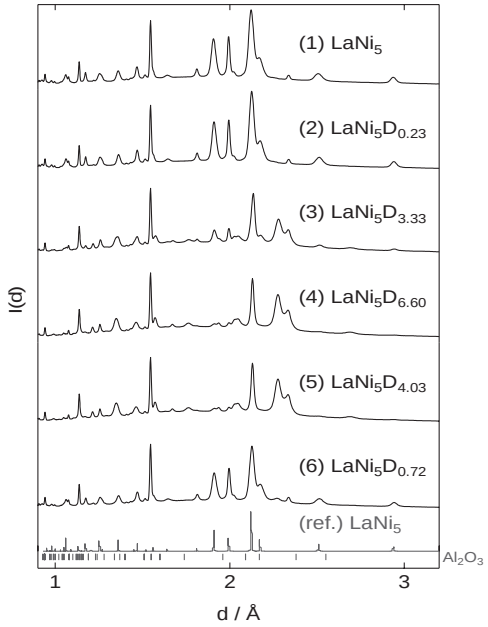

Figure 3. Neutron diffraction of $LaNi_5$-D_x measured on NOVA. Numbers enclosed in parentheses correspond to hydrogen contents shown in Fig. 2.

closing a valve and certain pressure of D_2 gas was filled in PCT (3 MPa in Figure 4). Opening the valve begins hydrogen absorption process. In 400 sec, it is clearly observed that the sample became hydride ($LaNi_5D_{6.6}$) through two-phase region.

In Figure 4, diffraction profiles were obtained by integrate neutron counts at every 8 sec. The time-interval can be optimized after the experiment taking accounts the statistics. Since the pulsed neutron at MLF generated at every 40 msec, minimum time interval is 40 msec.

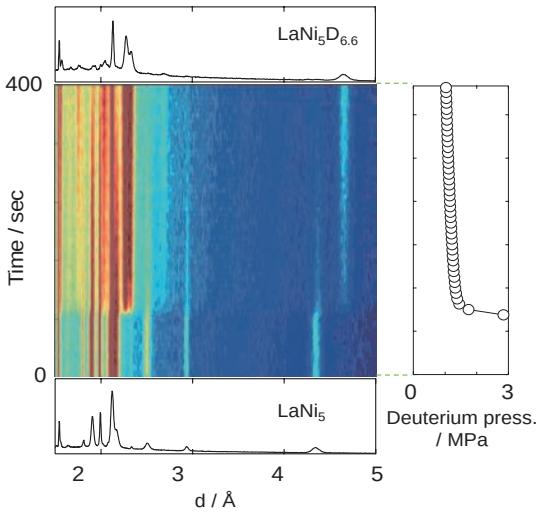

Figure 4. shows diffraction data that was summed event data with time-interval of 8 sec.

Even J-PARC, one-pulse measurement is quite challenging but shorter time interval may be feasible by selecting neutron counts at same sample environments (temperature, pressure, magnetic fields and so on) if the phenomenon is reversible.

It is noteworthy that such time-transient measurements are feasible at every beam lines at J-PARC. Utilization of event-mode recording will be progressed and expected to open new opportunities for materials & life science researches.

T. Otomo[1,2], K. Ikeda[2], H. Ohshita[1,2], N. Kaneko[1,2], T. Seya[1,2], and K. Suzuya[1]

[1]Neutron Science Section, Materials and Life Science Division, J-PARC Center; [2]Institute of Materials Structure Science, KEK

Development of Remote Access

Introduction

A lot of users of MLF perform a variety of experiments by using the MLF instruments. Because many experiments are performed automatically, it is necessary to monitor their experiment status from the users' desk or the dormitory. Additionally, these experiments produce an enormous amount of raw data whose total size is about a petabyte per year at the full performance of J-PARC. It is unrealistic that the users coming from the outside of MLF bring back these data to their home laboratories. It is required that analysis and visualization of stored data in MLF can be performed from their home laboratories via a network.

We have investigated and considered several remote access patterns and started to develop the three remote access methods shown in Fig.1. By using these remote access methods, the users can monitor the progress status of their experiments and analyze and visualize their data from the outside of MLF.

Development

To monitor the currently-executing experiment status, we have developed the web service which monitors the current status of the data acquisition (DAQ) system in each instrument. We have developed the web-based data reduction and visualization with the database, called MLF Experiment Database (MLF EXP-DB). The MLF EXP-DB is connected with our software framework [1], called IROHA and manages not only the produced raw data but also the experimental metadata. The MLF EXP-DB automatically registers the experimental raw data and metadata produced with the DAQ system and the IROHA. We can do the standard data reduction and visualization of the registered data through a web browser as shown in Fig.2. For the advanced analysis from the outside of MLF, the users will login to the MLF computational resources via a network and analyze their data stored in MLF interactively. The authentication system is under-development that is connecting with the user-identification information in the database of the J-PARC Users Office by taking into account the security policy.

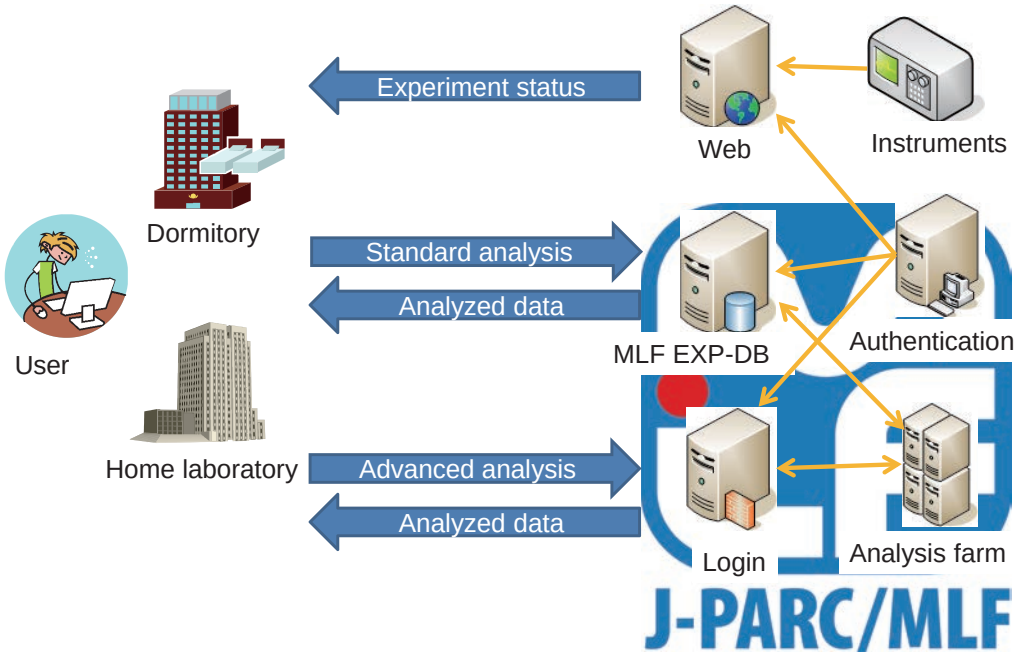

Figure 1. Three kinds of the remote access method in MLF.

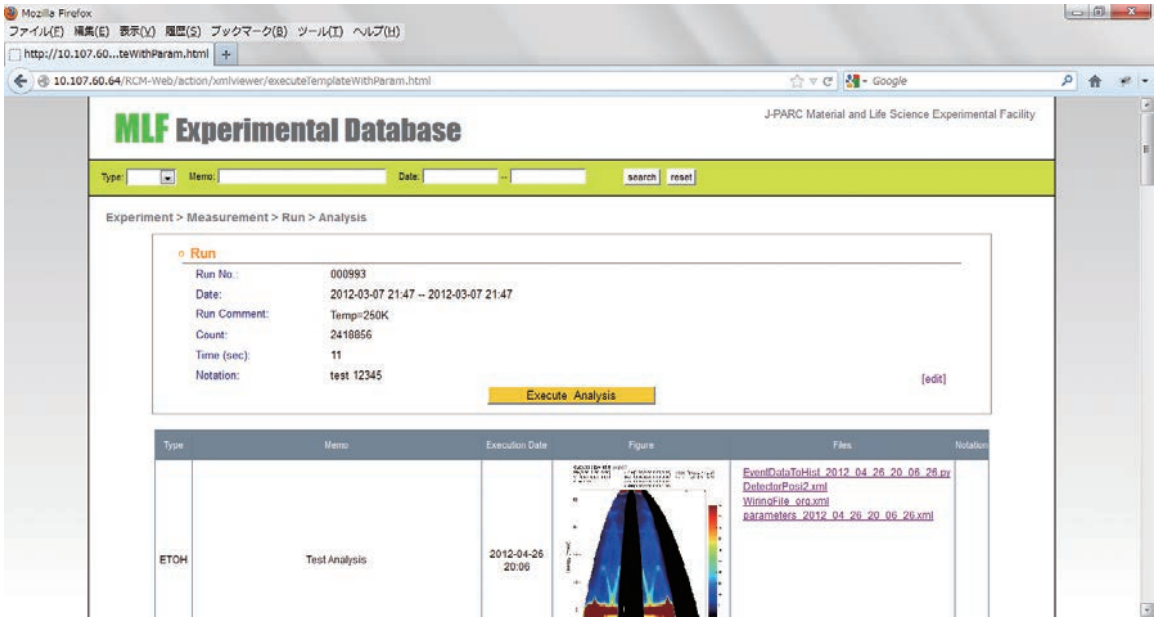

Figure 2. Standard analysis through a web browser.

Summary

We have developed the remote access in MLF, which includes monitoring of the DAQ status in each instrument as a web service and web-based data reduction and visualization with the MLF EXP-DB. Currently, these methods are available in J-PARC LAN, we are going to open them to the Internet in the next year.

References

[1] T. Nakatani, Y. Inamura, T. Ito, S. Harjo, R. Kajimoto, M. Arai, T. Ohhara, H. Nakagawa, T. Aoyagi, T. Otomo, J. Suzuki, T. Morishima, S. Muto, R. Kadono, S. Torii, Y. Yasu, T. Hosoya and M. Yonemura: Proceedings of ICALEPCS2009 673-675.

T. Nakatani[1], Y. Inamura[1], K. Moriyama[1], and T. Otomo[1,2]

[1]*Neutron Science Section, Materials and Life Science Division, J-PARC Center;* [2]*Institute of Materials Structure Science, KEK*

Current Status of Sample Environment at MLF

Introduction

Since the reorganization of the sample environment (SE) team in the MLF neutron facility in 2008, the SE team has discussed how we should contribute to the user support in SE to keep up with the demands for SE, in addition to the update of the SE protocol. After the earthquake in March 2011, the priority of SE in MLF might have not been so high because we needed to concentrate on the recovery from its damages. However, we achieved some progress in FY2011, including installation of new SE devices, preparation of the SE area, transportation of SE devices from KENS and other activities of the SE technical team.

SE Devices in MLF-neutron

A vertical-field superconducting magnet with asymmetric split coils and 7 T of the maximum field and a dilution refrigerator as its insert option were installed in March 2011 and the test operation was carried out in MLF (Fig. 1). Though these devices were purchased by the fund of BL17/18, they are designed rather as a general-purpose ones taking into account their compatibility with most beam lines. These devices will be available in MLF within FY2012 after some modification. Another device installed this fiscal year is a furnace with niobium heater which can be used to produce temperatures of up to 1600°C in a vacuum. This furnace is available for both instruments, which have the vacuum scattering tank and sample table (goniometer).

It is also noted that a pulse magnet system for neutron experiments has been developed by the Institute for Materials Research (IMR) group in Tohoku University (Nojiri et al.). 40 T of pulsed magnetic field has been successfully applied in an experiment in MLF. Its portable version will be also installed in the late fall of 2012.

As the number of general-purpose SE devices increases in MLF, it becomes important to establish the user support system in SE including their allocation. It is urgent to discuss the issue in the SE team.

Figure 1. Test operation of the 7 T vertical-field superconducting magnet, performed at the MLF experimental hall 2 in March 2012.

SE Area

In the last annual report we reported that we set the SE handling area in MLF experimental hall 1. In FY2011, the fence was fitted up at the SE area in experimental hall 1 (Fig. 2(a)). This is about 4 m x 8 m in area. Then test operation of some devices such as a new furnace and cryostat has been performed there. We will also prepare another SE area in experimental hall 2 (Fig. 2(b)). Its size is planned to be changeable depending on the period of beam-on/off so that the area can be effectively used during the time of construction.

Utilities for the SE area are now being prepared. The electric power supplies (100 V and 200 V 3p) have been prepared for both the MLF experimental halls 1 and 2,and the others areas such as cooling water and helium recovery lines will be also completed in both experimental halls within FY2012. This progressing work has enabled us to do a minimum SE support. When more SE devices are installed and the number of the users who need to use them increases in the near future, this area will not be enough to store and prepare the devices one after another. An area with a much better functionality should be further prepared for maintenance, storage, and so on.

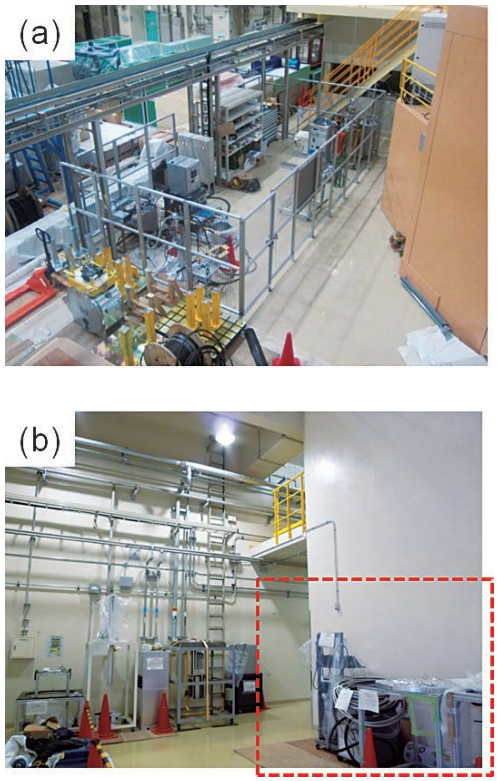

Figure 2. SE areas in MLF experimental hall 1 (a) and 2 (b).

KENS SE Devices

The KEK neutron facility (KENS) used to use many neutron SE devices until the proton synchrotron was shut down in 2006. For effective use of these resources, we selected some of those to bring to J-PARC, such as cryostats, compressors, sample changers etc. We finished ransporting them in November 2011. The SE technical staffs are now making a list of the devices and preparing their test operation to re-use them with minimum repairs and/or modifications. These are quite useful particularly for the beam lines which do not have any equipments. However, we need enough time, manpower, and funds to repair a part of them.

Figure 3. SE devices transported from Tsukuba Campus of KEK in November 2012.

Stepping Forward

The user program has already been restarted, so we should move to the next step where the practical works by the technical staffs is quite important. It is expected that the number of devices and the variety of users' experiments will increase, and then the contribution of the SE team becomes essential. The SE technical team will start training in operation of SE devices trough the users' experiments. Also, we should continue to require human resource and to consider improvement of the qualifications of it.

S. Ohira-Kawamura[1], T. Yokoo[1,2], Y. Yamauchi[1], and W. Kambara[1]
[1]*Neutron Science Section, Materials and Life Science Division, J-PARC Center;* [2]*Institute of Materials Structure Science, KEK*

Development of an in-situ SEOP ^{3}He Neutron Spin Filter

^{3}He has a very large absorption cross section only for a neutron whose spin is anti-parallel to that of a ^{3}He nuclei. Moreover, the neutron scattering cross section of ^{3}He is negligibly small. Therefore, nuclear spin-polarized ^{3}He gas functions as a neutron spin filter [1]. Compared with other spin filters such as Heusler alloys and magnetic super-mirrors, the ^{3}He gas neutron spin filters have the following advantages: they can polarize neutrons in a wide energy range; they are effective for a large divergent beam, etc [2, 3].

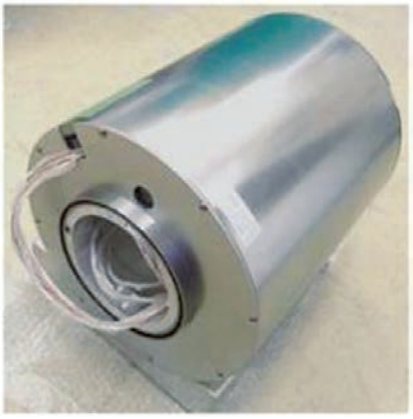

Figure 1. The developed magnetostatic cavity.

Thus, they are useful in various kinds of neutron beam experiments. So far, we have been developing an in-situ spin exchange optical pumping (SEOP) ^{3}He neutron spin filter to apply it to neutron scattering experiments at J-PARC [4]. To introduce the in-situ SEOP ^{3}He neutron spin filter into the instruments of the pulsed neutron beam facility of J-PARC, it is important to make the system compact and stable, because the system is located inside thick and bulky radiation shields for high energy gamma rays and neutrons. In this study, we have developed a compact magnetostatic cavity with a double layered permalloy shield and solenoid coils and a compact laser optics system with a volume holographic grating (VHG) element for the SEOP system.

Figures 1 and 2 show the developed magnetostatic cavity and its drawing. The magnetic cavity is composed of a magnetic shield and field coils. The outer dimensions of the cavity are 272 mm in diameter and 364 mm in length. The magnetic shield is made of Permalloy plates with a thickness of 2 mm, and it has a double-layered structure. The main coil has dimensions of 220 mm in diameter and 300 mm

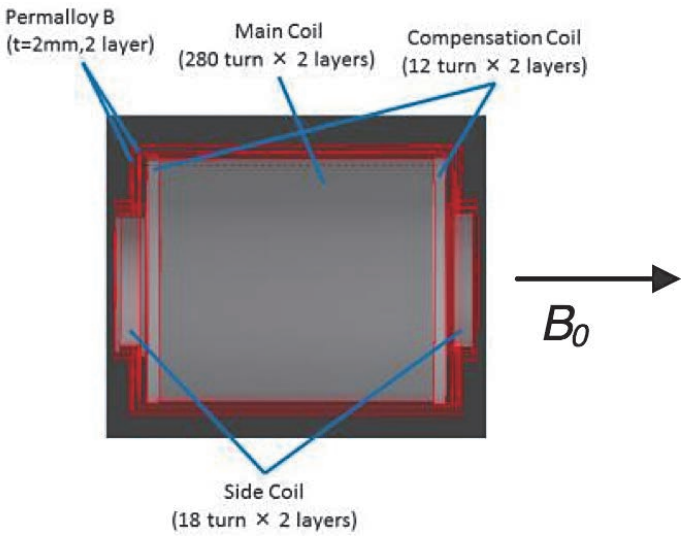

Figure 2. The developed magnetostatic cavity.

in length, and it is 560 turn-Cu wire. Two compensation coils with 24 turns are located at both edges to realize homogeneous magnetic field distribution. Two 36 turn-side coils with size of 120 mm in diameter and 20 mm in length are equipped at both ends to transport neutron adiabatically.

We calculated the magnetic field distribution generated inside the cavity. The field strength at the center position is 2.339 mT and $\left|\Delta B_{\perp}/B_0\right| \leq 5.34\mathrm{cm}^{-1}$. This corresponds to the ^{3}He relaxation time of ~200 hours. Moreover, the cavity can keep the magnetic field homogeneity which leads to sufficiently long ^{3}He relaxation time, over 100 hours, under the existence of an external field of 3.5 mT.

To make the in-situ SEOP system compact and stable, we also developed a compact laser optics system with a volume holographic grating (VHG) element. Its schematic layout is shown in Fig. 3. The output laser power is 30 W, and the laser spectrum width is 0.35 nm. The laser emitting diode is cooled by an air cooling system with a peltier element, and we don't use cooling water in this laser optics, so that we can easily install this system into the neutron beam instrument and operate it stably. We have done the ^{3}He polarization test by using this laser optics based on the SEOP, and observed that ^{3}He nuclear spin is polarized by the NMR technique.

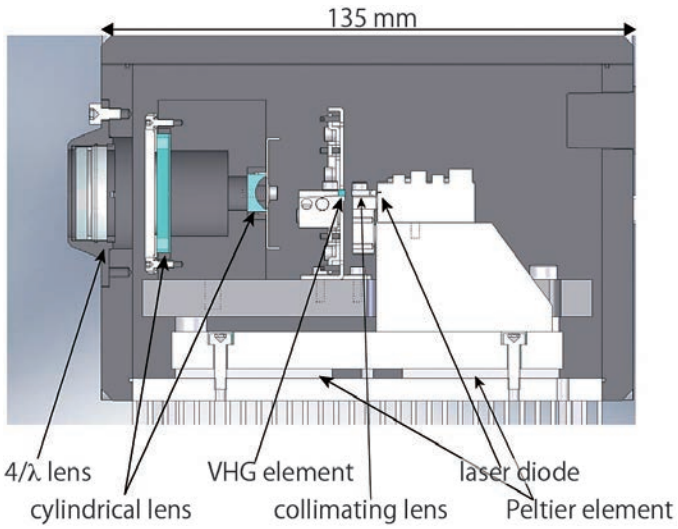

Figure 3. The developed Schmatic layout of the new laser optics.

References

[1] L. D. Cussen, D. J. Goossens and T.J. Hicks, NIM-A **440**, 409-420 (2000).

[2] C. G. Shull and J. S. Smart, Phys. Rev. **76**, 1256 (1949).

[3] R. N. Sinclair and B. N. Brockhouse, Phys. Rev. **120**, 1638 (1960).

[4] H. Kira, Y. Sakaguchi, T. Oku *et al.*, J. Physics: Conference Seiese 294, 012014 (2011).

T. Oku[1], H. Kira[2], K. Sakai[3], T. Shinohara[1], Y. Sakaguchi[2], T. Ino[1,4], Y. Arimoto[4], K. Ohoyama[5], H. Hiraka[5], L.J. Chang[6], M. Nakamura[1], J. Suzuki[2], H.M. Shimizu[7], M. Arai[8], Y. Endo[4], and K. Kakurai[9]

[1]Neutron Science Section, Materials and Life Science Division, J-PARC Center; [2]Neutron R&D Division, CROSS-Tokai; [3]Neutron Source Section, Materials and Life Science Division, J-PARC Center; [4]Institute of Materials Structure Science, KEK; [5]Institute for Material Research, Tohoku University; [6]Nuclear Science and Technology Center, National Tsing Hua University; [7]Graduate School of Science, Nagoya University [8]Materials and Life Science Division, J-PARC Center; [9]Quantum Beam Science Directorate, JAEA

Status of the Muon Kicker System at D-line

Introduction

The double pulse proton beam from the J-PARC 3GeV Rapid Cycling Synchrotron (RCS) hits the muon production target in the Materials and Life Science Facility (MLF), and produces muon pulses. The muon pulses are then transported through the decay muon line to two experimental areas (D1 and D2). A kicker system is used to separate the muon pulses and feed them to each experimental area simultaneously. The kicker system was installed as shown in Figure 1 in the summer of 2011. A beam operation with the kicker system started in the winter of 2011. Dividing the single pulse beam was successful, but anti-noise measures were required.

Measure to reduce the kicker noise

When the kicker is excited, noises of 10MHz appear in the detector signals as shown in Figure 2.

Later, however, the kicker noise level was dramatically improved through the ground line of the kicker system that was separated from the other earth lines. Figure 3 shows μe-decay count rates with kicker on/off. In the case of kicker-on, the noise level was improved after refining the ground line. However, further improvements are required when Multi Pixel Photon Counters (MPPC) will be used to replace the standard photomultiplier counters of the DΩ1 spectrometer.

Measures to reduce the electrical noise from the kicker are trial-and-error processes in parallel with the

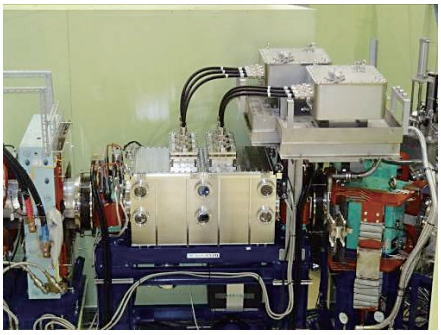

Figure 1. Kicker system in the decay muon line.

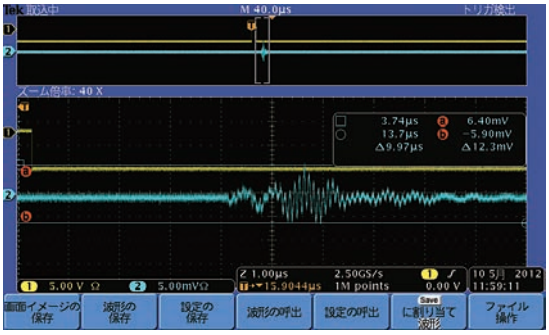

Figure 2. Typical kicker noise in a μe-decay counter.

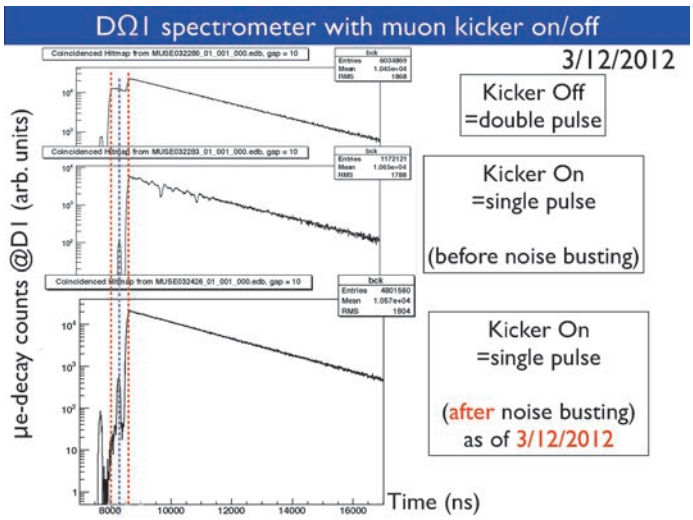

Figure 3. μe-decay spectra with kicker on/off.

improvements of the ground line. Some noise sources were overlaid with copper sheets as shown in Figure 4. The effect in the D2 area was confirmed with a radio wave detector. The results are shown in Figure 5.

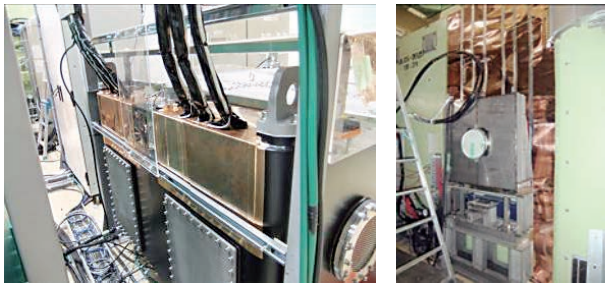

Figure 4. Trial-and-error for noise reduction measures.

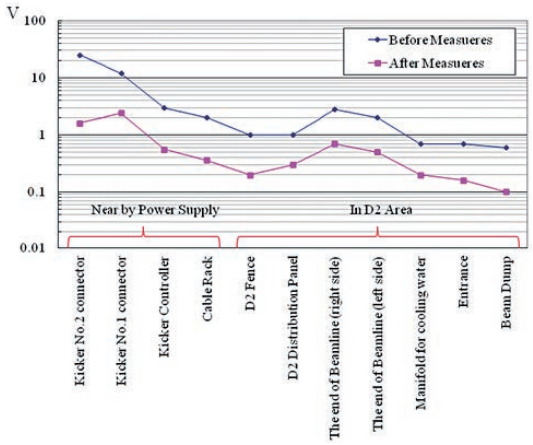

Figure 5. The noise distribution surrounding D2 area.

Summary

A kicker system was installed to separate the double-pulsed muon beams in the summer of 2011. The kicker system directed the two single-pulsed muon beams to the two existing experimental areas D1 and D2 simultaneously in March 2012. Experimental studies with the spectrometer in D1 area became possible with kicker-on, but the kicker noise level is still high according to the S/N ratio of some detectors.

Further measures to reduce the kicker noise are in progress for the beam operation in the autumn of 2012.

References

[1] H. Fujimori *et al*., KEK-MSL Report 2010, 10

[2] P. Strasser, H. Fujimori *et al*., New Muon Kicker System for the Decay Muon Beamline at J-PARC, Proceedings of the International Conference on Muon Spin Rotation, Relaxation and Resonance (μSR2011), May 16-20, 2011, Cancun, Mexico

[3] H. Fujimori *et al*., Proceedings of the 8th Annual Meeting of Particle Accelerator Society of Japan, August 1-3, 2011, Tsukuba, Japan

H. Fujimori[1,2], Y. Irie[2,3], K.M. Kojima[1,2], T. Nagatomo[1,2], S. Sakata[4], M. Meguro[4], N. Kurosawa[4], P. Strasser[1,2], and Y. Miyake[1,2]

[1]Muon Science Section, Materials and Life Science Division, J-PARC Center; [2]Institute of Materials Structure Science, KEK; [3]Accelerator Laboratory, KEK; [4]Nippon Advanced Technology Co. Ltd. (NAT)

Development of a Time Projection Chamber for the Precision Neutron Lifetime Measurement

A time projection chamber (TPC) has been developed to measure the neutron lifetime at BL05 – the NOP beamline in MLF. The neutron plays an important role in the Big Bang nucleosynthesis (BBN). The abundance of light elements in the universe is directly coupled with the neutron lifetime, and a better understanding of the BBN requires the precise length of the neutron lifetime. The neutron lifetime can be measured by identifying neutron decays in flight. At BL05, the decay electrons are tagged by the TPC with the four dimensional position. The TPC also measures deposit energy as low as 200 eV so that more than 99.9% of the decay electrons are to be detected to minimize the systematic uncertainty regarding the tagging efficiency.

It is essential to strongly reduce the background events. The TPC is surrounded by lead shielding, cosmic ray veto counters, and extra iron shielding. In addition, the TPC itself is made of special synthetic plastic, polyether ether ketone, to minimize the natural radioactive contamination. The inner walls of the TPC are covered with neutron absorber, ^{6}Li enriched LiF tiles, to further reduce the background events caused by the gas-scattered neutrons. It is also crucial to know the accurate neutron flux. A small amount of 3He gas is added to the TPC, and the neutron flux is measured by detecting the neutron absorption reactions, 3He(n,p)3H. An additional advantage of the process is that it unambiguously defines the neutron decay volume or the fiducial area of the TPC. The TPC can be normally operated under different gas pressures so that any background events resulting from the interactions of neutrons and the TPC gas can be statistically identified and subtracted. The apparatus is essentially a reproduction of the neutron lifetime measurement by Kossakowski et. al. [1] with the use of recent advanced technologies – a high intensity neutron source, a spin flip chopper, high-tech data acquisition electronics, synthetic materials, precise computer simulation, etc. After the disastrous earthquake hit northeastern Japan in March, 2011, J-PARC had been shut down for almost a year. However, there was enough time to study and improve the performance of the TPC as well as to develop sophisticated analysis methods to minimize the systematic uncertainties in the measurement. The physics run will start in 2012.

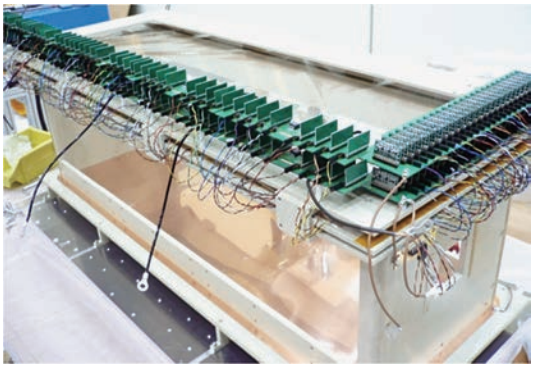

Figure 1. The time projection chamber for the precision neutron lifetime measurement at BL05.

References

[1] R. Kossakowski, P. Grivot, P. Liaud, K. Schreckenbach, G. Azuelos, Nucl. Phys. **A503**, (1989) 473.

T. Ino[1,2]

[1]*Neutron Science Section, Materials and Life Science Division, J-PARC Center;* [2]*Institute of Materials Structure Science, KEK*

What's new at the MLF ?

CROSS-Tokai

The Public Neutron Beam Facility at J-PARC MLF

Consistent with its longstanding policy of promoting open access to major publicly-funded research facilities, the Japanese government in July 2009 designated the accelerators (linac and 3 GeV proton synchrotron) and a proportion of beamlines at J-PARC MLF that are used for the generation and experimental exploitation of neutron beams as the Public Neutron Beam Facility. under the terms of the so-called "Public Use Promotion" legislation (Figure 1).

The aim of the legislation is to advance science and technology through the effective promotion and operation of general user access programs at designated large-scale research facilities. In practice, this is achieved by attracting and supporting use by researchers from a wide range of fields that spans from fundamental and applied research to industrial applications.

The establishment of the Public Neutron Beam Facility brings J-PARC MLF into line with the SPring-8 - SACLA synchrotron radiation and XFEL facility and the "K Computer" – a next-generation supercomputer project – where the "Public Use Promotion" legislation has already been successfully applied.

The Public Beamlines at J-PARC MLF

The MLF has capacity to accommodate up to 23 neutron beamlines around the present target station. There are currently thirteen neutron and two muon beam instruments in operation and six new neutron instruments in commissioning or under construction. Of these, five beamlines – all built and owned by JAEA – are a part of the Public Neutron Beam Facility and have been designated as Public Beamlines (Figure 2).

The Public Beamlines cover a wide range of neutron scattering techniques and research applications. Specifically, they are:

- BL01 *4SEASONS* - 4D-Space Access Neutron Spectrometer
- BL02 *DNA* - Biomolecular Dynamics Spectrometer
- BL15 *TAIKAN* - Small and Wide Angle Neutron Scattering Instrument

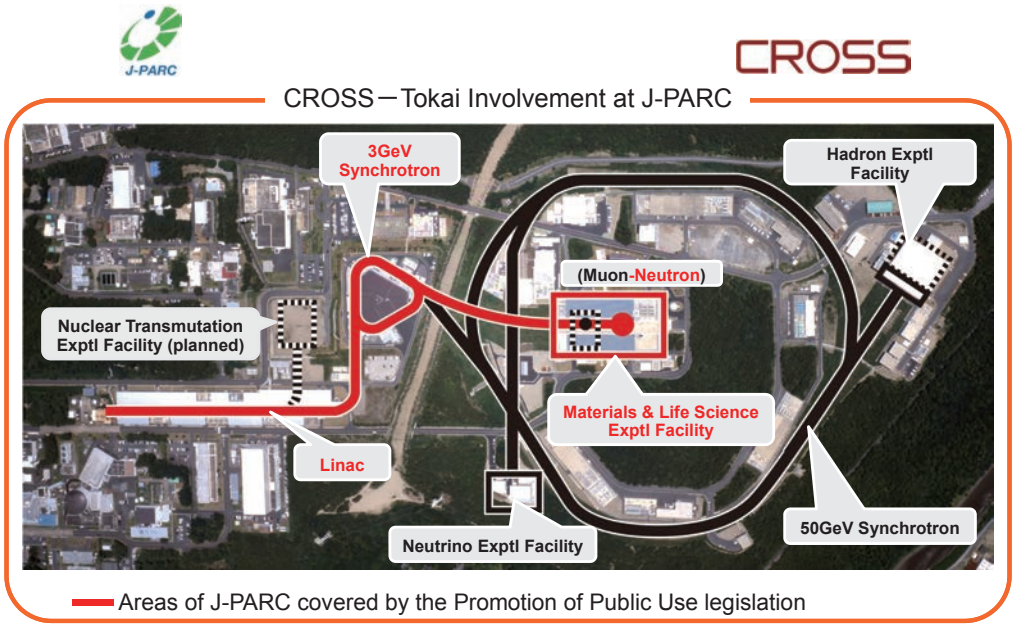

Figure 1. The Public Neutron Beam Facility at J-PARC (Shown in red).

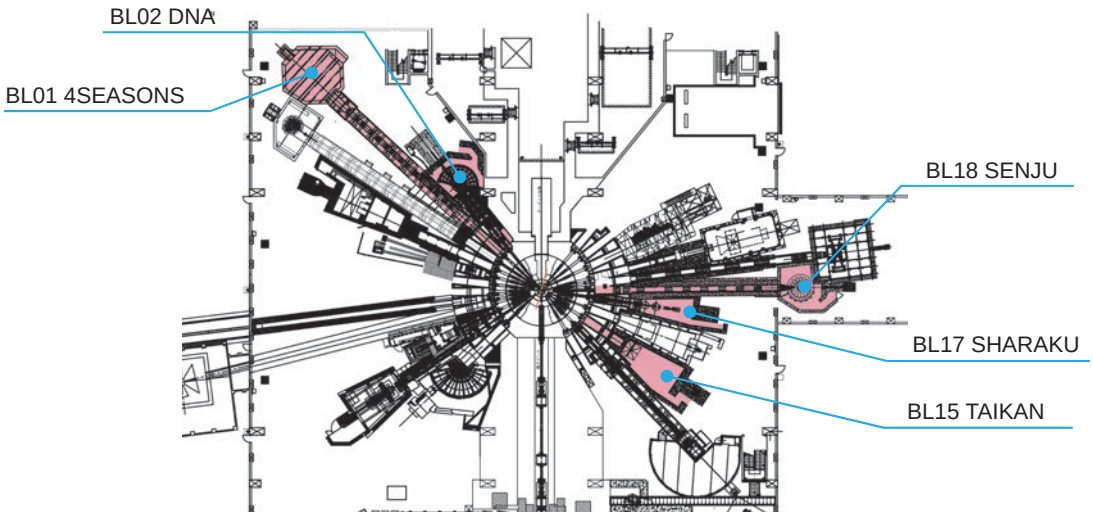

Figure 2. Layout of the Public Beamlines in the MLF Experimental Hall.

- BL17 *SHARAKU* - Polarized Neutron Reflectometer
- BL18 *SENJU* : Extreme Environment Single Crystal Neutron Diffractometer

CROSS and the Public Beamlines

The "Public Use Promotion" legislation requires that the user program on the Public Beamlines be managed and supported by an independent, third-party organization in preference to the original builder of these instruments (JAEA). This organization is known as the "Registered Institution for Facility Use Promotion" (Registered Institution).

CROSS submitted an application to be appointed as the Registered Institution for the Public Beamlines at J-PARC to the Ministry of Education, Culture, Sports, Science and Technology (MEXT) in February 2011 and was formally confirmed in the role by the Minister the following month. Accordingly, CROSS commenced operations from its Tokai offices within the Ibaraki Quantum Beam Research Center building adjacent to the J-PARC site on the 1st of April 2011 and CROSS-Tokai was born.

The Relationship between CROSS-Tokai and J-PARC Center

Although the Public Use Promotion legislation stipulates that CROSS-Tokai must be independent of JAEA and KEK – the co-owners and operators of J-PARC MLF – there is an inevitable and desirable level of cooperation and collaboration that is driven by the common objectives and interdependence of CROSS-Tokai and J-PARC Center. Indeed, the most recent publication of the MEXT basic policy governing the Public Neutron Beam Facility (February 2011) requires a level of cooperation between the stakeholders that will yield high quality research results while maintaining the support and confidence of the Japanese public. Accordingly, CROSS-Tokai is committed to operating in close collaboration with JAEA and KEK and, at the same time, building research cooperation and personnel networks with related facilities – both domestic and international – local authorities and the wider community.

Figure 3 shows a schematic representation of the operational and functional relationship between CROSS-Tokai and JAEA.

The Role of CROSS-Tokai

As Registered Institution for the Public Beamlines at J-PARC MLF, CROSS has wide-ranging responsibilities. Specific operational requirements and organizational expectations are set out in the Public Use Promotion legislation and associated policy documents (See the CROSS-Tokai website for details http://www.cross-tokai.jp/).

In practical terms, the core functions of CROSS-Tokai can be summarized as follows:

- *Proposal Selection and Beamtime Allocation on the Public Beamlines*
  - Develop and administer a fair and open proposal submission and evaluation process that

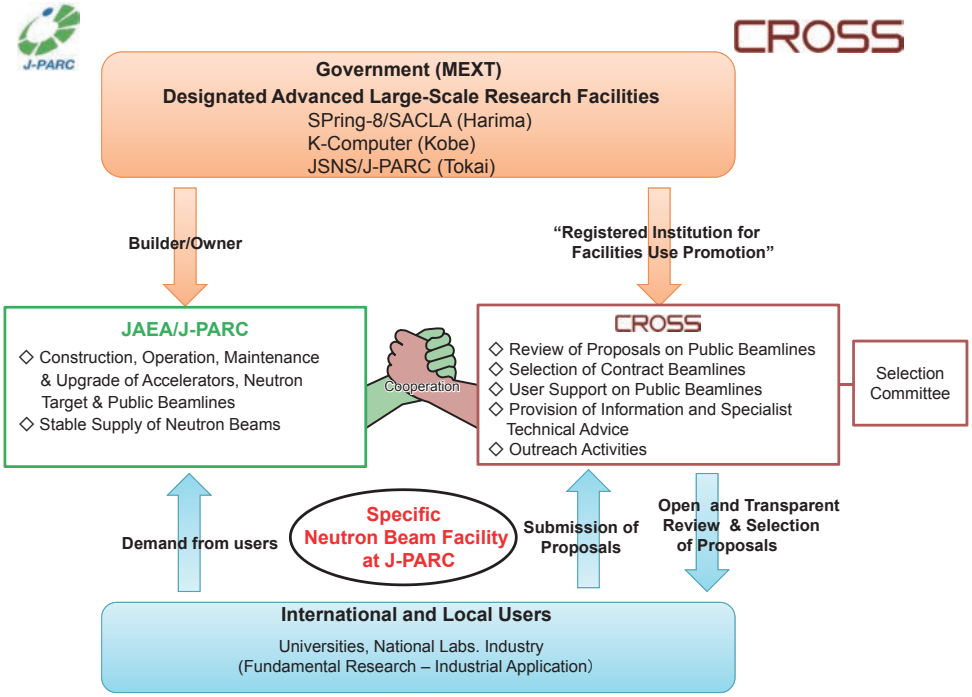

Figure 3. The relationship between and respective functions of JAEA and CROSS-Tokai.

facilitates neutron-based experiments from fundamental, applied and industrial research fields
  - Establish and coordinate the activities of the Selection Committee
  - Provide mechanisms to promote and support strategic research areas as identified through government policy and in response to changing national and international circumstances
- *User Support on the Public Beamlines*
  - Provide coordinated and user-oriented support to the experimental activity on the Public Beamlines
  - Provide beamline services and associated facilities that are responsive to user expectations and reflect international best practice
- *Information Resource for Facility Users*
  - Build and maintain a website that serves to provide information about:
    - Facility news and events
    - User program and other services
    - Beamline and support facility details
    - Organizational and staff contact details
    - Organizational, technical and research publications
  - Provide specialist technical advice via Science Coordinators and other expert staff
- *Outreach and Facility Promotion*
  - Promote leading-edge research and publicize outcomes via symposiums and online media
  - Host and organize conferences, workshops and seminars
  - Produce and distribute promotional brochures, pamphlets etc.
  - Enhance User Program – online systems, modes of service delivery etc.
  - Proactively promote international conferences and symposiums and present CROSS-Tokai activities and the Public Beamlines in these forums
  - Support and promotion of science and technology related activity in the local area
  - Strengthening Industry-Academia collaboration
- *Contract Beamline Assessment and Selection*
  - Manage the assessment, selection and implementation of proposals to build beamlines put forward by external organizations
  - These activities to be undertaken in close cooperation with the government and facility owners within an equitable selection framework

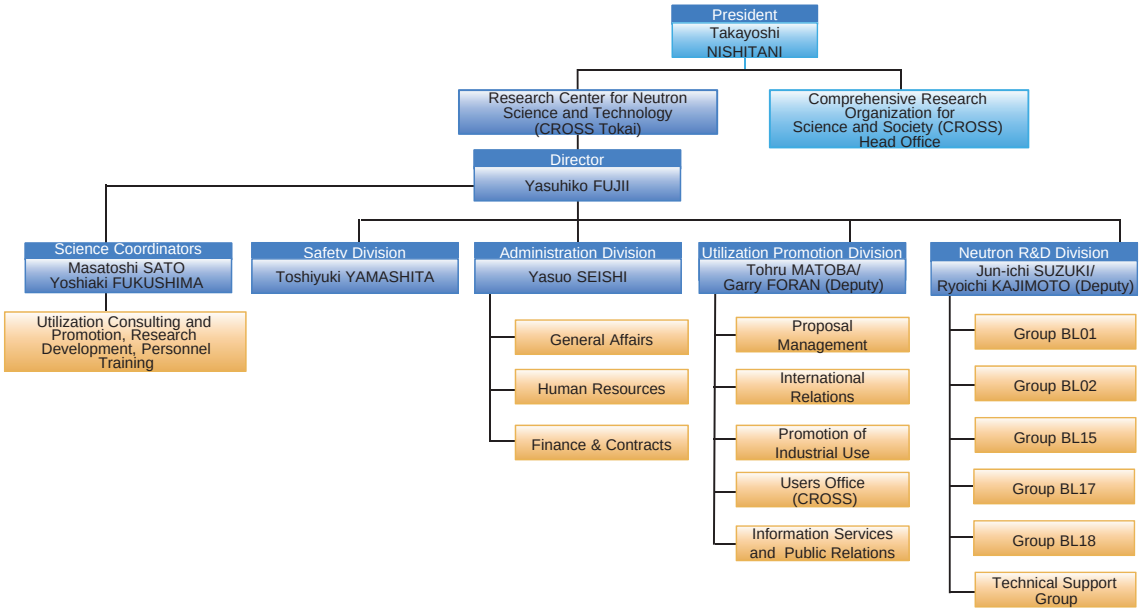

Figure 4. The CROSS-Tokai Organization Chart and Leadership Team.

The Activities of CROSS-Tokai in 2011

Overview

It is now one year since CROSS-Tokai commenced operations in support of the Public Beamlines at J-PARC MLF. It has been a year in which great progress has been made: not only in recovering from the effects of the 11 March 2011 earthquake, but also in establishing and building the presence of CROSS-Tokai at J-PARC.

The CROSS-Tokai team is now comprised of a full complement of 48 research and support staff engaged in activities across the full scope of the CROSS-Tokai mission (Figure 4).

During FY2011, the footprint of CROSS-Tokai in the J-PARC precinct dramatically increased not only in terms of personnel, but also from the viewpoint of supporting facilities and infrastructure. The hub of CROSS-Tokai's activities outside the MLF Experimental Hall has been established in the IQBRC Building – home to the J-PARC Center Users Office – with office space and user facilities being fitted out and put into service progressively throughout the year (See details below).

Key CROSS-Tokai activities and achievements in FY2011 include:

User Support

- Now supporting user operations and ongoing commissioning activities on the five Public Beamlines with Neutron R&D team of 23 scientists, programmers, engineers and technicians
- User Facilities under construction in the IQBRC
  - User Experiment Preparation Laboratory I - Hard Matter
  - User Experiment Preparation Laboratory – Soft Matter & Biomaterials
  - User Data Analysis Room
  - User Lounge
  - "Refresh Rooms"

Proposal Selection

- Established a framework and mechanism for proposal selection on the Public Beamlines
- 2011B Call for Proposals – July-Aug 2011
- 2012A Call for Proposals – Nov-Dec 2011
- Supported the work of committees associated with proposal selection:
  - Selection Committee – Convened 13 Jul 2011, 14 Nov 2011 & 13 Mar 2012
  - Proposal Evaluation Committee & Expert Panels – Convened 3-4 Nov 2011 & 29 Feb-1 Mar 2012
  - CROSS Development Proposal Evaluation Panel – Convened 17 Feb 2012
  - "Trial Use Access System" Task Force – Convened 31 Aug 2011, 10 Oct 2011 & 2 Feb 2012

User Experiment Preparation Laboratory I

User Experiment Preparation Laboratory II

User Data Analysis Room

User Lounge

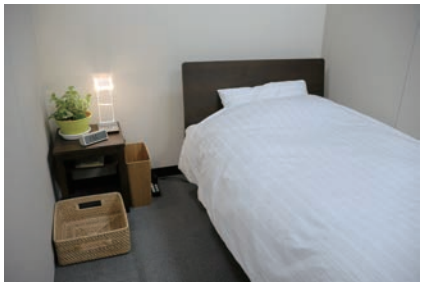

Refresh Rooms

Figure 5. CROSS-Tokai User Facilities in the IQBRC Building.

The 1st Selection Committee Meeting 13 Jul 2011

The 2nd Selection Committee Meeting 14 Nov 2011

The 3rd Selection Committee 13 Mar 2012

Figure 6. Scenes from the meetings of the Selection Committee in FY2011.

Outreach and Facility Promotion

- **CROSS*roads* Workshop Series**
  - CROSSroads Workshop on Strongly-Correlated Systems – Tokai, 17-18 Oct 2011
  - CROSSroads Workshop on SANS Research at J-PARC MLF – Tokai, 14 Mar 2012
- **CROSS Industry Seminars**
  - NISSAN Motor Company – 21 Dec 2011
  - Toyota Central Laboratories – 23 Jan 2012
- **Other Conferences, Symposiums and Workshops**
  - Workshop on Magnetic Structure Analysis from Neutron Powder Diffraction – Tokyo, 9 Aug 2011
  - Workshop on Battery Materials – Tokyo, 17 Nov 2011†
  - 1st Asia-Oceania Conference on Neutron Scattering (AOCNS) – Tsukuba, 20-24 Nov 2011†
  - Workshop on Advances in Neutron Science for the Study of Materials Anisotropy, Strength and Deformation Properties – Tokyo, 29-30 Nov 2011†
  - 1st CROSS-JASRI Workshop - New Opportunities for Neutrons and SR in Solar Battery R&D – Tokyo, 16 Jan 2012†
  - 3rd MLF Symposium – Tokai, 19-20 Jan 2012†

Figure 7. Scenes from the Trial Use Information Days
Tokyo, 8-9 Feb 2012.

Figure 8. Dr Kazuki Ohishi of CROSS-Tokai (second from left).
At his award presentation

- Trial Use Information Days – Tokyo, 8-9 Feb 2012 (Figure 7)
- Workshop on SANS Data Analysis – Osaka, 28-29 Feb 2012†

† Co-hosted by CROSS-Tokai

Other Activities and Achievements

- **Awards and Prizes**
  - The Society of Materials Science, Japan Annual Activity Prize
    Awarded to: Koji Kiriyama (CROSS-Tokai Neutron R&D Division) – 25 Apr 2011
  - The Japanese Society for Neutron Science Technology Award
    Awarded to: Ryoichi Kajimoto*, Mitsutaka Nakamura, Yasuhiro Inamura, Takeshi Nakatani, Wataru Kambara, Tetsuya Yokoo and Fumio Mizuno (* CROSS-Tokai Neutron R&D Division) – Nov 2011
  - The Crystallographic Society of Japan Nishikawa Prize
    Awarded to: Yasuhiko Fujii (Director, CROSS-Tokai) – Nov 2011
    JAEA Chairman's Award for Research and Development
    Awarded to: Satoshi Koizumi, Youhei Nouda, Daisuke Yamaguchi, Takayuki Oku, Jun-ichi Suzuki* and Hiroki Iwase* (* CROSS-Tokai Neutron R&D Division) – Nov 2011
  - The Iron and Steel Institute of Japan Research Publication Prize
    Awarded to: Hisao Yasuhara, Kaoru Sato, Tohji Yuki, Ohnuma Masato, Jun-ichi Suzuki* and Yo Tomota (* CROSS-Tokai Neutron R&D Division) – 25 Mar 2012
  - The Society of Muon and Meson Science of Japan Young Researcher Encouragement Prize (Figure 8)
    Awarded to: Kazuki Ohishi (CROSS Neutron R&D Division) – 26 Mar 2012

BL02: Si Crystal Analyzer near Backscattering TOF Spectrometer DNA

Introduction

A Si crystal analyzer near backscattering TOF spectrometer DNA was under construction and beam commissioning in JFY2011. The instrumental specifications for DNA are shown in Table 1.

Table 1. Instrumental specifications of DNA.

Items	Specification
Neutron source (NS)	Coupled Liquid H_2 Moderator
L_1 (source-sample)	42 [m]
L_2 (sample-analyzer)	~ 2.3 [m]
L_3 (analyzer-detector)	~2.0 [m]
Pulse sharpening chopper (PS-chopper)	
	Max speed: 300Hz at ~7.5m from NS
Crystal Analyzer	
Crystal and reflection index	Si(111)
	Si(311) in plan
Bragg angle of analyzers	~87.5 [deg.]
Energy resolution	~1.5 [μeV]: Si(111)
	~12 [μeV]: Si(111)
	without PS-chopper
	~5 [μeV]: Si(311)
Momentum range	0.07 < Q < 1.98 [A^{-1}]: Si(111)
	0.60 < Q < 3.80 [A^{-1}]: Si(311)
Scan energy range	-25 < E < 45 [μeV]:
	Single pulse scan around E_f
	-500 < E < 500 [μeV]:
	without PS-chopper in second frame

(the plan as of the end of march 2012)

This type spectrometer covers the area of the micro-eV energy range in the *Q-E* space. Many users program will be expected in science field such as biophysics, confined liquids, fast ionic conductors and so on.

Construction works in JFY2011

In JFY2011, main construction works were the installation of super mirror guides, vacuum chamber, analyzer crystal units and detector amplifier units as shown in the following photos.

Figure 1. The insertion of a super mirror guide into a metal jacket. (October 22, 2011)

Figure 2. The alignment works of super mirror guide in BL02 beam line by laser tracker. (October 22, 2011)

Figure 3. The delivery of the DNA vacuum chamber. (September 30, 2011)

Figure 4. The installation of the DNA vacuum chamber. (October 13, 2011)

Figure 5. The installation of analyzer crystal units. (January 06, 2012)

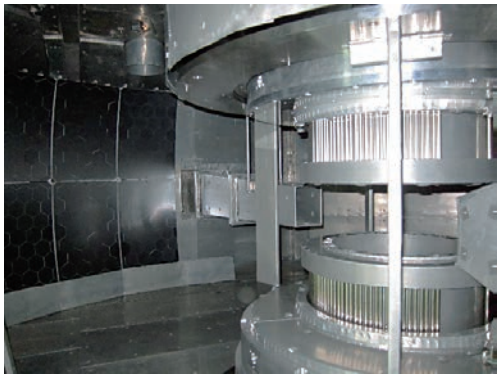

Figure 6. The installation of analyzer crystal units and detector amplifier units. (March 02, 2012)

Results of Beam Commissioning in JFY2011

The commissioning has been started from the beginning of February 2012. In this period, the pulse sharpening high speed chopper could not be operated, then we operated DNA spectrometer without the pulse sharpening chopper at energy resolution dE~12μeV. Figure 7 shows the comparison in the measurements of tunneling spectrum between BL14 and BL02. The level of background was found to be of the same order between two spectrometers.

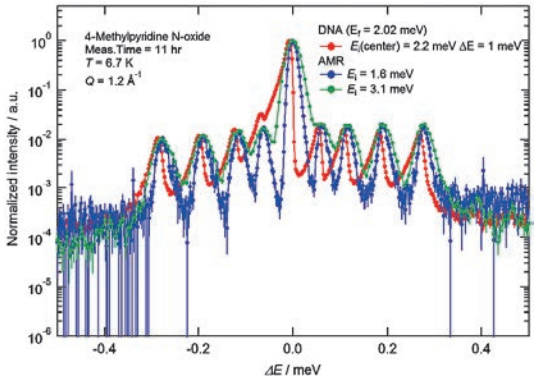

Figure 7. A comparison the measurements of tunnel spectrum for 4-Methylpyridine N-oxide powder between BL14 and BL02.

Schedule in JFY2012

The user program will start form 2012A period. And the commissioning with pulse sharpening chopper will start form the autumn of 2012.

References

[1] N. Takahashi, *et al.*, Journal of Physics and Chemistry of Solids 68, 2199-2203 (2007).

K. Shibata[1], N. Takahashi[2], Y. Kawakita[2], K. Kamazawa[1], T. Yamada[1], K. Nakajima[2], W. Kambara[2], Y. Inamura[2], T. Nakatani[2], K. Soyama[3], K. Oikawa[4], N. Hosoya[2], T. Iwahashi[2], Y. Ito[2], H. Tanaka[2] , K. Aizawa[2], M. Arai[5], and S. Fujiwara[6]

[1]Neutron R&D Division, CROSS-Tokai; [2]Neutron Science Section, Materials and Life Science Division, J-PARC Center; [3]Neutron Instrumentation Section, Materials and Life Science Division, J-PARC Center; [4]Neutron Source Section, Materials and Life Science Division, J-PARC Center; [5]Materials and Life Science Division, J-PARC Center; [6]Quantum Beam Science Directorate, JAEA

Development of BL09 SPICA

East Japan Earthquake

The Great East Japan Earthquake hit the east area of Japan at 14:46 JST on March 11, 2011. At J-PARC the earthquake was felt at level 6 of the seismic intensity scale. The BL09 annex building moved to the north by 3 cm and to the west by 7 cm, and subsided by 10 cm. Fortunately, the construction of SPICA had not been started yet at the time when the quake occurred.

Design concept of SPICA

SPICA has been designed to be of high resolution and high intensity. This means the moderator should be sharp enough (a decoupled-poisoned moderator was chosen), the flight path should be long and the focusing guide should be incorporated. The flight path between the moderator and the sample position is L_1 = 52 m. Since, according to the simulation of the guide tube, the elliptical guide shows an excellent performance over a wide range of wavelengths, we adopted the elliptical super-mirrors guide tube to keep high intensity at the sample position. Figure 1 shows the calculated map of the neutron intensity distribution at the sample position.

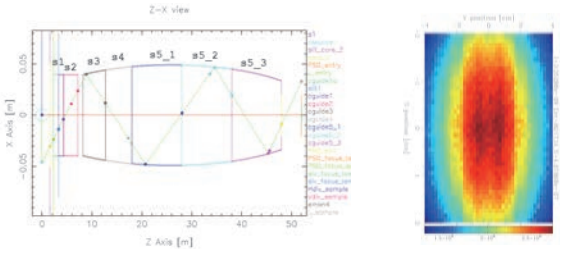

(a) (b)

Figure 1. Schematic diagram of the elliptic supermirrors in the guide tube of SPICA (a) and the neutron intensity distribution map at the sample position (b).

SPICA was designed to consist of three detector banks: the backward detector bank (150-175º), the multipurpose detector bank (13-140º) and the small angle detector bank (1-25º). The distance L_2 from the sample to the detectors is about 2 m for all banks. To cover this large detector area, about 1600 one-dimensional ^{3}He position-sensitive detectors (60 cm in length and half inch in diameter) are used.

Construction of SPICA

The photographs of the construction of the beamline and its shieldings are shown in Fig. 2. In Fig. 2(a), we look in the direction of the neutron target from SPICA and Fig. 2(b) indicates the view from the upper stream of the neutron source.

(a) (b)

Figure 2. The BL09 beamline line with the elliptical supermirrors. The Fig. 2(a) is the view from SPICA and (b) is the view from the neutron target.

The beamline and the SPICA instrument are shielded with neutron shielding concrete. The shield optimization with new novel neutron shielding concrete was performed to reduce the skyshine dose rate of neutron and γ-ray radiations instead of a conventional shield configuration of iron, polyethylene and B_4C resin.

First beam at SPICA

On February 8, 2011, we detected the first neutron beam at the position of 1 m away from the end of the guide tube. Fig. 4 indicates the detected neutron beam without and with silhouette characters made of cadmium sheets, and the group photographs.

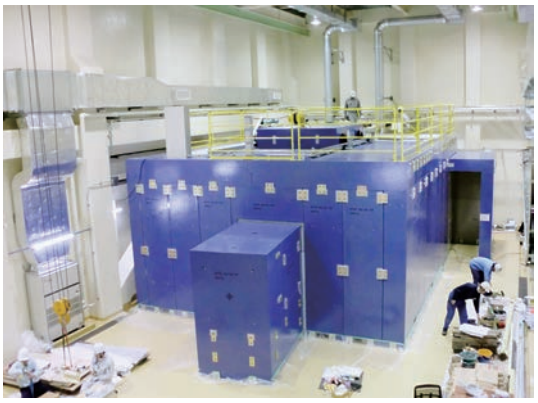

Figure 3. The shield of SPICA diffractometer at BL09.

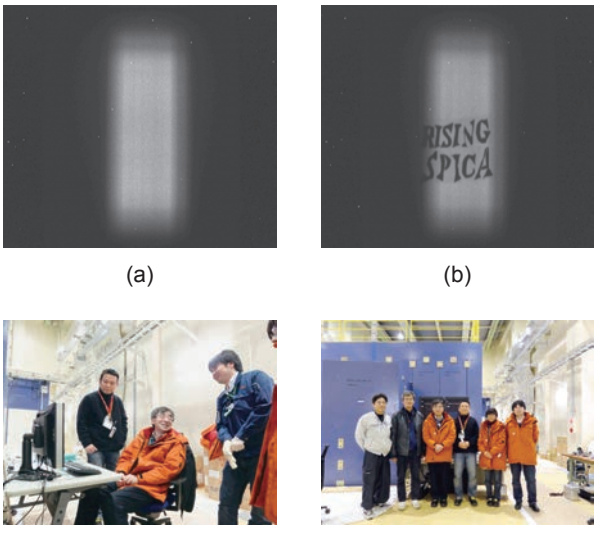

(a) (b)

(c) (d)

Figure 4. The neutron beam imaging and group photographs. The silhouette shown in (b) (RISING SPICA) was made of cadmium foil.

As shown in Fig. 5, the homogeneities of neutron beam intensities along the line A-B (horizontal direction) and C-D (vertical direction) are in fair condition, which means considerable good efficiency of the guide tube equipped with the elliptical supermirors.

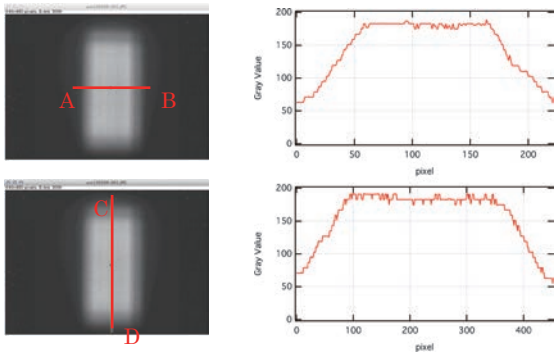

Figure 5. The homogeneity of neutron beam (see text).

M. Yonemura[1,2], T. Kamiyama[1,2], M. Nagao[1,2], Y. Onodera[3], S. Torii[1,2], M. Kawai[1,2], K. Mori[3], and T. Fukunaga[3]

[1]Neutron Science Section, Materials and Life Science Division, J-PARC Center; [2]Institute of Materials Structure Science, KEK; [3]Research Reactor Institute, Kyoto University

BL11: Completion of High Pressure Neutron Diffractometer PLANET

PLANET is a powder diffractometer designed specifically for high-pressure experiments. This year started with checking the damage to the beamline caused by the earthquake. Then, we repaired it and continued the construction.

In March 2012, we finished the construction and the commissioning started. Here, we introduce these issues in the above order.

The evaluation of the incident beam

Due to the robust design of the beamline, we did not see any substantial damage to the beamline devices. The only substantial effect was the inclination of the experimental hall and the resulting shift of the super-mirror guide from its original position. Figure 1 shows the shift of the center of the mirror components at each section. To check the effects on the incident beam nature, we measured the spatial distribution and the beam flux at the sample position. Figure 2 shows the difference of the beam center from the designed position. The beam center deviated by 1.5 mm in the upward and 1.5 mm toward the BL12 side. The beam flux was estimated from the radioactivation of the Au foil placed at the sample position. The beam flux within the area of 10 mmϕ amounted to 98% of the designed value, while that within the area of 3 mmϕ showed a worse correspondence.

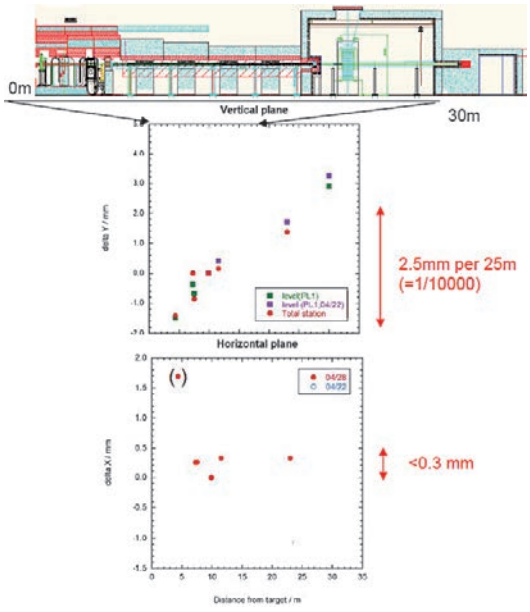

Figure 1. Shift of the center position of the supermirror at each section.

Construction of the beamline

We installed two components which are the key to the success of this beamline. The one is the 90 deg. detector bank equipped with foldable neutron shielding panels and the radial collimator alignment system. In spite of the complex mechanism in folding the panels, the detector bank system worked well.

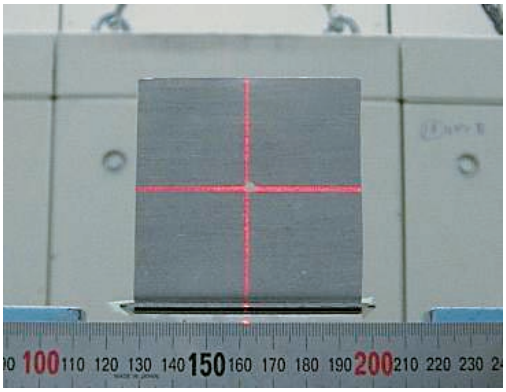

Figure 2. Shift of the beam center (hole in Cd) from the designed position (red cross).

Figure 3. Detector banks with the foldable shielding panels and the alignment system for radial collimators.

Figure 4. The 6-axis multi-anvil press “ATSUHIME” installed in the experimental hutch.

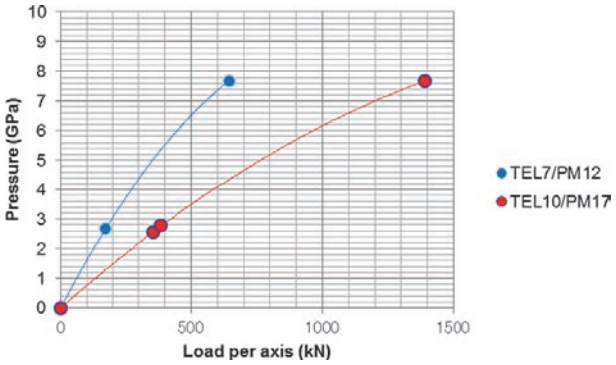

Figure 5. Pressure generation curve of the multi-anvil press when using the WC anvils and ZrO_2 pressure transmitting medium.

The second one is the 6-axis multi-anvil press which was installed on Feb. 29, (see Fig.4). Figure 5 shows the results of the high-pressure generation test. By using a pressure transmitting medium with the size of 17 mm cube, we can approach the pressure of 7.7 GPa (Bi III-V transition). This result indicates that we can conduct high-pressure neutron experiments at 10 GPa using a relatively large sample with a volume of 21 mm^3.

The construction of the hardware has been almost finished, and now we are installing the software. The commissioning will be finished in the spring of 2012, and the PLANET will be used by project members in the next autumn. The beamline will be opened for general users after JFY 2013.

This project is supported by Grant-in-Aid for Creative Scientific Research (19GS0205) from the Japan Society for Promotion of Science and Grant-in-Aid for Scientific Research on Innovative Areas (No. 20103001) from the Ministry of Education, Culture, Sports, Science and Technology (MEXT) of Japan.

T. Hattori[1,2], A. Sano[1,2], H. Arima[3], A. Yamada[4] W. Utsumi[1,2], H. Kagi[5], and T. Yagi[4]

[1]Neutron Science Section, Materials and Life Science Division, J-PARC Center; [2]Quantum Beam Science Directorate, JAEA; [3]Institute for Material Research, Tohoku University; [4]Geodynamics Research Center, Ehime Univ; [5]Graduate School of Science, The University of Tokyo

Development and Commissioning of TAIKAN

The small and wide angle neutron scattering instrument TAIKAN (BL15) restarted beam operation on January 24, 2012 following repair and upgrading after the Great East Japan Earthquake, which occurred on March 11, 2011. TAIKAN was developed more than on March 8, 2011, which was the first day of beam operation. But the greatest change occurred in the staff. TAIKAN was registered as one of public beamlines under the legislation for the "Promotion of Public Utilization of Specific Advanced Large Research Facilities" in 2011 and a new staff of CROSS-Tokai joined the group of TAIKAN. The staff of the J-PARC center and CROSS-Tokai shown in Fig. 1 has engaged in user support and research activities at TAIKAN.

Figure 1. A souvenir picture taken on the day of restarting the beam operation.

Figure 2 shows a 3D image of TAIKAN. TAIKAN is composed of a set of components: optical devices, 4 choppers, a sample stage, a vacuum chamber, and 5 detector banks. On the small-angle and the middle-angle detector banks in the vacuum scattering chamber, 632 and 136 ^{3}He PSD tubes with 8 mm in diameter and about 0.6 MPa in ^{3}He gas pressure have been installed, respectively. On the high-angle detector bank in the atmosphere 104 ^{3}He PSD tubes have been installed.

Figure 3 shows the small-angle and the middle-angle detector banks. The minimum q value, q_{min}, reaches 1.5 nm^{-1} with the small-angle detectors and the neutron wavelength of 0.78 nm. At the central part of the small-angle detector bank there is a square area without ^{3}He PSD tubes. The size of the area is about 200 mm^H×200 mm^W. In the rear of this area 32 short ^{3}He PSD tubes and a high resolution 2D detector will be installed as small-angle and an ultra-small-angle detector to make q_{min} smaller down to 5×10^{-3} nm^{-1}.

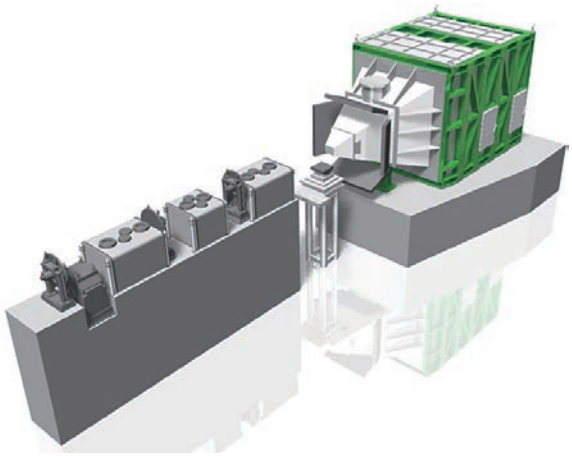

Figure 2. A 3D image of TAIKAN.

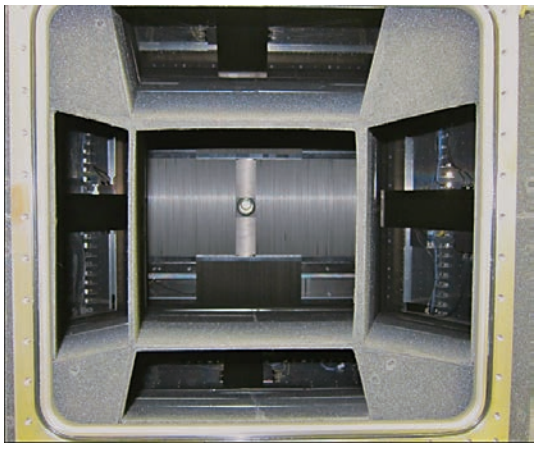

Figure 3. A small-angle and a middle-angle detector banks.

A sample changer was provided. 10-sample set in sample holders can be mounted simultaneously on the sample changer. The temperature of the samples can be controlled between -25 and 125 °C. The sample changer is set on a sample stage with 4-axes (x, y, R_x, R_y(=ω)) goniometer, where the z-axis is defined as it is parallel to the beam axis.

The characteristics of TAIKAN were evaluated with a neutron beam. Figures 4 and 5 show scattering profiles obtained for standard samples of silver behenate and glassy carbon with the small-angle detector bank, respectively. The beam sizes of the samples of silver behenate and glassy carbon are 12 mm×12 mm and 10 mm×10 mm, respectively. The neutron wavelength used in data analysis is from 0.07 to 0.76 nm. For the sample of silver behenate 5 diffraction peaks were observed clearly as shown in Fig. 4. The full width at half maximum of the first diffraction peak is 0.084 nm^{-1}. The ratio of this value and the q value of the peak center (q=1.08 nm^{-1}) is 0.078, even when the scattering profile obtained with short neutron wavelength is included in data analysis. For the sample of glassy carbon Guinier region and Porod region were observed clearly as shown in Fig. 5. A Guinier radius R_g obtained with this scattering profile is 0.69 nm. On the figure an USAXS profile measured by Dr. Ilavsky, who kindly provided us with the sample, of APS is also plotted in arbitrary unit. It was confirmed that the SANS profile almost agreed with the USAXS profile.

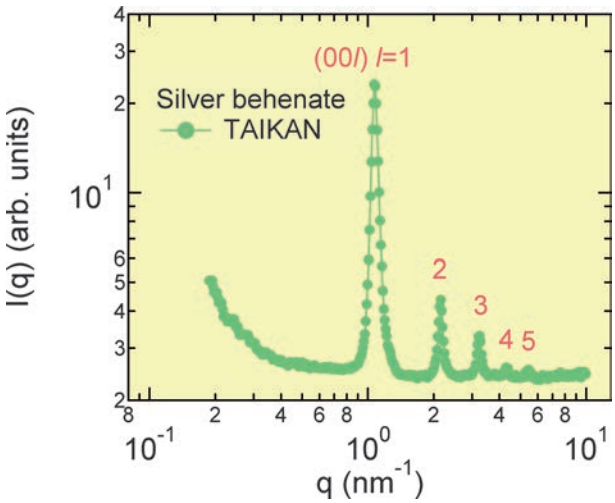

Figure 4. A scattering profile of silver behenate.

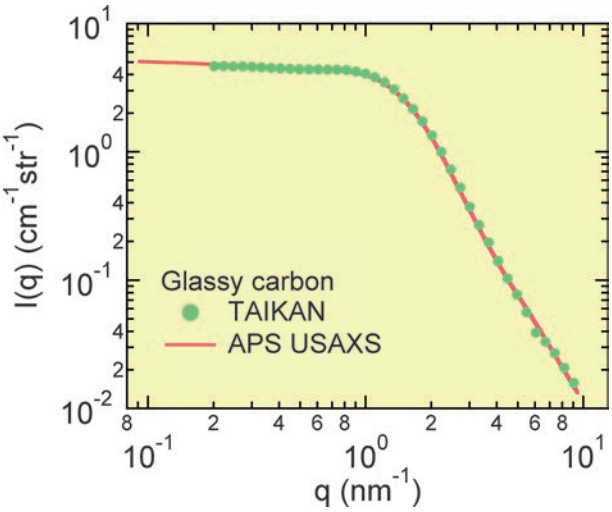

Figure 5. Scattering profiles of glassy carbon.

J. Suzuki[1], S. Takata[2], T. Shinohara[2], T. Oku[2], T. Tominaga[2], T. Nakatani[2], Y. Inamura[2], K. Suzuya[2], K. Aizawa[2], M. Arai[3], T. Otomo[2,4], K. Ohishi[1], H. Iwase[1], T. Ito[1], and M. Sugiyama[5]

[1]Neutron R&D Division, CROSS-Tokai; [2]Neutron Science Section, Materials and Life Science Division, J-PARC Center; [3]Materials and Life Science Division, J-PARC Center; [4]Institute of Materials Structure Science, KEK; [5]Research Reactor Institute, Kyoto University

Polarized Neutron Reflectometer SHARAKU Started User Program

Neutron reflectometry has been widely recognized as an indispensable tool to analyze structures of nanomaterials which have layered structure. In such layered structure, there is existence of interfaces between different materials where new physical phenomena are expected to emerge. This is very important for nanotechnology because it has a close relation to the practical devices. SHARAKU was installed at BL17 as the second neutron reflectometer of MLF reflecting that situation.

SHARAKU was designed to routinely use polarized neutrons while the first neutron reflectometer of MLF, SOFIA, is dedicated to the free surface and interface investigation. Therefore targets of SHARAKU are solid thin films, especially magnetic thin films, and films which contain hydrogenous materials. The hydrogen in the latter sample sometimes causes dominant incoherent scattering. The polarized neutron technique can remove the incoherent scattering background in the neutron reflectivity measurements.

The installation of SHARAKU was almost complete when the earthquake struck in March last year (2011). SHARAKU itself was not seriously damaged by the earthquake. However, we had to do some extra work. We reconstructed a part of the biological shield, and realigned the beam line components such as choppers, beam slits, a polarizer, and so on.

The first neutron beam was introduced to SHARAKU at the end of this January, and we started the commissioning. Typical unpolarized neutron reflectivities are shown in Figs. 1 and 2.

Figure 1 shows unpolarized neutron reflectivity curves from a Ni thin film on a Si substrate. An example of a reflectivity profile of a multilayer sample is shown in Fig. 2. The sample is 20 stacks of a Ni/Ti bilayer on a Si substrate. The designed thickness of both Ni and Ti layer is 5.0 nm. The clear total reflection is observed in the lower-q region, and the fringes appear in the middle-q region in both figures. Bragg peaks from the periodic bilayer of Ni/Ti are seen in addition to the fringes in the data of the multilayer.

A neutron polarizer of SHARAKU consists of $4Q_c$ Fe/Si polarizing supermirrors which align with double-transmission geometry. A stack of the same $4Q_c$ Fe/Si polarizing supermirrors are used for the analyzer. The mirrors are horizontally stacked with a single-reflection geometry in this case. Spin flippers are two-coil Drabkin flippers.

Figure 3 shows the wavelength dependence of the flipping ratios. The maximum flipping ratio is 130, and it linearly decreases with the increase of the wavelength. There is no additional fine structure.

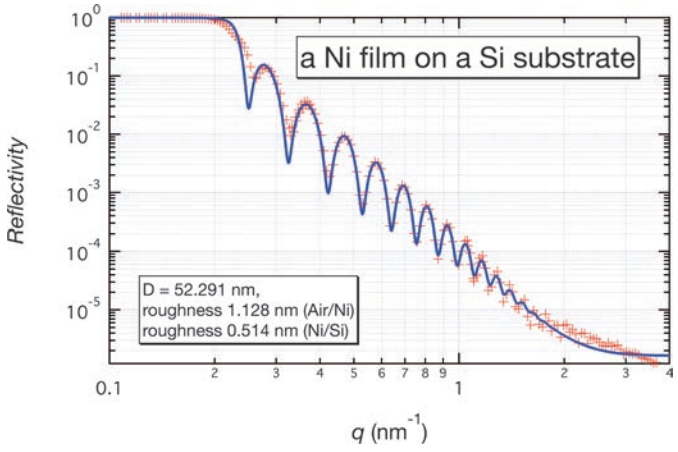

Figure 1. Unpolarized neutron reflectivity of a Ni thin film on a Si substrate. Experimental data are plotted by "+", and the best fitting curve is drawn by a solid line.

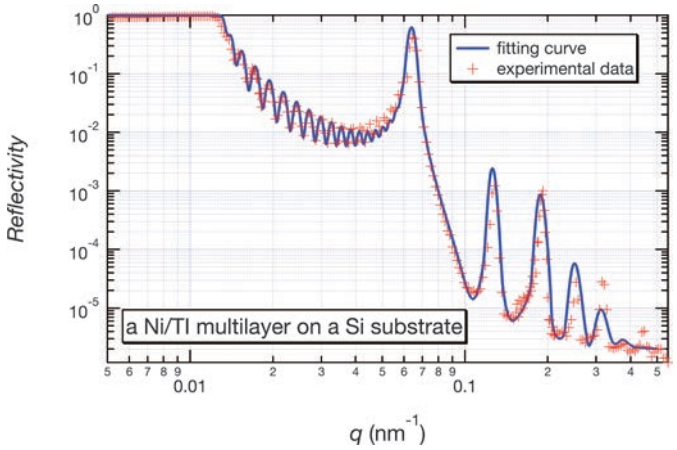

Figure 2. Unpolarized neutron reflectivity of a [Ni(5nm)/Ti(5nm)] ×20 multilayer on a Si substrate. Experimental data are plotted by "+", and the best fitting curve is drawn by a solid line.

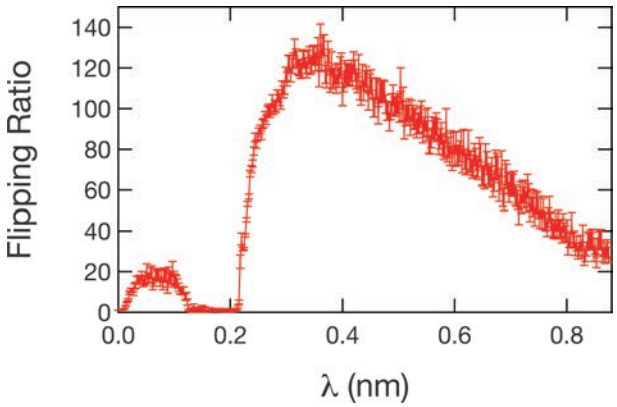

Figure 3. The wavelength dependence of flipping ratio using the polarizer and the analyzer of SHARAKU.

It enables us to do a simple data correction. We did not evaluate the flipping efficiencies of the two-coil flippers, but this graph shows that they work properly.

In the end of fiscal year 2011, SHARAKU was ready to use although the reflectometer was still at a commissioning stage. We started the user program in the 2011B MLF operation. We are waiting for your proposals and are looking forward to seeing you in the BL17 cabin.

References

[1] M. Takeda *et al.*, Chinese J. Phys. **50**, (2012) 161.

M. Takeda[1,2], D. Yamazaki[2,3], K. Soyama[2,3], R. Maruyama[3], H. Hayashida[3], H. Asaoka[1,2], T. Yamazaki[2], K. Aizawa[1], M. Arai[1], Y. Inamura[1], T. Itoh[1], W. Kambara[1], K. Kaneko[1,2], T. Nakamura[3], T. Nakatani[1], K. Oikawa[4], T. Ohhara[5], K. Sakasai[3], T. Shinohara[1], K. Suzuya[1], N. Takahashi[1], S. Takata[1], I. Tamura[6], K. Toh[3], H. Yamagishi[3], T. Hirano[7], N. Yoshida[5], Y. Sakaguchi[5], M. Mizusawa[5], J. Suzuki[5], J. Sato[5], and K. Kiriyama[5]

[1]Neutron Science Section, Materials and Life Science Division, J-PARC Center; [2]Quantum Beam Science Directorate, JAEA; [3]Neutron Instrumentation Section, Materials and Life Science Division, J-PARC Center; [4]Neutron Source Section, Materials and Life Science Division, J-PARC Center; [5]Neutron R&D Division, CROSS-Tokai; [6]Department of Research Reactor and Tandem Accelerator, JAEA; [7]Hitachi Research Laboratory, Hitachi Ltd., Hitachi

Commissioning of BL18 SENJU

SENJU is a new TOF single-crystal neutron diffractometer. SENJU is designed for precise crystal and magnetic structure analyses under multiple extreme environments such as low-temperature, high-pressure and high-magnetic field. SENJU is also designed for taking diffraction measurement of small single crystals less than 1.0mm^3 in volume.

The commissioning of SENJU had been scheduled to begin in April 2011 but was delayed due to severe damage to the instrument shield caused by the earthquake of March 11, 2011. The SENJU instrument team (Fig. 1) spent one year to deconstruct the beamline, repair damaged components, and rebuild the instrument.

On March 5, 2012, the first neutron beam was delivered to the sample position. Subsequently, the 2-dimensional detectors, goniometers, sample environment equipment and the device control software were tested and conditioned. At the same time, diffraction images of several organic and inorganic single crystals such as NaCl, 12CaO· 7Al_2O_3 (Fig. 2), glycine and sucrose were measured at room temperature (RT). In these measurements, Bragg reflections in the high-Q region (d-spacing < 0.5 Å) were successfully observed in some organic and inorganic crystals.

Figure 1. The SENJU instrument team.

In the case of a 1 x 1 x 1 mm^3 size NaCl crystal, intensity data were acquired with a duration time of 7.5 hours. The calculated unit cell parameters from the positions of the observed Bragg reflections (a = 5.640(2) Å, b = 5.660(6) Å, c = 5.643(8) Å, α = 90.2(2)º, β = 89.95(5) º, γ = 90.09(5)º) coincided well with the expected values (a = b = c = 5.64 Å, α = β = γ = 90º). The total of 88 Bragg reflections were recorded and used in the structural analysis. The final R-factor was R = 3.25% and the obtained parameters well agreed with the previously reported ones.

Bragg reflections were also successfully observed from a small, laboratory X-ray size single crystal of NaCl (0.3 x 0.3 x 0.1 mm^3) with a 50 hour exposure time at 200 kW beam power. This result suggests that the structural analyses of laboratory X-ray size crystals using neutron diffraction on SENJU should become feasible when the J-PARC accelerators achieve 1MW.

The data processing procedure has also been developed and tested. The successful structural analysis of a 1 mm^3 NaCl crystal at SENJU as described above indicates that both the data meas-

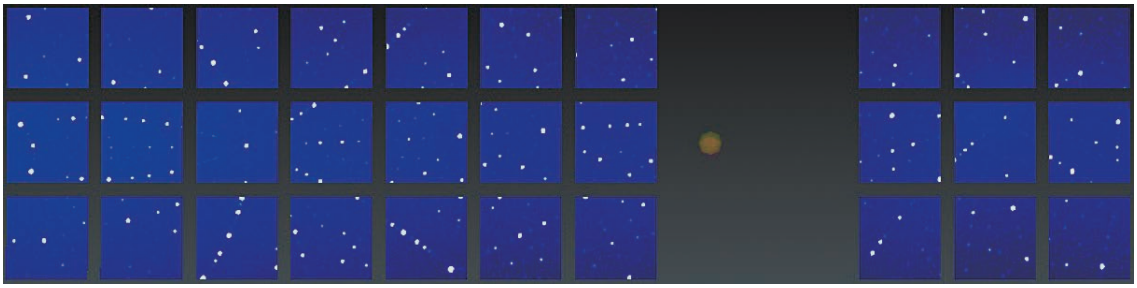

Figure 2. The diffraction image of a 12CaO•7Al_2O_3 single crystal measured at SENJU.

urement and processing procedure at SENJU are reliable.

A commissioning of a 4K cryostat for SENJU was also started. Inside the cryostat, a small piezo-electric motor based fixed-χ type two-axis goniometer, rotatable at low temperature, is attached to a cold finger. By optimizing the wiring of the motors, a base temperature of 3.0 K at the top of the goniometer was achieved within a 3-hour cool down from RT. The first low-temperature experiment using the cryostat was carried out on $TbCoGa_5$ which shows an antiferromagnetic order below 35 K [1] The measurement at 50 K and 10 K reveals that magnetic Bragg reflections derived from the ordering with ***q***=(1/2 0 1/2) were clearly observed at 10 K (Fig. 3).

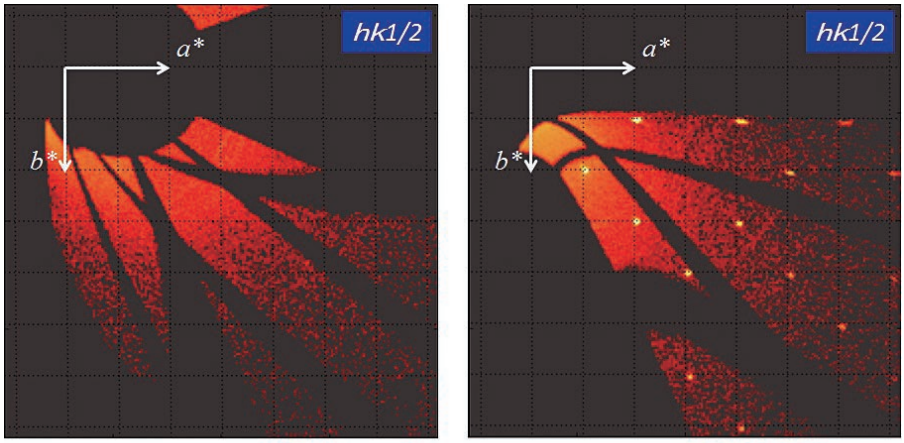

Figure 3. The (*h k 0.5*) plane of $TbCoGa_5$ at 50 K (left) and 10 K (right) measured on SENJU. Magnetic Bragg reflections derived from antiferromagnetic ordering is clearly observed at 10 K.
(the sample was provided by Suzuki group, Yokohama National University.)

Reference

[1] R. Watanuki *et al.*: J. Phys. Soc. Jpn. **80** (2011) SA083.

T. Ohhara[1], R. Kiyanagi[2], T. Kawasaki[2], K. Oikawa[3], I. Tamura[4], K. Kaneko[2,5], A. Nakao[1], T. Hanashima[1], and K. Munakata[1]
[1]Neutron R&D Division, CROSS-Tokai; [2]Neutron Science Section, Materials and Life Science Division, J-PARC Center; [3]Neutron Source Section, Materials and Life Science Division, J-PARC Center; [4]Department of Research Reactor and Tandem Accelerator, JAEA; [5]Quantum Beam Science Directorate, JAEA

TAKUMI at BL19

Damages from the earthquake & recovery

TAKUMI suffered significant damages from the big earthquake on March 11; the satellite building sank by about 15 cm, the beam line shields at the joint part between the main building and the satellite building were tilted and 4 m of the neutron guides parts, including the supporting parts inside the shields, were broken. The bolts used to fix the alignment positions of the detector frames were also broken and the frames hit the sample table, but fortunately both the detectors and the sample table themselves were saved. The broken neutron guides are shown in Figure 1. To recover TAKUMI, all parts, including the spectrometer shields, were removed, the sunken satellite building was jacked-up, the broken parts were repaired and/or repurchased, and all parts were reinstalled as they were at the time of the construction. The recovery of the main part of TAKUMI finished at the end of February 2012, while the reinstallation of the sample environments is still to be continued. TAKUMI was managed by Kazuya Aizawa and Stefanus Harjo as instrument scientists, Jun Abe as a postdoc and Takaaki Iwahashi as an engineer (not full time) during FY 2011.

Re-commissioning

TAKUMI finally started its re-commissioning on March 6th, 2012. Figure 2 shows the main spectrometer in which all of the main parts have been re-installed, being in the same condition as before the earthquake on March 11. TAKUMI is now ready for experiments. In Figure 3 (top), K. Aizawa is starting the shutter operation of TAKUMI's first beam after the recovery, and the direct beam image observed by neutron camera is shown in Figure 3 (bottom).

TAKUMI's sample table and detector positions, chopper parameters, detector parameters, TOF to d-spacing conversion parameter, 2 mm gauge definition radial collimator setting parameter, and other calibration parameters, had been fixed during its commissioning.

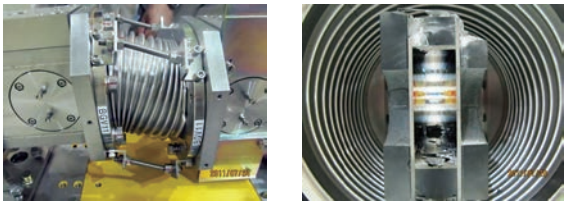

Figure 1. Lattice strain evolution during tensile deformation of A2024 alloy

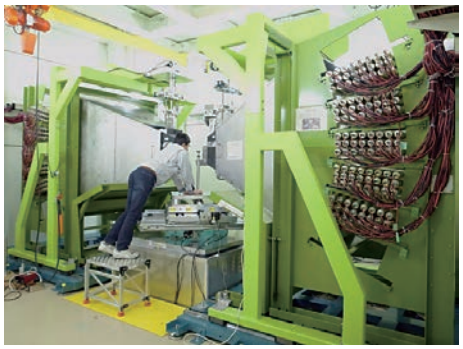

Figure 2. TAKUMI spectrometer room after the recovery (back to its normal condition)

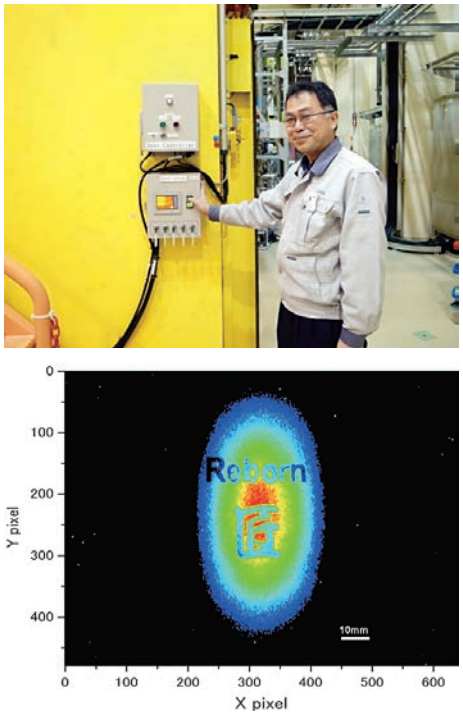

Figure 3. Shutter operation for the first beam for re-commissioning (top), and the direct beam image observed by neutron camera (bottom).

The commissioning of TAKUMI has not been finished yet, but strain mapping measurements and in situ measurements during loading at RT, has been ready to be conducted. Residual strain mapping test on shrink-fit ring & plug of Al alloy has been conducted using a prototype VAMAS sample made in house. The sample used for the measurement is shown in Figure 4 (top), and the results in Figure 4 (bottom). Gauge volumes of 2×2×10 mm^3 and 2×2×2 mm^3 were used for the hoop/radial strain components and axial strain component, respectively. The d0 measurement was not done, but the strain distributions can be seen from the lattice parameter distributions. Hoop and radial components for the same positions were measured at different -90 and +90 deg scattering detector banks to test our setting conditions of the sample table, radial collimators and detector arrangement. As seen in Figure 4 (bottom), both hoop and radial strain components are well reproducibly measured at different detector banks. The three strain components also show good balance.

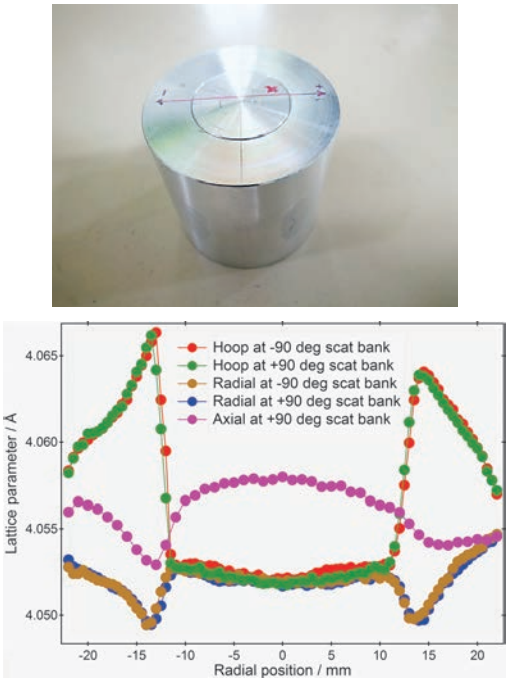

Figure 4. Shrink-fit ring & plug of Al alloy(top), and lattice parameter distributions with respect to the radial position (bottom).

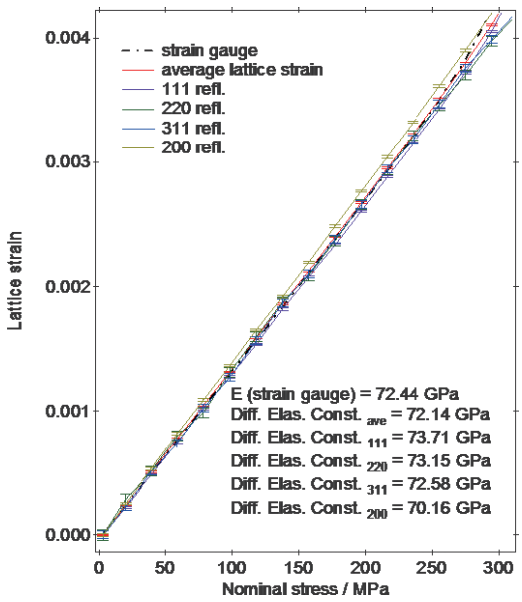

Figure 5. Lattice strain – nominal stress curves obtained during tensile test of alu-minum (A2024) alloy.

A dog bone flat specimen made by aluminum (A2024) alloy was prepared and in situ measurements during tensile deformation were conducted. Strain gauges were glued to the specimen to monitor macroscopic strains. Several stress steps were applied for the elastic region. Figure 5 shows the results of lattice strains plotted with respect to the applied stress. The average lattice strains were in good agreements with the macroscopic strains measured from the strain gauges, showing that the strain accuracy for tensile deformation done at TAKUMI was very good. Moreover, the anisotropy of diffraction elastic constant is also very clearly observed.

User programs

There were many proposals that have been approved to be done at TAKUMI for 2011A. Since TAKUMI and J-PARC were not able to conduct them, several have been transferred to SNS (VULCAN) and ISIS (ENGIN-X). For that, we express our appreciation to the scientists of both instruments.

S. Harjo, K. Aizawa, J. Abe, and T. Iwahashi
Neutron Science Section, Materials and Life Science Division, J-PARC Center

Radiation Shield of U-Line

The U-line construction was started in this fiscal year. A part of the beam line shield was settled in the 2nd experimental hall toward the complete of U-line construction in the summer of 2012 to provide the ultra slow muon beam from the autumn.

A radiation shield was designed along the established strategy [1]. Namely, we developed a technique to use Monte-Carlo simulation to take measures against the complicated facility structure. The simulated result was fed back to the deice design, and the revised one was simulated again. The feedback procedure was repeated until obtaining a design satisfying all requirements. Both the accumulated dose and the heat generation are evaluated by a Monte-Carlo code, PHITS [2]. In the simulation, protons are created just upstream of the muon target with a practical emittance, and then protons and secondary particles originating from nuclear reactions are transported. For safety reasons, we multiplied the simulated result by the margin factor of two, and the radiation dose was required to be below the design limit at the boundary between the controlled area and the public area, which was introduced in the J-PARC site. We optimized the amount, the arrangement and the material of the radiation shield. For this purpose, using Monte-Carlo simulation is suitable because of the flexibility of modeling.

Figure 1 shows the determined shield layout to be submitted to MEXT for operation from the autumn of 2011. D1 area was also modified for the future extension of U-line. In this case, the radiation dose was evaluated as shown in Fig. 2. In comparison with D-line, U-line has a large beamline aperture, and thus

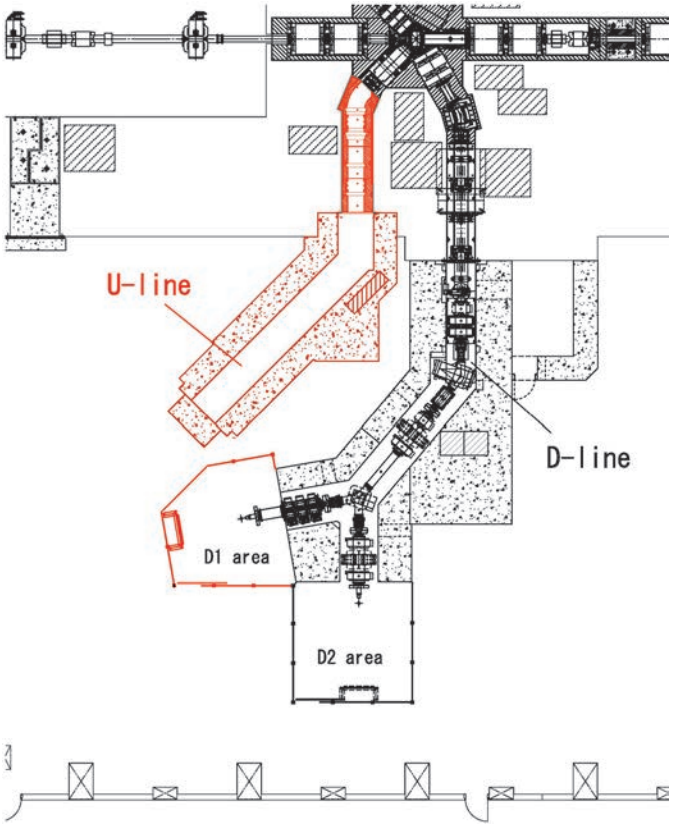

Figure 1. The shield layout in the 2nd experimental hall submitted to MEXT in FY2011.

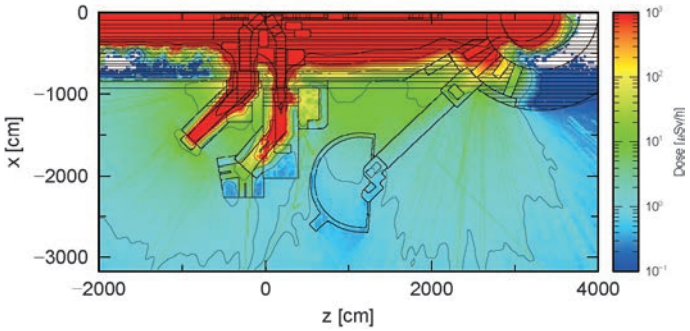

Figure 2. A typical evaluated result of radiation dose assuming the shield layout shown in Fig. 1.

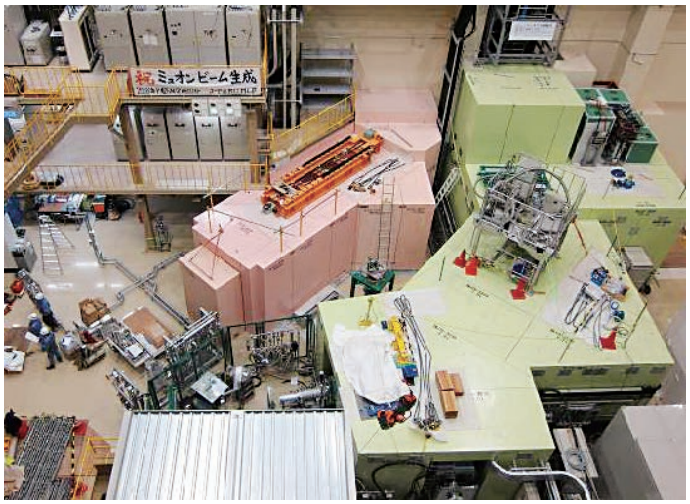

Figure 3. A photo taken after the installation of the shield blocks.

the effect of streaming neutrons becomes serious. To stop these neutrons, a temporary shield block was settled at the exit of U-line. This shield block will be removed in the installation of the beamline magnets.

The installation work of the shield blocks was completed in December 2011, just before restarting the accelerator operation after the disaster in March. In January 2012, the settlement of shield blocks for the extension of U-line, *i.e.* ultra-slow muon beamline, was started. Due to the space limitation, temporal movement of shield blocks will become difficult after the completion of U-line, and thus well-considered maintenance scenario will be required.

References

[1] N. Kawamura *et al.* 2009 *Nucl. Inst. and Meth. A* **600** 114.
[2] H. Iwase, K. Niita, T. Nakamura 2002 *J. Nucl. Sci. Technol.* **39** 1142.
[3] K. Niita *et al.* 2006 *Radiat. Meas.* **41** 1080.

N. Kawamura[1,2], and Muon Sci. Sec., J-PARC
[1]*Muon Science Section, Materials and Life Science Division, J-PARC Center;* [2]*Institute of Materials Structure Science, KEK*

Status of the Superomega Muon Beamline

The Superomega muon beamline is now being installed on U-line in experimental hall No.2 of the Materials and Life Science Facility (MLF) in J-PARC. The U-line is the second muon beamline of MLF/J-PARC, and the Superomega muon beamline is the muon extraction and transportation part of U-line. The features of Superomega are a large solid angle acceptance and simultaneous extraction of the both positive and negative muons, and all of its beamline magnets consist of solenoids. The first goal of the Superomega is the surface muon source for the ultra-slow muon beam, which is energy tunable low energy muon beam for a variety of experiments, such as surface-interface magnetism, and muon g-2 measurement.

The Superomega muon beamline consists of three parts, the normal-conducting capture solenoid, the superconducting curved transport solenoid, and the axial focusing solenoid. At present, the capture solenoid had been already installed in March 2009. The fabrication of the curved transport solenoid and the axial focusing solenoid is already completed. And they all will be installed in the summer of 2012.

The design of the superconducting transport solenoid was described previously [1]. Here, we focus on the design and concept of the axial focusing solenoid. The axial focusing solenoid is installed on the downstream of the curved transport solenoid. The axial focusing solenoid consists of five beamline vacuum chambers and six warm bore cryostats. Each cryostat has two thin solenoids, which can be individually applied to the current to transport and focus the muon beam onto the experimental target. The axial focusing solenoid is cooled down by thermal conducting method using a 1.5-W Gifford-McMahon (GM) refrigerator.

The various functions, which are muon beam blocker, three stage Wien-filter type positron separators, and muon beam slits, are added on the beamline chambers. To avoid radiation exposure in the experimental area, the beam blocker is inserted into the muon beamline for stopping the muons and any other particles. The electrodes of the positron separators have 30-cm gap, 75-cm length and 50-cm width. They can be applied ±400 kV by using Cockroft-Walton type high voltage power supplies

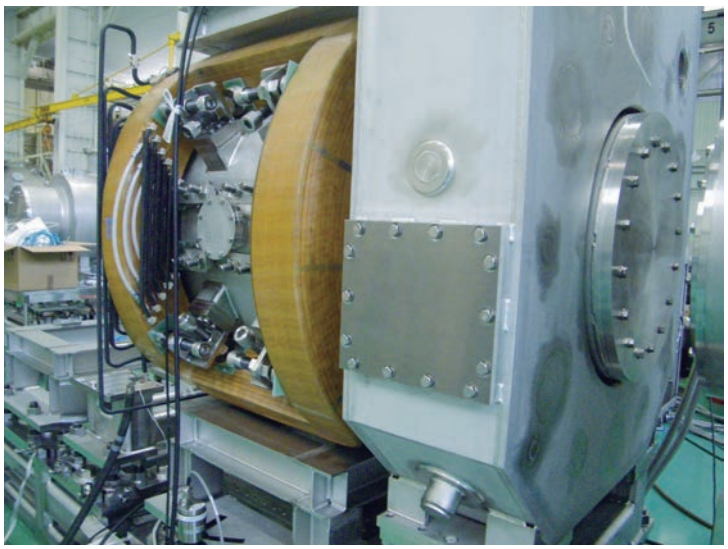

Figure 1. Picture of the vacuum chamber of the positron separator and the cryostats of the superconducting coils of the axial focusing solenoid.

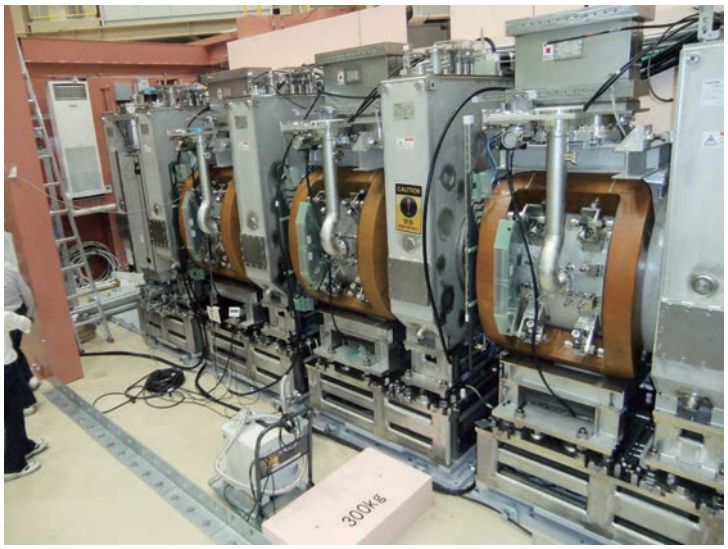

Figure 2. Picture of the axial focusing solenoid.

directory set on the beamline chamber, to eliminate almost all positrons from the muon beam, which are simultaneously transported with the muon.

The beam transportation and trajectories of axial focusing solenoid were calculated using a GEANT4-based simulation package called G4Beamline [2]. According to the simulations, the 2 x 10^8 muons/s can be focused on to the final experimental target (70 x 50 mm) placed on the 700-mm downstream of the last focusing solenoid. This indicates that the Superomega muon beamline will be the highest intensity pulsed muon source in the world. The first beam extraction experiment of Superomega beamline will be conducted in October 2012.

References

[1] Y. Makida *et al.*, IEEE TRANSACTIONS ON APPLIED SUPERCONDUCTIVITY, 21, (2011) 1725.

[2] Muons, Inc. 552 Nm Batavia Avenue, Batavia, IL, available at http://www.muonsinc.com.

Y. Ikedo[1,2] Y. Miyake[1,2], K. Shimomura[1,2], P. Strasser[1,2], K. Nishiyama[1,2], N. Kawamura[1,2], H. Fujimori[1,2], S. Makimura[1,2], A. Koda[1,2], Y. Kobayashi[1,2], T. Nagatomo[1,2], J. Nakamura[1,2], T. Ogitsu[2], Y. Makida[2], T. Adachi[3], M. Yoshida[2], H. Ohhata[2], T. Okamura[2], A. Yamamoto[2], T. Nakamoto[2], K. Sasaki[2], W. Higemoto[1,4], and K. Ishida[5]

[1]Muon Science Section, Materials and Life Science Division, J-PARC Center; [2]Institute of Materials Structure Science, KEK; [3]School of Science, University of Tokyo; [4]Advanced Science Research Center, JAEA; [5]Nishina Center, RIKEN

Facility Report

Beam Operation Status at MLF

After remarkably quick recovery from the damage caused by the great earthquake, the proton beam was introduced to the target on December 22nd 2011 as scheduled. After only one shot of the beam, it could be confirmed that it reached the mercury target. After the tuning of the proton beam, the beam operation for users restarted on January 24th 2012. In order to confirm the status of the target facilities, we delivered proton beam with power of 120 kW, which was smaller than the one used before the great earthquake. The beam power has been increased gradually. Since March 15th 2012, proton beam with power of 220 kW is being delivered to the target. The level of availability has reached more than 90%, as shown in Table 1, during Run # 40 performed from January to February. On February 11th and 12th, the beam was stopped for modification of the neutron beam lines. From the 5th of March, Run #41 has started. In Run #41, the user operation was terminated on March 22nd 2012, due to the failure of the high voltage power supply (HVPS) for the LINAC, which was fixed on April 9th 2012. As a result of problems with the HVPS, which caused low availability in Run # 41, 9 days of beam schedule had been cancelled.

Table 1. Run cycle, scheduled time and availability.

Run#	Scheduled Time (h).	Availability
40	549	94.3
41	547	57.7

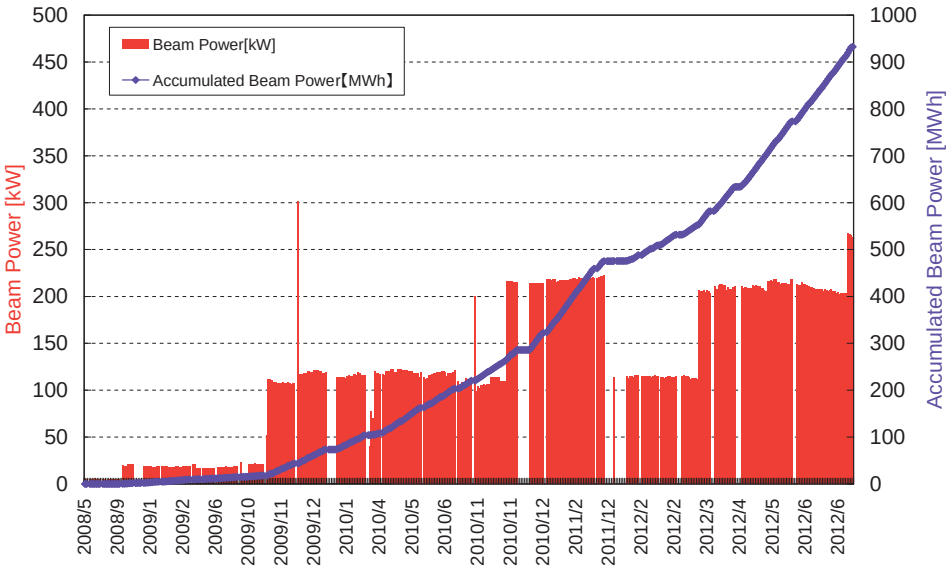

Figure 1. Beam power trend at MLF and cumulative beam power from the first beam to the summer 2012.

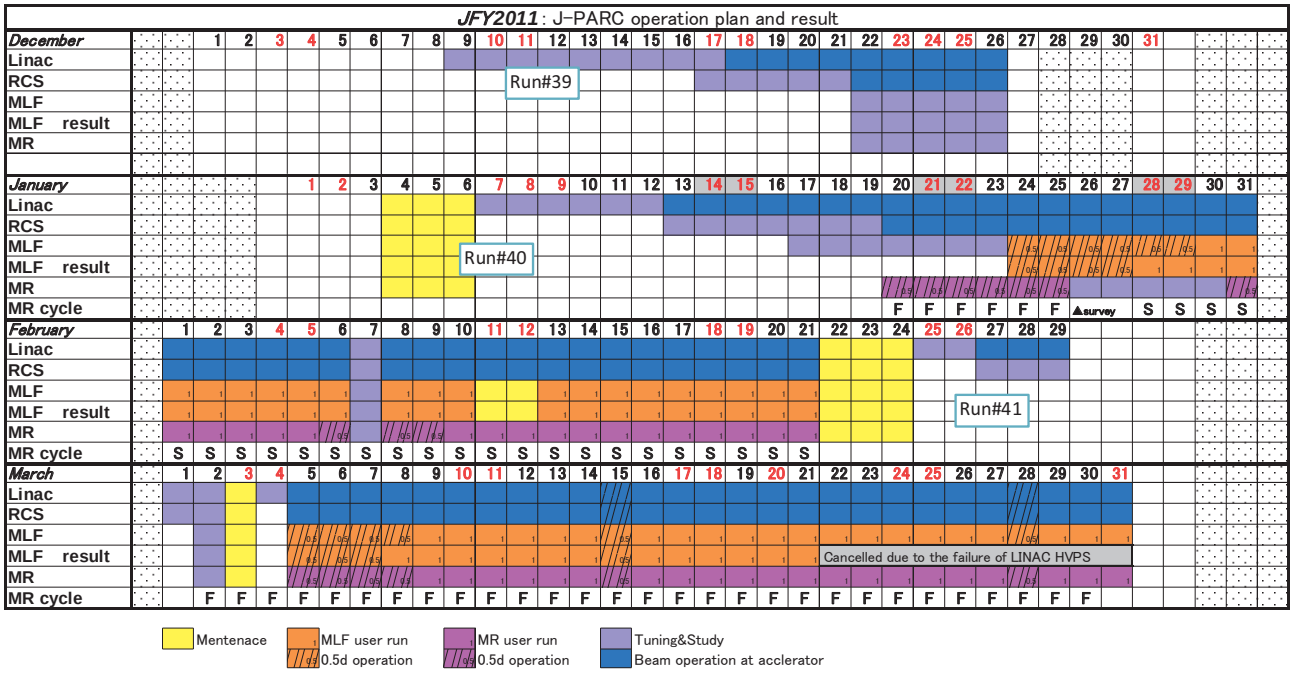

Figure 2. Scheduled plan and actual results for the beam operation in JFY2011 at J-PARC. Unfortunately, due to the failure of the high voltage power supply for the LINAC, the beam operation was cancelled after March 22nd 2012.

Users at MLF

In FY2010, the number of users at MLF (both for neutron and muon experiments) tripled compared to FY2008 when we officially started the user program. At that time, the operation power was 200 kW of proton beam, and 6 neutron beam lines (instruments) and 2 muon beam ports were available for the research program. In FY2011, in contrast, a big decrease of the number of users was caused by the earthquake on March 11th. Until the end of FY2011, refurbishment works were done on the accelerator, beamline systems, instruments, and buildings to provide proper facilities for scientific research. It is greatly expected that the number of users will increase again in the next year. The number of users in the period of fiscal year are summarized in Table and Figure for domestic and foreign users of neutron and muon experimental facilities.

Table. The number of domestic and foreign users in the period of fiscal year

	FY2008		FY2009		FY2010		FY2011	
	Domestic Users	Foreign Users	Domestic Users	Foreign Users	Domestic Users	Foreign Users	Domestic Users	Foreign Users
Neutron	182		378		529		222	
	161	21	353	25	485	44	198	24
Muon	12		57		55		30	
	12	0	55	2	48	7	28	2

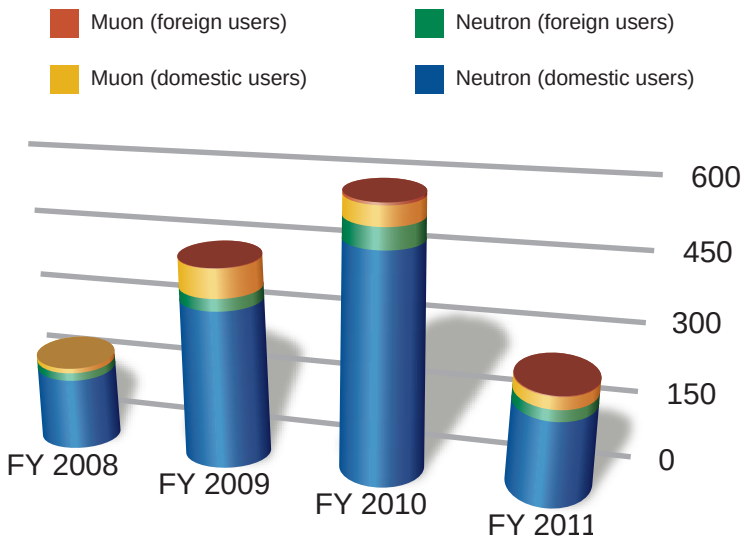

Figure. The number of domestic and foreign users in the period of fiscal year

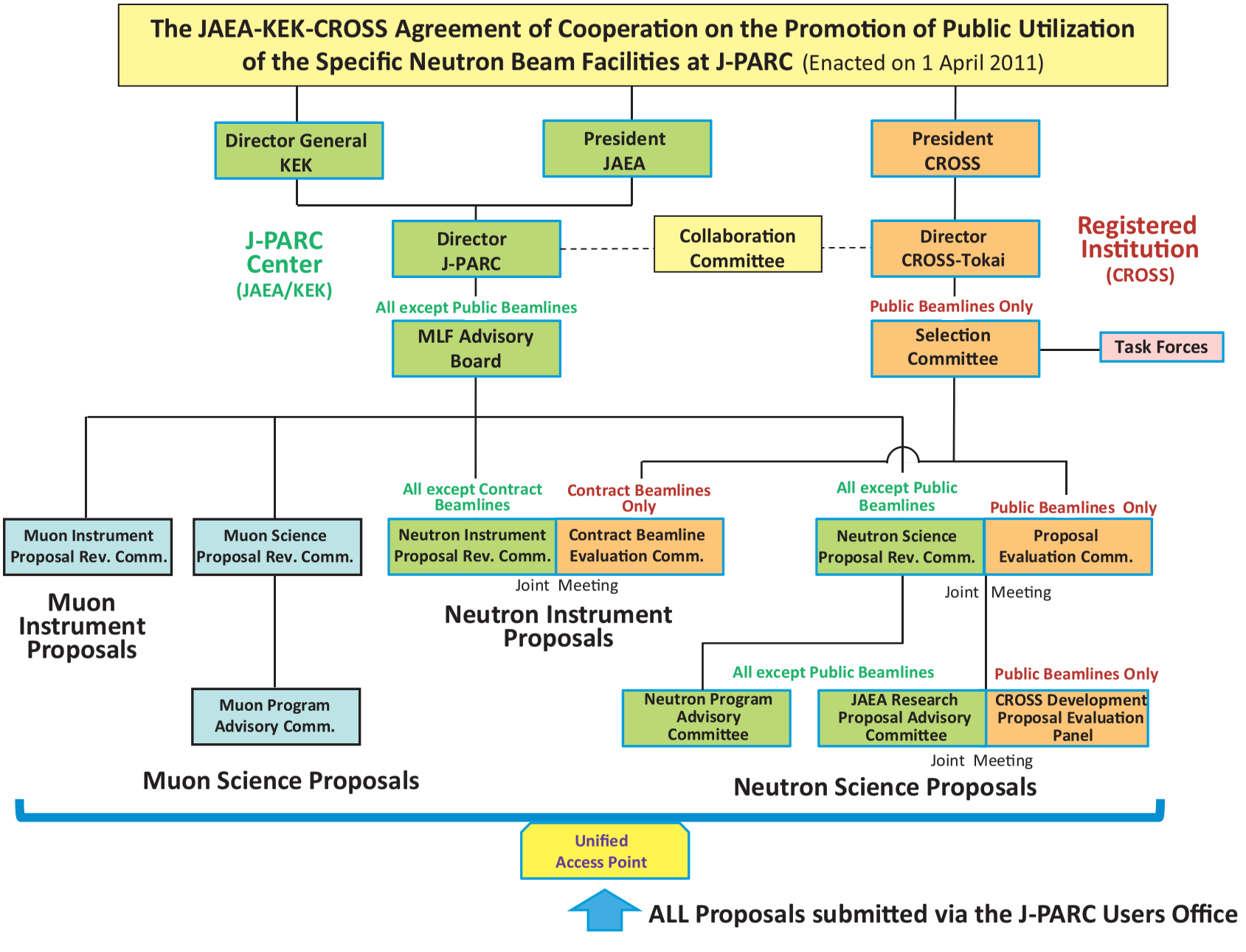
The JAEA-KEK-CROSS Agreement of Cooperation on the Promotion of Public Utilization of the Specific Neutron Beam Facilities at J-PARC (Enacted on 1 April 2011)
Director General KEK
President JAEA
President CROSS
J-PARC Center (JAEA/KEK)
Director J-PARC
Collaboration Committee
Director CROSS-Tokai
Registered Institution (CROSS)
All except Public Beamlines
Public Beamlines Only
MLF Advisory Board
Selection Committee
Task Forces
All except Contract Beamlines
Contract Beamlines Only
All except Public Beamlines
Public Beamlines Only
Muon Instrument Proposal Rev. Comm.
Muon Science Proposal Rev. Comm.
Neutron Instrument Proposal Rev. Comm.
Contract Beamline Evaluation Comm.
Neutron Science Proposal Rev. Comm.
Proposal Evaluation Comm.
Joint Meeting
Joint Meeting
Muon Instrument Proposals
Neutron Instrument Proposals
All except Public Beamlines
Public Beamlines Only
Muon Program Advisory Comm.
Neutron Program Advisory Committee
JAEA Research Proposal Advisory Committee
CROSS Development Proposal Evaluation Panel
Joint Meeting
Muon Science Proposals
Neutron Science Proposals
Unified Access Point
ALL Proposals submitted via the J-PARC Users Office

MLF Proposals Summary – FY2011

Table 1. Breakdown of Proposal Numbers for the 2011A & 2011B Rounds

Beam-line	Instrument		2011A						2011B					
			Submitted			Approved			Submitted			Approved		
			GU	PU/S	IU	GU	PU/S	IU	GU	PU/S	IU	GU	PU/S	IU
BL01	4D-Space Access Neutron Spectrometer - ***4SEASONS***		14	2	1	10	2	1	1	0	1	1	0	1
BL02	Biomolecular Dynamics Spectrometer - ***DNA***								3	0	1	1	0	1
BL03	Ibaraki Biological Crystal Diffractometer - ***iBIX***	(100-β)‡	4	0	1	3	0	1	0	0	0	0	0	0
		(β)†	1	16	0	3	9	0	0	4	0	0	4	0
BL04	Accurate Neutron-Nucleus Reaction Measurement Instrument - ***ANNRI***		0	1	0	0	1	0	4	0	1	4	1	0
BL05	Neutron Optics and Physics - ***NOP***		0	1	0	0	1	0	0	1	0	0	1	0
BL08	Super High Resolution Powder Diffractometer -***S-HRPD***		16	1	0	12	1	0	4	1	0	4	1	0
BL10	Neutron Beamline for Observation and Research Use - ***NOBORU***		10	3	1	10	3	1	5	3	1	5	3	1
BL12	High Resolution Chopper Spectrometer - ***HRC***		4	1	0	2	1	0	1	1	0	1	1	0
BL14	Cold-neutron Disk-chopper Spectrometer - ***AMATERAS***		13	3	1	8	3	1	3	3	1	2	3	1
BL15	Small and Wide Angle Neutron Scattering Instrument - ***TAIKAN***								7	0	1	4	0	1
BL16	High-Performance Neutron Reflectometer with a Horizontal Sample Geometry - ***SOFIA***		10	1	0	10	1	0	6	1	0	6	1	0
BL17	Polarized Neutron Reflectometer - ***SHARAKU***								5	0	1	2	0	1
BL19	Engineering Diffractometer - ***TAKUMI***		20	2	1	18	2	1	4	2	1	2	2	1
BL20	Ibaraki Materials Design Diffractometer - ***iMATERIA***	(100-β)‡	11	0	0	7	0	0	6	0	0	6	0	0
		(β)†	17	18	0	17	18	0	10	5	0	10	5	0
BL21	High Intensity Total Diffractometer - ***NOVA***		1	1	0	1	1	0	0	1	0	0	1	0
D1	Muon D1		15	1	1	9	1	1	5	1	1	4	1	1
D2	Muon D2		5	0	1	5	0	1	4	0	1	4	0	1
Subtotal			141	51	7	115	44	7	68	23	10	56	24	9
Total			199			166			101			89		

GU : General Use **PU** : Project Use or Ibaraki Pref. Project Use **IU :** Instrument Group Use
S : S-type Proposals **†** : Ibaraki Pref. Exclusive Use Beamtime (β = 80% in FY2011)
‡ : J-PARC Center General Use Beamtime ((100-β = 20% in FY2011)

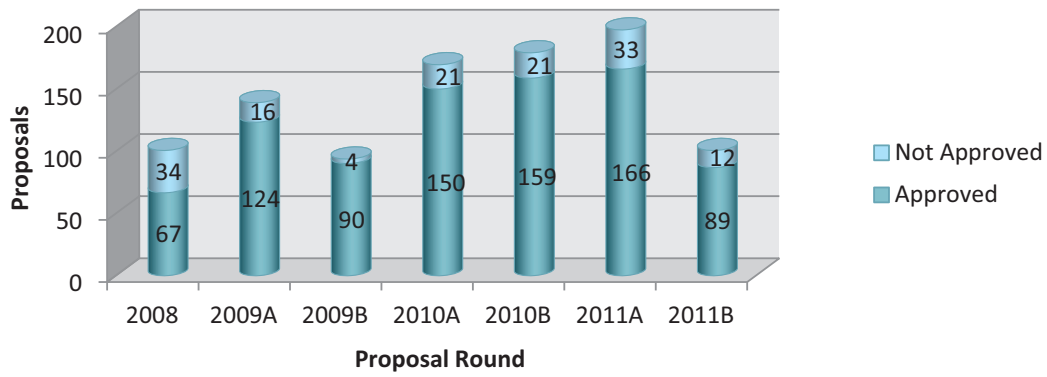

Figure 1. MLF Proposal Numbers over Time

Table 2. Principal Investigator Affiliations in FY2011

Universities (Japan)	JAEA	Companies (Japan)	KEK	Foreign Organizations	Research Institutes (Japan)
111	73	56	26	21	13

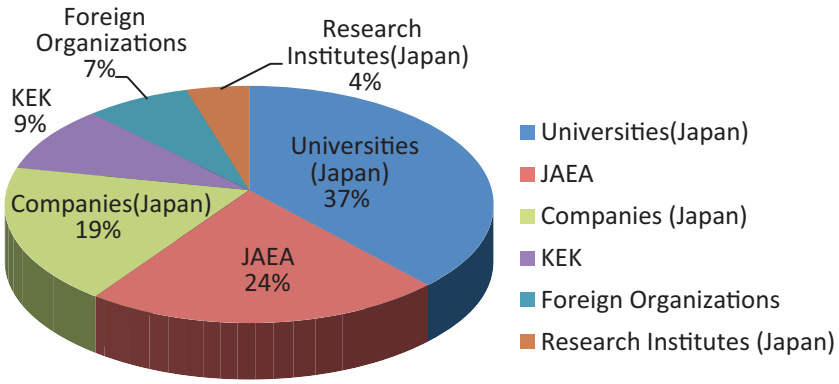

Figure 2. Origin of Proposals in FY2011

Table 3. Proposals by Sub-committee/Expert Panel – FY2011

Sub-committee Expert Panel	P1	P2	P3	P4	P5	P6	P7	P8	Q1	Q2
No. of Proposals	53	11	13	7	32	5	23	9	11	18

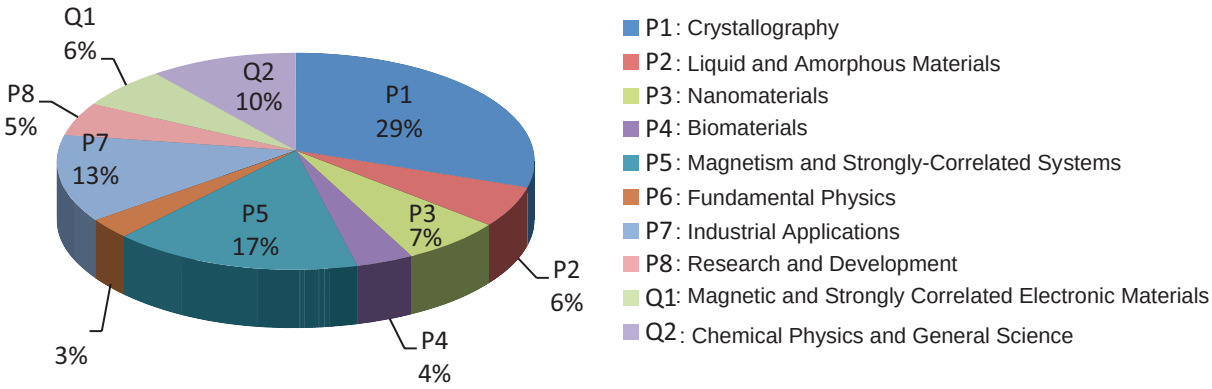

Figure 3. Submitted Proposals by Sub-committee/Expert Panel – FY2011

MLF Division Staff 2011

Director	Masatoshi Arai (JAEA)
Vice Director	Hideki Seto (KEK)
	Takashi Kato (JAEA)

Neutron Source Section

	JAEA	
Leader	Masatoshi Futakawa	Akira Ogawa
Sub-Leader	Hiroshi Takada	Kiichi Ohtsu
	Fujio Maekawa	Toshiaki Uehara
	Shinichi Sakamoto	Kiyomi Ikezaki
	Katsuhiro Haga	Kohei Hanano
	Shinichiro Meigo	Hideki Tatsumoto
	Sakai Kenji	Motoki Ohi
	Yoshimi Kasugai	Yoshihiko Kawakami
	Makoto Teshigawara	Manabu Ito
	Tomokazu Aso	Hisashi Sakurayama
	Hidetaka Kinoshita	Takeshi Naoe
	Kenichi Oikawa	Atsushi Akutsu
	Masahide Harada	Toru Suzuki
	Shoichi Hasegawa	Masato Ida
	Hiroyuki Kogawa	Kenichi Kanomata
	Takasi Wakui	Tatsuhiro Nakajima
	Tetsuya Kai	Hiroki Matsui
	Masakazu Seki	Shizuka Yoshinari
	Akihiko Watanabe	Chieko Higuchi

Neutron Science Section

	KEK	
Leader	Takashi Kamiyama	Hidenori Sagehashi
	Susumu Ikeda	Suguru Muto
	Toshiya Otomo	Naokatsu Kaneko
	Tetsuya Yokoo	Masao Yonemura
	Norifumi Yamada	Miki Nagao
	Shuki Torii	
	Tomohiro Seya	JAEA
	Masataka Sakaguchi	Sub-Leader Kazuya Aizawa
	Zhang Junrong	Kentarao Suzuya
	Koichiro Sadakane	Kenji Nakajima
	Hirohiko Shimizu	Takayuki Oku
	Shinichi Ito	Mitsutaka Nakamura
	Takashi Ino	Stefanus Harjo
	Setsuo Satoh	Takeshi Nakatani

Shinichi Takata
Nobuaki Takahashi
Takenao Shinohara
Yukinobu Kawakita
Seiko Kawamura
Hiroshi Arima
Yasuhiro Inamura
Hiroshi Kira
Tatsuya Kikuchi
Takuro Kawasaki
Jun Abe
Taiki Tominaga
Hirotaka Sato
Fumio Mizuno
Hironori Shimakura
Hiroki Ueno
Yuhua Su
Wu Gong
Hiromichi Tanaka
Wataru Kambara
Yukihiro Ito

Takaaki Iwahashi
Tomonori Hosoya
Yasuhiro Yamauchi
Kentaro Moriyama
Masayasu Takeda
Toyotaka Osakabe
Kazuo Kurihara
Wataru Utsumi
Shuichi Wakimoto
Takanori Hattori
Itaru Tamura
Koji Kaneko
Asami Sano
Hideo Harada
Atsushi Kimura
Hidehito Asaoka
Masato Kubota
Chiho Tobe
Naoko Shimizu
Junko Akutsu

Neutron Instrumentation Section

JAEA

Leader
Kazuhiko Soyama
Kaoru Sakasai
Dai Yamazaki
Kentaro Toh
Tatsuya Nakamura
Ryuji Maruyama

Hirotoshi Hayashida
Hideshi Yamagishi
Satoru Okayasu
Takuro Sakai
Ryo Yasuda
Mana Hirayama

Muon Section

KEK

Leader
Yasuhiro Miyake
Ryosuke Kadono
Koichiro Shimomura
Kenji Kojima
Patrick Strasser
Naritoshi Kawamura
Akihiro Koda
Hiroshi Fujimori
Shunsuke Makimura
Yasuhisa Nemoto
Yasuo Kobayashi

Kusuo Nishiyama
Yutaka Ikedo
Tetsuya Masuda
Jumpei Nakamura
Toyofusa Yoshimura

JAEA

Wataru Higemoto
Takashi Ito
Kazuhiko Ninomiya

CROSS-Tokai Staff 2011

Director Yasuhiko Fujii

Science Coordinators

Masatoshi Sato
Yoshiaki Fukushima

Neutron R&D Division

Head	Jun-ichi Suzuki	Takayasu Hanashima
Head (Deputy)	Ryoichi Kajimoto	Koji Munakata
	Sungdae Ji	Koji Kiriyama
	Kazuhiko Ikeuchi	Takayoshi Ito
	Kaoru Shibata	Yukihiko Kawamura
	Kazuya Kamazawa	Hiroshi Kira
	Takeshi Yamada	Motoyuki Ishikado
	Kazuki Ohishi	Kazuhiro Akutsu
	Hiroki Iwase	Makoto Kobayashi
	Tazuko Mizusawa	Akifumi Kishi
	Yoshifumi Sakaguchi	Tadashi Futagami
	Noboru Yoshida	Kaoru Sato
	Takashi Ohhara	Junichi Sato
	Akiko Nakao	Satoshi Kasai

Health and Safety Division

Toshiyuki Yamashita

Utilization Promotion Division

Head	Tohru Matoba	Megumi Kawakami
Head (Deputy)	Garry Foran	Aya Yamada
	Toshiki Asai	Katsumi Kunigihara
	Rei Ohuchi	Asami Inoue
	Junko Ohta	Emi Takaha
	Shin-ichi Yamaguchi	

Admin and Finance Division

Head	Yasuo Seishi	Tomoyuki Yabana
Head (Deputy)	Masaru Yokoyama	Mutsumi Shiraishi
	Takahiro Koizumi	Mika Gunji

Committee and Meetings

Materials and Life Science Facility Advisory Board

物質・生命科学実験施設利用委員会

Masatoshi Arai	Japan Atomic Energy Agency, Japan
Yasuhiko Fujii	Comprehensive Research Organization for Science and Society, Japan
Toshiharu Fukunaga	Kyoto University, Japan
Masatoshi Futakawa	Japan Atomic Energy Agency, Japan
Makoto Hayashi	Ibaraki Prefecture, Japan
Mitsuhiro Hirai	Gunma University, Japan
Yujiro Ikeda	Japan Atomic Energy Agency, Japan
Susumu Ikeda	High Energy Accelerator Research Organization, Japan
Kazuaki Iwasa	Tohoku University, Japan
Masahiko Iwasaki	RIKEN, Japan
Ryosuke Kadono	High Energy Accelerator Research Organization, Japan
Kazuhisa Kakurai	Japan Atomic Energy Agency, Japan
Shinichi Kamei	Mitsubishi Research Institute, Inc., Japan
Takashi Kamiyama	High Energy Accelerator Research Organization, Japan
Toshiji Kanaya (Chair)	Kyoto University, Japan
Takashi Kato	Japan Atomic Energy Agency, Japan
Youji Koike	Tohoku University, Japan
Yasuhiro Miyake	High Energy Accelerator Research Organization, Japan
Junichirou Mizuki	Japan Atomic Energy Agency, Japan
Toshiya Otomo	High Energy Accelerator Research Organization, Japan
Hideki Seto	High Energy Accelerator Research Organization, Japan
Mitsuhiro Shibayama	University of Tokyo, Japan
Jun Sugiyama	Toyota Central R&D Labs., Inc., Japan
Eiko Torikai	University of Yamanashi, Japan
Kazuyoshi Yamada	Tohoku University, Japan

Neutron Instrument Proposal Review Committee

中性子実験装置部会

Masatoshi Arai	Japan Atomic Energy Agency, Japan
Koichiro Asahi	Tokyo Institute of Technology, Japan
Muneyuki Imafuku	Tokyo City University, Japan
Takashi Kamiyama	High Energy Accelerator Research Organization, Japan
Takashi Kato	Japan Atomic Energy Agency, Japan
Hideaki Kitazawa	National Institute for Material Science, Japan
Yoshiaki Kiyanagi (Chair)	Hokkaido University, Japan
Yukio Morii	Ibaraki Prefecture, Japan
Yukio Morimoto	Kyoto University, Japan
Kenji Nakajima	Japan Atomic Energy Agency, Japan
Toshiya Otomo	High Energy Accelerator Research Organization, Japan
Kenji Ohoyama	Tohoku University, Japan

Mamoru Sato	Yokohama City University, Japan
Hideki Seto	High Energy Accelerator Research Organization, Japan
Junichi Suzuki	Comprehensive Research Organization for Science and Society, Japan
Naoya Torikai	Mie University, Japan
Hideki Yoshizawa	University of Tokyo, Japan

Neutron Science Proposal Review Committee

中性子課題審査部会

Yoshiaki Akiniwa	Yokohama National University, Japan
Masatoshi Arai	Japan Atomic Energy Agency, Japan
Takahisa Arima	University of Tokyo, Japan
Sung-Min Choi	Korea Advanced Institute of Science and Technology, Korea
Hideto En'yo	RIKEN, Japan
Toshiharu Fukunaga	Kyoto University, Japan
Makoto Hayashi	Ibaraki Prefecture, Japan
Susumu Ikeda	High Energy Accelerator Research Organization, Japan
Kazuhisa Kakurai	Japan Atomic Energy Agency, Japan
Takashi Kamiyama	High Energy Accelerator Research Organization, Japan
Toshiji Kanaya	Kyoto University, Japan
Takashi Kato	Japan Atomic Energy Agency, Japan
Brendan Kennedy	University of Sydney, Australia
Yoshiaki Kiyanagi	Hokkaido University, Japan
Yasuhiro Miyake	High Energy Accelerator Research Organization, Japan
Yukio Morii	Ibaraki Prefecture, Japan
Yukio Noda	Tohoku University, Japan
Yuji Ohashi	Ibaraki Prefecture, Japan
Je-Geun Park	Seoul National University, Korea
Mamoru Sato	Yokohama city University, Japan
Hideki Seto	High Energy Accelerator Research Organization, Japan
Mitsuhiro Shibayama (Chair)	University of Tokyo, Japan
Junichi Suzuki	Comprehensive Research Organization for Science and Society, Japan
Peter Timmins	Institut Laue-Langevin, France
Yo Tomota	Ibaraki University, Japan
Xun-Li Wang	Oak Ridge National Laboratory, U.S.A
Kazuyoshi Yamada	Tohoku University, Japan
Hideki Yoshizawa	University of Tokyo, Japan

JAEA Research Proposal Advisory Committee

J-PARC物質・生命科学実験施設におけるJAEA研究課題諮問委員会

Masatoshi Arai	Japan Atomic Energy Agency, Japan
Toshiharu Fukunaga	Kyoto University, Japan
Mitsuhiro Hirai	Gunma University, Japan
Yujiro Ikeda	Japan Atomic Energy Agency, Japan

Masayuki Imai	Ochanomizu University, Japan
Toshiji Kanaya	Kyoto University, Japan
Yuji Kawabata	Kyoto University, Japan
Yukinobu Kawakita	Japan Atomic Energy Agency, Japan
Hideaki Kitazawa	National Institute for Material Science, Japan
Yoshiaki Kiyanagi	Hokkaido University, Japan
Michiyasu Mori	Japan Atomic Energy Agency, Japan
Yoichi Murakami	High Energy Accelerator Research Organization, Japan
Kenji Nakajima	Japan Atomic Energy Agency, Japan
Tsuneyoshi Nakayama (Chair)	Hokkaido University, Japan
Hiroyuki Oigawa	Japan Atomic Energy Agency, Japan
Taku Sato	University of Tokyo, Japan
Hideki Seto	High Energy Accelerator Research Organization, Japan
Shinichi Shamoto	Japan Atomic Energy Agency, Japan
Hirohiko Shimizu	Nagoya University, Japan
Junichi Suzuki	Comprehensive Research Organization for Science and Society, Japan
Keisuke Tanaka	Meijo University, Japan
Yo Tomota	Ibaraki University, Japan
Eiko Torikai	University of Yamanashi, Japan
Kazuyoshi Yamada	Tohoku University, Japan

Neutron Program Advisory Committee

中性子共同利用実験審査委員会

Koichiro Asahi	Tokyo Institute of Technology, Japan
Yasushi Idemoto	Tokyo University of Science, Japan
Susumu Ikeda	High Energy Accelerator Research Organization, Japan
Shinichi Itoh	High Energy Accelerator Research Organization, Japan
Kazuaki Iwasa	Tohoku University, Japan
Ryosuke Kadono	High Energy Accelerator Research Organization, Japan
Hiroshi Kageyama	Kyoto University, Japan
Hiroyuki Kagi	University of Tokyo, Japan
Takashi Kamiyama	High Energy Accelerator Research Organization, Japan
Toshiji Kanaya	Kyoto University, Japan
Mikio Kataoka	Nara Institute of Science and Technology
Nomura Masaharu	High Energy Accelerator Research Organization, Japan
Yutaka Moritomo	University of Tsukuba, Japan
Youichi Murakami	High Energy Accelerator Research Organization, Japan
Toshiya Otomo	High Energy Accelerator Research Organization, Japan
Hideki Seto (Chair)	High Energy Accelerator Research Organization, Japan
Hirohiko Shimizu	High Energy Accelerator Research Organization, Japan
Masaaki Sugiyama	Kyoto University, Japan
Junichi Suzuki	Comprehensive Research Organization for Science and Society, Japan
Noboru Yamamto	High Energy Accelerator Research Organization, Japan
Osamu Yamamuro	University of Tokyo, Japan
Kiyanagi Yoshiaki	Hokkaido University, Japan

Muon Instrument Proposal Review Committee

ミュオン実験装置部会

Masatoshi Arai	Japan Atomic Energy Agency, Japan
Koichiro Asahi (Chair)	Tokyo Institute of Technology, Japan
Wataru Higemoto	Japan Atomic Energy Agency, Japan
Masahiko Iwasaki	RIKEN, Japan
Ryosuke Kadono	High Energy Accelerator Research Organization, Japan
Takashi Kato	Japan Atomic Energy Agency, Japan
Kenji Kojima	High Energy Accelerator Research Organization, Japan
Kenya Kubo	International Christian University, Japan
Yoshitaka Kuno	Osaka University, Japan
Yasuhiro Miyake	High Energy Accelerator Research Organization, Japan
Nobuhiko Nishida	Tokyo Institute of Technology, Japan
Hiroyuki Nojiri	Tohoku University, Japan
Toru Ogitsu	High Energy Accelerator Research Organization, Japan
Koichiro Shimomura	High Energy Accelerator Research Organization, Japan
Yasunori Yamazaki	RIKEN, Japan

Muon Science Proposal Review Committee

ミュオン課題審査部会

Masatoshi Arai	Japan Atomic Energy Agency, Japan
Koichiro Asahi	Tokyo Institute of Technology, Japan
Kim H. Chow	University of Alberta, Canada
Roberto De Renzi	University of Parma, Italy
Wataru Higemoto	Japan Atomic Energy Agency, Japan
Katsuhiko Ishida	RIKEN, Japan
Kenji Ishida	Kyoto University, Japan
Ryosuke Kadono	High Energy Accelerator Research Organization, Japan
Shinsaku Kambe	Japan Atomic Energy Agency, Japan
Takashi Kamiyama	High Energy Accelerator Research Organization, Japan
Hiroshi Kobori	Chiba University, Japan
Youji Koike (Chair)	Tohoku University, Japan
Kenya Kubo	International Christian University, Japan
Yasuhiro Miyake	High Energy Accelerator Research Organization, Japan
Yuichiro Nagame	Japan Atomic Energy Agency, Japan
Yasuo Nozue	Osaka University, Japan
Masao Ogata	University of Tokyo, Japan
Shinji Tsuneyuki	University of Tokyo, Japan
Soichi Wakatsuki	High Energy Accelerator Research Organization, Japan

Muon Program Advisory Committee

ミュオン共同利用実験審査委員会

Hiroshi Amitsuka	Hokkaido University, Japan
Masaharu Aoki	Osaka University, Japan
Wataru Higemoto	Japan Atomic Energy Agency, Japan
Susumu Ikeda	High Energy Accelerator Research Organization, Japan
Katsuhiko Ishida	RIKEN, Japan
Kenji Ishida	Kyoto University, Japan
Kenji Itoh	High Energy Accelerator Research Organization, Japan
Ryosuke Kadono (Chair)	High Energy Accelerator Research Organization, Japan
Shinsaku Kambe	Japan Atomic Energy Agency, Japan
Yoh Kobori	Chiba University, Japan
Yoji Koike	Tohoku University, Japan
Kenji Kojima	High Energy Accelerator Research Organization, Japan
Tadashi Koseki	High Energy Accelerator Research Organization, Japan
Kenya Kubo	International Christian University, Japan
Yasuyuki Matsuda	University of Tokyo, Japan
Yasuhiro Miyake	High Energy Accelerator Research Organization, Japan
Yuichro Nagame	Japan Atomic Energy Agency, Japan
Hironori Nakao	High Energy Accelerator Research Organization, Japan
Yasuo Nozue	Osaka University, Japan
Masao Ogata	University of Tokyo, Japan
Hideki Seto	High Energy Accelerator Research Organization, Japan
Atsushi Shinohara	Osaka University, Japan
Shinji Tsuneyuki	University of Tokyo, Japan

Selection Committee (CROSS)

選定委員会

Toshio Akai	Mitsubishi Rayon Co., Ltd., Japan
Hidetoshi Fukuyama (Chair)	Tokyo University of Science, Japan
Makoto Hayashi	Ibaraki Prefecture, Japan
Kazuaki Iwasa	Tohoku University, Japan
Shinichi Kamei	Mitsubishi Research Institute Inc., Japan
Toshiji Kanaya	Kyoto University, Japan
Mikio Kataoka	Nara Institute of Science and Technology, Japan
Naoki Kishimoto	National Institute of Material Science, Japan
Tomoko Nakanishi	University of Tokyo, Japan
Kazumi Nishijima	Mochida Pharmaceutical Co., Ltd., Japan
Mitsuhiro Shibayama	University of Tokyo, Japan
Masaki Takada	RIKEN, Japan
Kiyoyuki Terakura	Japan Advanced Institute of Science and Technology, Japan
Eiko Torikai	University of Yamanashi, Japan

Neutron Advisory Committee (NAC)

NAC-2012 convened 8-10 Feb 2012 at the IQBRC, Tokai

List of NAC-2012 Members

Kurt N. Clausen	Paul Scherrer Institute, Switzerland
John R. Haines	Oak Ridge National Laboratory, USA
Toshiji Kanaya	Kyoto University, Japan
Mahn Won Kim	Korea Advanced Institute of Science and Technology, Korea
Yoshiaki Kiyanagi	Hokkaido University, Japan
Dan A. Neumann	National Institute of Standards and Technology, USA
Robert Robinson	Australian Nuclear Science and Technology Organization, Australia
Uschi Steigenberger (Chair)	Science and Technology Facilities Council, UK
Werner Wagner	Paul Scherrer Institute, Switzerland

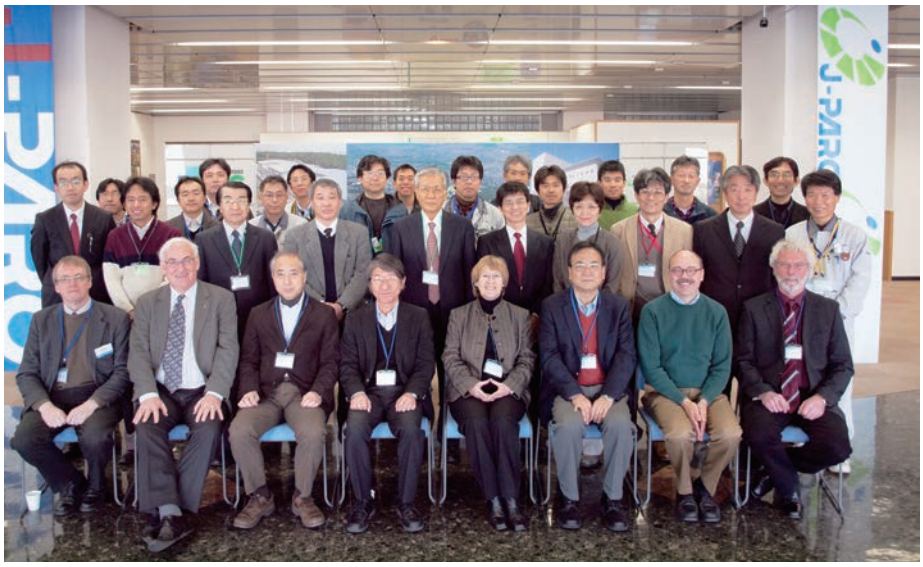

Group photo of NAC-2012

Muon Science Advisory Committee (MuSAC)

MuSAC-10 convened 17-18 Feb 2012 at the KEK Tokai Campus

List of MuSAC-10 Members

Jun Akimitsu	Aoyama-Gakuin University, Japan
Hiroshi Amitsuka	Hokkaido University, Japan
Robert Cywinski	University of Huddersfield, UK
Elvezio Morenzoni (Chair)	Paul Scherrer Institute, Switzerland
Jean-Michel Poutissou	TRIUMF, Canada
Atsushi Shinohara	Osaka University, Japan
Jeff E. Sonier	Simon Fraser University, Canada
Eiko Torikai	University of Yamanashi, Japan

Group photo of MuSAC-10

The Government Review of J-PARC

Hiroaki Aihara	University of Tokyo, Japan
Hidetoshi Fukuyama (Chair)	Tokyo University of Science, Japan
Takaaki Kajita	University of Tokyo, Japan
Toshiji Kanaya	Kyoto University, Japan
Michiyo Kaneko	Toyota Motor Corporation, Japan
Akio Komori	National Institutes of Natural Sciences, Japan
Noritaka Kumagai	Japan Synchrotron Radiation Research Institute, Japan
Kazumi Nishijima	Mochida Pharmaceutical Co., Ltd., Japan
Kiyotaka Okada	National Institutes of Natural Sciences, Japan
Nobuyuki Osakabe	Hitachi, Ltd., Japan
Hirokazu Tamura	Tohoku University, Japan
Eiko Torikai	University of Yamanashi, Japan
Yuriko Yamagata	Kumamoto University, Japan
Hiromi Yokoyama	University of Tokyo, Japan

The Government started their review of J-PARC on March, 2012. The accomplishment of early recovery from the Great East Japan Earthquake was highly appreciated. The major focus of this review was to establish the future five year plan. For Neutrons, the extensive efforts will be made to improve the environments for sample preparations and data analyses. For Muons, the best effort for the coming five years for the Muon group will be to fill up two beamlines, called S and H. The construction of a research building and an isotope storage building were also discussed.

Award List

The AONSA Prize 2011
For his pioneering development of accelerator-based neutron sources and instrumentations, and his great contribution to the establishment of neutron science community and finally to the realization of one of the most powerful pulsed neutron scattering facility at J-PARC
The Asia-Oceania Neutron Scattering Association (AONSA)
Noboru Watanabe, November 2011

The JSNS Young Scientist Award
Neutron Diffraction Study on Hydrogen Bond in Mineral in the Deep Earth
The Japanese Society for Neutron Science
Asami Sano-Furukawa, November 2011

The JSNS Young Scientist Award
Quantitative Imaging of Crystalline Structural Information by Pulsed Neutron Transmission
The Japanese Society for Neutron Science
Hirotaka Sato, November 2011

The JSNS Technology Award
Development of High-efficient Inelastic Neutron Scattering Method with Multiple Incident Energies on a Chopper Spectrometer
The Japanese Society for Neutron Science
Ryoichi Kajimoto, Mitsutaka Nakamura, Yasuhiro Inamura, Takeshi Nakatani, Wataru Kambara, Tetsuya Yokoo, Fumio Mizuno, November 2011

The Awards of CrSJ, S. Nishikawa Award
Neutron and X-ray Scattering Study of Structure and Dynamics of Condensed Matters
The Crystallographic Society of Japan
Yasuhiko Fujii, November 2011

平成 23 年度理事長表彰　研究開発功績賞（日本原子力研究開発機構）
物質階層構造のマルチスケール解析を目指した先端的中性子超小角散乱法の開発
小泉智、能田洋平、山口大輔、奥隆之、鈴木淳市、岩瀬裕希
平成 23 年 10 月 1 日

日本鉄鋼協会俵論文賞
中性子小角散乱法による鉄鋼中ナノ析出物のサイズ評価
安原久雄、佐藤馨、田路勇樹、大沼正人、鈴木淳市、友田陽
平成 23 年 3 月 25 日

日本中間子科学会若手奨励賞
μ^+SR 法による分子磁性体の磁気構造キラリティの研究
大石一城
平成 24 年 3 月 26 日

日本材料学会関東支部年間活動賞
桐山幸治
平成 23 年 4 月 25 日

日本非破壊検査協会第 19 回超音波による非破壊評価シンポジウム 新進賞
Cavitation damage evaluation by nonlinear ultrasonic technique
万濤
平成 24 年 1 月 27 日

平成 23 年度日本結晶学会年会 ポスター賞
新しい粉末指数づけアルゴリズムとその実行結果について
富安亮子
2011 年 11 月 24 日

2011 年日本金属学会秋期大会 ポスター賞
中性子および X 線回折による超イオン伝導体 $Li_7P_3S_{11}$ の構造研究
小野寺陽平
2011 年 12 月 7 日

MLF Publication 2011

1 T. Adachi, Y. Tanabe, K. Suzuki, Y. Koike, T. Suzuki, T. Kawamata, and I. Watanabe
Development of Cu-Spin Correlation in the $Bi_{1.74}Pb_{0.38}Sr_{1.88}Cu_{1-y}Zny O_{6+\delta}$ High-Temperature Superconductors Observed by Muon Spin Relaxation
Physical Review B **83** 184522 (2011)

2 M. Arai
Pulsed Neutron Sources and Facilities
Neutrons in Soft Matter, edt T. Imae et al., John Wiley & Sons Publication 601 (2011)

3 Y. Arimoto, T. Yoshioka, H.M. Shimizu, K. Mishima, T. Ino, K. Taketani, S. Muto, M. Kitaguchi, S. Imajo, Y. Iwashita, S. Yamashita, Y. Kamiya, A. Yoshimi, K. Asahi, T. Shima, and K. Sakai
Longitudinal-gradient magnet for time focusing of ultra-cold neutrons
Physics Procedia **17** 20 (2011)

4 Y. Arimoto, T. Ino, H.M. Shimizu, T. Kamiyama, H. Kira, T. Oku, Y. Sakaguchi, K. Kakurai, K. Sakai, J. Suzuki, S. Koizumi, M. Arai, Y. Endo, M. Nakamura, T. Shinohara, M. Takeda, S. Wakimoto, D. Yamazaki, K. Ohoymama, H. Hiraka, et al.
External cavity design of high-power diode laser for polarized helium-3 neutron spin filters based on spin-exchange optical pumping
Physica B **406** 2439 (2011)

5 K.H. Chow, M. Månsson, Y. Ikedo, J. Sugiyama, O. Ofer, E.J. Ansaldo, J.H. Brewer, M. Isobe, H. Gotou, T. Yagi, Y Ueda, and C. Baines
μSR Investigation of the Hollandite Vanadate $K_2V_8O_{16}$
Physics Procedia (2011)

6 藤井保彦
J-PARC 特定中性子線施設における登録機関の役割
日本中性子科学会誌「波紋」**21** 184 (2011)

7 藤井保彦
こんにちは、AONSA です
日本中性子科学会誌「波紋」**21** 192 (2011)

8 T. Fukuda, A.Q.R. Baron, H. Nakamura, S. Shamoto, M. Ishikado, M. Machida, H. Uchiyama, A. Iyo, H. Kito, J. Mizuki, M. Arai, and H. Eisaki
Phonon Spectra of $PrFeAsO_{1-y}$ via Inelastic X-ray Scattering
Journal of the Physical Society of Japan **80** SB015-1 (2011)

9 T. Fukuda, A.Q.R. Baron, H. Nakamura, S. Shamoto, M. Ishikado, M. Machida, H. Uchiyama, A. Iyo, H. Kito, J. Mizuki, M. Arai, and H. Eisaki
Soft and Isotropic Phonons in $PrFeAsO_{1-y}$
Physical Review B **84** 064504 (2011)

10 R. Fukuta, S. Miyasaka, K. Hemmi, S. Tajima, D. Kawana, K. Ikeuchi, Y. Yamasaki, A. Nakao, H. Nakao, Y. Murakami, and K. Iwasa
Effect of cation-size variation on spin and orbital orders in $Eu_{1-x}(La_{0.254}Y_{0.746})_xVO_3$
Physical Review B **84** 140409 (2011)

11 二川正敏、前川藤夫、坂元眞一
1-MW pulsed spallation neutron source (JSNS) at J-PARC
Neutron News **22** 15 (2011)

12 二川正敏、直江崇
Dynamic responses of a solid wall in contact with a bubbly liquid excited by thermal shock loading
Experimental Thermal and Fluid Science **35** 1177 (2011)

13 H. Gretarsson, A. Lupascu, J. Kim, D. Casa, T. Gog, W. Wu, S.R. Julian, Z.J. Xu, J.S. Wen, G.D. Gu, R.H. Yuan, Z.G. Chen, N.-L. Wang, S. Khim, K.H. Kim, M. Ishikado, I. Jarrige, S. Shamoto, J.-H. Chu, I.R. Fisher, and Y.-J. Kim
Revealing the dual nature of magnetism in iron pnictides and iron chalcogenides using x-ray emission spectroscopy
Physical Review B **84** 100509 (R) (2011)

14 H. Harada, S. Goko, A. Kimura, M. Ohta, M. Oshima, F. Kitatani, Y. Toh, K. Furutaka, T. Kin, M. Koizumi, S. Nakamura, M. Igashira, T. Katabuchi, M. Mizumoto, T. Ohsaki, J. Hori, T. Fujii, K. Takamiya, J. Goto, Y. Kiyanagi, K. Kino,x M. Furusaka, F. Hiraga, and T. Kamiyamah
Study of Neutron Capture Reactions Using the 4-pai Ge Spectrometer
Journal of the Korean Physical Society **59** 1547 (2011)

15 T. Hemmi, S. Harjo, T. Ito, K. Matsui, Y. Nunoya, N. Koizumi, Y. Takahashi, H. Nakajima, K. Aizawa, H. Suzuki, S. Machiya, H. Oguro, Y. Tsuchiya, and K. Osamura
Neutron Diffraction Measurements of Internal Strain in Nb_3Sn Cable-In-Conduit Conductors
IEEE Trans. Appl. Supercond. **21** 2028 (2011)

16 J. Hori, K. Furutaka, S. Goko, H. Harada, A. Kimura, T. Kin, F. Kitatani, M. Koizumi, S. Nakamura, M. Ohta, M. Oshima, Y. Toh, M. Igashira, T. Katabuchi, M. Mizumoto, T. Kamiyama, K. Kinox, and Y. Kiyanagi
Measurement of Neutron Capture Gamma Rays from the Resonances of ^{91}Zr and ^{96}Zr at the J-PARC/MLF/ANNRI
Journal of the Korean Physical Society **59** 1777 (2011)

17 Y. Idemoto, Y. Tsukada, N. Kitamura, A. Hoshikawa, and T. Ishigaki.
Charge in Crystal Structure of $LiNi_{0.8}Co_{0.19}Cu_{0.01}O_2$ Cathode during Charge of Coin Cell Observed by Ex situ Time-of-flight Neutron Diffraction.
Chemistry Letters **40** 168 (2011)

18 K. Iida, M. Kofu, N. Katayama, J. Lee, R. Kajimoto, Y. Inamura, M. Nakamura, M. Arai, Y. Yoshida, M. Fujita, K. Yamada, and S.-H. Lee
Inelastic neutron scattering study of the magnetic fluctuations in Sr_2RuO_4
Physical Review B **84** 060402 (2011)

19 H. Iikura, N. Tsutsui, T. Nakamura, M. Katagiri, M. Kureta, J. Kubo, and M. Matsubayashi
Evaluations of the new LiF-scintillator and optional brightness enhancement films for neutron imaging
Nuclear Instruments and Methods in Physics Research Section A **651** 100 (2011)

20 R. Iizuka, H. Kagi, K. Komatsu, D. Ushijima, S. Nakano, A. Sano-Furukawa, T. Nagai, and T. Yagi
Pressure responses of portlandite and H-D isotope effects on pressure-induced phase transitions

Physics and Chemistry of Minerals **38** 777 (2011)

21 K. Ikeda, H. Ohshita, N. Kaneko, J. Zhang, M. Yonemura, T. Otomo, K. Suzuya, H.Yukawa, M. Morinaga, H.-W. Li, S. Semboshi, and S. Orimo
Data Acquisition System for High Resolution Chopper Spectrometer (HRC) at J-PARC
Materials Transactions **52** 598 (2011)

22 Y. Ikedo Y. Miyake, K. Shimomura, P. Strasser, K. Nishiyama, N. Kawamura, H. Fujimori, S. Makimura, A. Koda, K. Nakahara, T. Ogitsu, Y. Makida, T. Adachi, M. Yoshida, A. Yamamoto, T. Nakamoto, K. Sasaki, K. Tanaka, N. Kimura, W. Higemoto, Y. Ajima, K. Ishida, Y. Matsuda, and A. Satof
The Status of the Superomega Muon Beamline
AIP Conference Proceedings **1382** 220 (2011)

23 V.A. Innis-Samson, M. Mizusawa, and K. Sakurai
X-ray Reflection Tomography: A New Tool for Surface Imaging
Analytical Chemistry **83** 7600 (2011)

24 T. Ino, Y. Arimoto, T. Yoshioka, K. Mishima, K. Taketani, S. Muto, H.M. Shimizu, H. Kira, Y. Sakaguchi, T. Oku, K. Sakai, T. Shinohara, J. Suzuki, H. Otono, H. Oide, S. Yamashita, S. Imajo, H. Funahashi, M. Yamada, Y. Iwashita, *et al.*
Measurement of the neutron beam polarization of BL05/NOP beamline at J-PARC
Physica B **406** 2424 (2011)

25 R. Inoue, K. Kawashima, K. Matsui, M. Nakamura, K. Nishida, T. Kanaya, and N.L. Yamada
Interfacial properties of polystyrene thin films as revealed by neutron reflectivity
Physical Review E **84** 031802 (2011)

26 K. Ishii, S. Ishihara, Y. Murakami, K. Ikeuchi, K. Kuzushita, T. Inami, K. Ohwada, M. Yoshida, I. Jarrige, N. Tatami, S. Niioka, D. Bizen, Y. Ando, J. Mizuki, S. Maekawa, and Y. Endoh
Polarization-analyzed resonant inelastic x-ray scattering of the orbital excitations in $KCuF_3$
Physical Review B **83** 241101 (2011)

27 K. Ishii, K. Tsutsui, K. Ikeuchi, I. Jarrige, J. Mizuki, H. Hiraka, K. Yamada, T. Tohyama, S. Maekawa, Y. Endoh H. Ishii, and Y.Q. Cai
Electronic excitations around the substituted atom in $La_2Cu_{1-y}Ni_yO_4$ as seen via resonant inelastic x-ray scattering
Physical Review B **85** 104509 (2011)

28 M. Ishikado, Y. Nagai, K. Kodama, R. Kajimoto, M. Nakamura, Y. Inamura, S. Wakimoto, H. Nakamura, M. Machida, K. Suzuki, H. Usui, K. Kuroki, A. Iyo, H. Eisaki, M. Arai, and S. Shamoto
$s_{\pm}$-like spin resonance in the iron-based nodal superconductor $BaFe_2(As_{0.65}P_{0.35})_2$ observed using inelastic neutron scattering
Physical Review B **84** 144517 (2011)

29 M. Ishikado, K. Kodama, R. Kajimoto, M. Nakamura, Y. Inamura, S. Wakimoto, A. Iyo, H. Eisaki, M. Arai, and S. Shamoto
Inelastic neutron scattering on iron-based superconductor $BaFe_2(As,P)_2$
Physica C **471** 643 (2011)

30 T.U. Ito, W. Higemoto, K. Ninomiya, A. Amato, T. Sugai, Y. Haga, and H. S. Suzuki
Possible Long-periodic Magnetic Structure in $SmPb_3$
Journal of the Physical Society of Japan **80** SA075 (2011)

31 T.U. Ito, W. Higemoto, K. Ninomiya, H. Luetkens, T. Sugai, Y. Haga, and H.S. Suzuki
Incommensurate-to-Commensurate Magnetic Phase Transition in $SmIn_3$ Observed by Muon Spin Relaxation
Journal of the Physical Society of Japan **80** 033710 (2011)

32 伊藤晋一、中山恒義
パーコレーション磁性体における反強磁性フラクトン
日本中性子科学会誌「波紋」**21** 234 (2011)

33 S. Itoh, T. Nakayama, and M.A. Adams
Antiferromagnetic Fractons in Diluted Heisenberg Systems $RbMn_{0.4}Mg_{0.6}F_3$ and $Rb_2Mn_{0.598}Mg_{0.402}F_4$
Journal of the Physical Society of Japan **80** 104704 (2011)

34 S. Itoh, T. Yokoo, S. Satoh, S. Yano, D. Kawana, J. Suzuki, and T.J. Sato
High Resolution Chopper Spectrometer (HRC) at J-PARC
Nuclear Instruments and Methods in Physics Research Section A **631** 90 (2011)

35 S. Itoh, K. Ueno, R. Ohkubo, H. Sagehashi, Y. Funahashi, and T. Yokoo
Irradiation properties of T0 chopper components
Nuclear Instruments and Methods in Physics Research Section A **654** 527 (2011)

36 H. Iwase, H. Endo, M. Katagiri, and M. Shibayama
Modernization of the small-angle neutron scattering spectrometer SANS-U by upgrade to a focusing SANS spectrometer
Journal of Applied Crystallography **44** 558 (2011)

37 K. Iwase, K. Mori, Y, Hishinuma, Y. Hasegawa, S. Iimura, H. Ishikawa, T. Kamoshida, and T. Ishigaki
Development of sample holder for in situ neutron measurement of hydrogen absorbing alloy
International Journal of hydrogen energy **36** 3062 (2011)

38 T. Kai, M. Segawa, M.Ooi, E. Hashimoto, T. Shinohara, M. Harada, F. Maekawa, K. Oikawa, T. Sakai, M. Matsubayashi, and M. Kureta
First demonstration of neutron resonance absorption imaging using a high-speed video camera in J-PARC
Nuclear Instruments and Methods in Physics Research A **651** 126 (2011)

39 T. Kai, M. Segawa, M. Ooi, E. Hashimoto, T. Shinohara, M. Harada, F. Maekawa, K. Oikawa, T. Sakai, M. Matsubayashi, and M. Kureta
First demonstration of neutron resonance absorption imaging using a high-speed video camera in J-PARC
Nuclear Instruments and Methods in Physics Research Section A **651** 126 (2011)

40 梶本亮一、前川藤夫、有馬寛、吉成静香、新井正敏
「J-PARC/MLF JAEA プロジェクト研究に関する研究会」講演資料集：2010 年 9 月 29 日、10 月 28 日、10 月 29 日、いばらき量子ビーム研究センター、東海村
JAEA-Review 2011-014 213 (2011)

41 R. Kajimoto, M. Nakamura, Y. Inamura, F. Mizuno, K. Nakajima, S. Ohira-Kawamura, T. Yokoo, T. Nakatani, R. Maruyama, K. Soyama, K. Shibata, K. Suzuya, S. Sato, K. Aizawa, M. Arai, S. Wakimoto, M. Ishikado, S. Shamoto, M. Fujita, H. Hiraka, K. Ohoyama, K. Yamada, and C.-H. Lee
The Fermi Chopper Spectrometer 4SEASONS at J-PARC
Journal of the Physical Society of Japan **80** SB025 (2011)

42 K. Kamada, H. Furukawa, T. Kurokawa, T. Tada, T. Tominaga, Y. Nakano, and J.P. Gong
Surfactant-induced friction reduction for hydrogels in the boundary lubrication regime
Journal of Physics: Condenced Matter **23** 284107-1 (2011)

43 N. Kamaya, K. Homma, Y. Yamakawa, M. Hirayama, R. Kanno, M. Yonemura, T. Kamiyama, Y. Kato, S. Hama, K. Kawamoto, and A. Mitsui
A lithium superionic conductor
Nature Materials **10** 682 (2011)

44 K. Kamazawa, H. Nozaki, M. Harada, K. Mukai, Y. Ikedo, K. Iida, T.J. Sato, Y. Qiu, M. Tyagi, and J. Sugiyama
Interrelationship between Li^+ diffusion, charge, and magnetism in $^7LiMn_2O_4$ and $^7Li_{1.1}Mn_{1.9}O_4$ spinels: Elastic, inelastic, and quasielastic neutron scattering
Physical Review B **83** 094401 (2011)

45 Y. Kasugai, M. Ooi, and T. Kai
Gamma dose measurements and spectroscopy analysis for spallation products in JSNS mercury circulation system
Progress in Nuclear Science and Technology **1** 501 (2011)

46 Y. Kasugai, N. Matsuda, Y. Iwamoto, Y. Sakamoto, H. Nakashima, N. Kinoshita, H. Iwase, T. Sanami, M. Hagiwara, H. Hirayama, H. Yashima, N. Sigyo, H. Arakawa, K. Ishibashi, N. Mokhov, A. Leveling, D. Boehnlein, K. Vaziri, G. Lauten, S. Wayne, V. Cupps, B. Kershisnik, S. Benesch, T. Nakamura, K. Oishi, and K. Niita
Shielding experiments under JASMIN Collaboration at Fermilab (I) Overview of the Research Activities
Journal of the Korean Physical Society **59** 2063 (2011)

47 D. Kawaguchi, A. Nelson, Y. Masubuchi, J.P. Majewski, N. Torikai, N.L. Yamada, A.R. Siti Sarah, A. Takano, and Y. Matsushita
Precise Analyses of Short-Time Relaxation at Asymmetric Polystyrene Interface in Terms of Molecular Weight by Time-Resolved Neutron Reflectivity Measurements
Macromolecules **44** 9424 (2011)

48 M. Kawai, M. Futakawa, T. Naoe, H. Yamada, and C.-N. Xu
Measurements of strain-rate distributions on material after SHPB impact
Engineering Transaction **59** 1 (2011)

49 S. Ohira-Kawamura, K. Nakajima, Y Inamura, Y. Tsujimoto, A. Kitada, F. Takeiri, H. Kageyama, Y. Ajiro, M. Nishi, and K. Kakurai
ToF Inelastic neutron scattering studies on quantum spin systems $(CuCl)LaB_2O_7$ (B = Nb, Ta)
Journal of Physics: Conference Series **320** 012037 (2011)

50 A. Kimura, K. Furutaka, S. Goko, H. Harada, T. Kin, F. Kitatani, M. Koizumi, S. Nakamura, M. Ohta, M. Oshima, Y. Toh, T. Fujii, S. Fukutani, J. Hori, K. Takamiya, M. Igashira, T. Katabuchi, M. Mizumoto, T. Kamiyama, K. Kino, and Y. Kiyanagi
Measurements of Neutron-capture Cross Sections of ^{244}Cm and ^{246}Cm at J-PARC/MLF/ANNRI
Journal of the Korean Physical Society **59** 1828 (2011)

51 T. Kin, K. Furutaka, S. Goko, H. Harada, A. Kimura, F. Kitatani, S. Nakamura, M. Ohta, M. Oshima, Y. Toh, J. Hori, M. Igashira, T. Katabuchi, M. Koizumi, M. Mizumoto, T. Kamiyama, K. Kino, and Y. Kiyanagi
The "4-pi Ge Spectrometer" for Measurements of Neutron Capture Cross Sections by the TOF Method at the J-PARC/MLF/ANNRI
Journal of the Korean Physical Society **59** 1769 (2011)

52 K. Kino, M. Furusaka, F. Hiraga, T. Kamiyama, Y. Kiyanagi, K. Furutaka, S. Goko, H. Harada, M. Harada, T. Kai, A. Kimura, T. Kin, F. Kitatani, M. Koizumi, F. Maekawa, S. Meigo, S. Nakamura, M. Ooi, M. Ohta, M. Oshima, Y. Toh, M. Igashira, T. Katabuchi, and M. Mizumoto
Measurement of energy spectra and spatial distributions of neutron beams provided by the ANNRI beamline for capture cross-section measurements at the J-PARC/MLF
Nuclear Instruments and Methods in Physics Research A **626-627** 58 (2011)

53 K. Kino, K. Mori, M. Yonemura, S. Torii, M. Kawai, T. Fukunaga, and T. Kamiyama
Design of Air Scattering Chamber for the Powder Diffractometer SPICA
Journal of the Physical Society of Japan **80** SB01 (2011)

54 木下秀孝、涌井隆、松井寛樹、前川藤夫、春日井好己、羽賀勝洋、勅使河原誠、明午伸一郎、関正和、坂元眞一、二川正敏
J-PARC MLF 使用済放射化機器保管計画検討結果
JAEA-Technology 2011-040

55 H. Kira, Y. Sakaguchi, T. Oku, J. Suzuki, M. Nakamura, M. Arai, Y. Endoh, L.J. Chang, K. Kakurai, Y. Arimoto, T. Ino, H.M. Shimizu, T. Kamiyama, K. Ohoyama, H. Hiraka, K. Tsutsumi, and K Yamada
Developments of In-Situ SEOP Polarized ^3He Neutron Spin Filter in Japan
Journal of Physics: Conference Series **294** 012014 (2011)

56 H. Kira, Y. Sakaguchi, T. Oku, J. Suzuki, M. Nakamura, M. Arai, K. Kakurai, Y. Endo, Y. Arimoto, T. Ino, H.M. Shimizu, T. Kamiyama, K. Tsutsumi, K. Ohoyama, H. Hiraka, K. Yamada, and L.-J. Chang
Development and test of SEOP neutron spin filter in Japan
Physica B **406** 2433 (2011)

57 Y. Kiyanagi, T. Kamiyama, H. Sato, T. Shinohara, T. Kai, K. Aizawa, M. Arai, M. Harada, K. Sakai, K. Oikawa, M. Ohi, F. Maekawa, T. Sakai, M. Matsubayashi, M. Segawa, and M. Kureta
Design study of the imaging beamline at J-PARC MLF, ERNIS
Nuclear Instruments and Methods in Physics Research A **651** 16 (2011)

58 Y. Kiyanagi, K. Kino, M. Furusaka, F. Hiraga, T. Kamiyama, K. Kato, M. Igashira, T.Katabuchi, M. Mizumoto, M. Oshima, H. Harada, J. Katakura, K. Furutaka, S. Goko, A.Kimura, T. Kin, F. Kitatani, M. Koizumi, S. Nakamura, M. Ohta, Y. Toh, T. Ohtsuki, K.Hirose, T. Fujii, J. Hori, K. Takamiya, S. Fukutani, M. Shibata, K. Yamada, and H. Utsunomiya
The Study on Nuclear Data by Using a High Intensity Pulsed Neutron Source for Advanced Nuclear System' Nuclear Data Project and the Characteristics of the Neutron Beam Line for the Capture Cross Section Experiments at J-PARC
Journal of the Korean Physical Society **59** 1781 (2011)

59 Y. Kiyanagi, T. Kamiyama, H. Sato, T. Shinohara, T. Kai, K. Aizawa, M. Arai, M. Harada, K. Sakai, K. Oikawa, M. Ohi, F. Maekawa, T. Sakai, M. Matsubayashi, M. Segawa, and M. Kureta
Design study of the imaging beam line at J-PARC MLF, ERNIS
Nuclear Instruments and Methods in Physics Research Section A **651** 16 (2011)

60 Y. Kiyanagi
Accurate Neutron Nucleus Reaction Measurement Instrument (ANNRI) for Capture Cross Section Measurements at J-PARC
Journal of the Korean Physical Society **59** 779 (2011)

61 M. Kobayashi, K. Mitamura, M. Terada, N.L. Yamada, and A. Takahara
Characterization of Swollen States of Polyelectrolyte Brushes in Salt Solution by Neutron Reflectivity
Journal of Physics: Conference Series **272** 012019 (2011)

62 W. Kobayashi, Y. Hayashi, M. Matsushita, Y. Yamamoto, I. Terasaki, A. Nakao, H. Nakao, Y. Murakami, Y. Moritomo, H. Yamauchi, and M. Karppinen
Anisotropic thermoelectric properties associated with dimensional

crossover in quasi-one-dimensional $SrNbO_{3.4+d}$ (d-0.03)
Physical Review B **84** 085118-1 (2011)

63 H.-J. Liu, U.-S. Jeng, N.L. Yamada, A.-C. Su, W.-R. Wu, C.-J. Su, S.-J. Lin, K.-H. Wei, and M.-Y. Chiu
Surface and interface porosity of polymer/fullerene-derivative thin films revealed by contrast variation of neutron and X-ray reflectivity
Soft Matter **7** 9276 (2011)

64 H. Mamiya, N. Terada, H. Kitazawa, A. Hoshikawa, and T. Ishigaki
Structural and Magnetic Properties of Dilute Spinel Ferrites: Neutron Diffractometry and Magnetmetry Investigation.
Journal of Magnetics **16** 134 (2011)

65 K. Matsubayashi, K. Munakata, M. Isobe, N. Katayama, K. Ohgushi, Y. Ueda, N. Kawamura, M. Mizumaki, N. Ishimatsu, M. Hedo, I. Umehara, and Y. Uwatoko
Pressure-induced changes in the magnetic and valence state of $EuFe_2As_2$
Physical Review B **84** 024502-1 (2011)

66 M. Matsui, K. Komatsu, E. Ikeda, A. Sano-Furukawa, H. Gotou, and T. Yagi
The crystal structure of δ-$Al(OH)_3$: Neutron diffraction measurements and ab initio calculations
American Mineralogist **96** 854 (2011)

67 H. Matsuo, Y. Kitanaka, Y. Noguchi, M. Miyayama, T. Ozaki, S. Mori, S. Torii, and T. Kamiyama,
Ferroelectric Properties and Domain Structures of $(Bi_{0.5}K_{0.5})TiO_3$-$BiFeO_3$ ceramics
Transactions of the Materials Research Society of Japan **36** 285 (2011)

68 吉良弘
オンビーム Spin Exchange Optical Pumping 型 ^{3}He 偏極フィルターシステムの開発
日本中性子科学会誌「波紋」**21** 146 (2011)

69 K. Mitamura, N.L. Yamada, H. Sagehashi, H. Seto, N. Torikai, T. Sugita, M. Furusaka, and A. Takahara
Advanced Neutron Reflectometer for Investigation on Dynamic/Static Structures of Soft-Interfaces in J-PARC
Journal of Physics: Conference Series **272** 012017 (2011)

70 Y. Miyake, K. Shimomura, N. Kawamura, P. Strasser, A. Koda, H. Fujimori, S. Makimura, K. Nakahara, M. Kato, S. Takeshita, K. Nishiyama, Y. Kobayashi, K. Kojima, R. Kadono, W. Higemoto, T. Ito, K. Ninomiya, M. Hiraishi, M. Miyazaki, and K. Kubo
Strongest Pulsed Muon Source at J-PARC MUSE
AIP Conference Proceedings **1382** 217 (2011)

71 Y. Miyake, N. Nishida, J. Yoshino, W. Higemoto, E. Torikai, K. Shimomura, Y. Ikedo, N. Kawamura, P. Strasser, S. Makimura, H. Fujimori, K. Nakahara, A. Koda, Y. Kobayashi, K. Nishiyama, R. Kadono, T. Ogitsu, Y. Makida, K. Sasaki, T. Adachi, and K. Nagamine
Ultra Slow Muon Microscopy for Nano-science
Journal of Physics: Conference Series **302** 012038 (2011)

72 M. Miyazaki, R. Kadono, M. Hiraishi, T. Masuda, A. Koda, K.M. Kojima, T. Yamazaki, Y. Tabata, and H. Nakamura
Quasi-One-Dimensional Spin Dynamics in d-Electron Heavy-Fermion Metal $Y_{1-x}Sc_xMn_2$
Journal of the Physical Society of Japan **80** 063707 (2011)

73 M. Mizusawa, and K. Sakurai
In-situ X-ray reflectivity measurement of polyvinyl acetate thin films during glass transition
IOP Conference Series: Materials Science and Engineering **24** 012013 (2011)

74 森井幸生、藤井保彦
連載講座「中性子回折の基礎と応用」を終わるにあたって
RADIOISOTOPES **60** 151 (2011)

75 S. Morooka, N. Sato, M. Ojima, S. Harjo, Y. Adachi, Y. Tomota, and O. Umezawa
In-situ Neutron Diffraction Study on Work-hardening Behavior in a Ferrite-Martensite Dual Phase Steel
International Journal of Automotive Engineering **2** 361 (2011)

76 K. Mukai, J. Sugiyama, K. Kamazawa, Y. Ikedo, D. Andreica, and A. Amato
Magnetic properties of the chemically delithiated $Li_xMn_2O_4$ with $0.07<x<1$
Journal of Solid State Chemistry **184** 1096 (2011)

77 M. Nagano, F. Yamaga, N. Zettsu, D. Yamazaki, R. Maruyama, K. Soyama, and K. Yamamura
Development of fabrication process for aspherical neutron focusing mirror using numerically controlled local wet etching with low-pressure polishing
Nuclear Instruments and Methods in Physics Research Section A **634** 112 (2011)

78 K. Nakajima, S. Ohira-Kawamura, T. Kikuchi, M. Nakamura, R. Kajimoto, Y. Inamura, N. Takahashi, K. Aizawa, K. Suzuya, K. Shibata, T. Nakatani, K. Soyama, R. Maruyama, H. Tanaka, W. Kambara, T. Iwahashi, Y. Itoh, T. Osakabe, S. Wakimoto, K. Kakurai, F. Maekawa, M. Harada, K. Oikawa, R.E. Lechner, F. Mezei, and M. Arai
AMATERAS: A Cold-Neutron Disk Chopper Spectrometer
Journal of the Physical Society of Japan **80** SB28 (2011)

79 M. Nakamura, K. Nakajima, Y. Inamura, S. Ohira-Kawamura, T. Kikuchi, T. Otomo, and M. Arai
A Possibility of Dynamical Study on Solid State Ionic Materials by Inelastic Neutron Scattering
Atom Indonesia **36** 116 (2010)

80 S. Nakamura, K. Furutaka, S. Goko, H. Harada, A. Kimura, T. Kin, F. Kitatani, M. Koizumi, M. Ohta, M. Oshima, Y. Toh, J. Hori, T. Fujii, S. Fukutani, K. Takamiya, M. Igashira, T. Katabuchi, M. Mizumoto, T. Kamiyama, K. Kino, and Y. Kiyanagi
Measurements of Neutron-capture Cross Sections of Palladium Isotopes at the J-PARC/MLF/ANNRI
Journal of the Korean Physical Society **59** 1773 (2011)

81 T. Nakamura, R. Yasuda, M. Katagiri, K. Toh, K. Sakasai, A. Birumachi, M. Ebine, and K. Soyama
Development of Wavelength-Shifting-Fiber Neutron Image Detector with a Fiber-Optic Taper with a High Spatial Resolution
2011 IEEE Nuclesr Scinece Symposium Conference Record, M-179 (2011)

82 Y. Nakano, T. Kurokawa, M. Du, J. Liu, T. Tominaga, Y. Osada, and J.P. Gong
Effect of Hyaluronan Solution on Dynamic Friction of PVA Gel Sliding on Weakly Adhesive Glass Substrate
Macromolecules **44** 8908 (2011)

83 中谷健、稲村泰弘
J-PARC と計算科学の連携
RIST NEWS **49** 20 (2010)

84 K. Nakayama, Y. Hirose, J. Soeda, M. Yoshizumi, T. Uemura, M. Uno, W. Li, M.J. Kang, M. Yamagishi, Y. Okada, E. Miyazaki, Y. Nakazawa, A. Nakao, K. Takimiya, and J. Takeya

Patternable Solution-Crystallized Organic Transistors with High Charge Carrier Mobility
Advanced Materials **23** 1575 (2011)

85 M. Uno, K. Nakayama, J. Soeda, Y. Hirose, K. Miwa, T. Uemura, A. Nakao, K. Takimiya, and J. Takeya
High-Speed Flexible Organic Field-Effect Transistors with a 3D Structure
Advanced Materials **23** 3047 (2011)

86 直江崇、粉川広行、二川正敏、井田真人
Mitigation technologies for damage induced by pressure waves in high-power mercury spallation neutron sources, 3; Consideration of the effect of microbubbles on pressure wave propagation through a water test
Journal of Nuclear Science and Technology **48** 865 (2011)

87 根本靖久
超伝導ソレノイド電磁石用ヘリウム冷凍機の運転および保守管理
Proceedings of the Meeting on the Technical Study at KEK
KEK Proceedings 2011-2 5 (2011)

88 I. Nishi, M. Ishikado, S. Ideta, W. Malaeb, T. Yoshida, A. Fujimori, Y. Kotani, M. Kubota, K. Ono, M. Yi, D.H. Lu, R. Moore, Z.-X. Shen, A. Iyo, K. Kihou, H. Kito, H. Eisaki, S. Shamoto, and R. Arita,
Angle-resolved photoemission spectroscopy study of $PrFeAsO_{0.7}$: Comparison with LaFePO
Physical Review B **84** 014504 (2011)

89 Y. Oba, S. Koppoju, M. Ohnuma, T. Murakami, H. Hatano, K. Sasakawa, A. Kitahara, and J. Suzuki
Quantitative Analysis of Precipitate in Vanadium-microalloyed Medium Carbon Steels Using Small-angle X-ray and Neutron Scattering Methods
ISIJ International **51** 1852 (2011)

90 O. Ofer, J. Sugiyama, J.H. Brewer, E.J. Ansaldo, M. Månsson, K.H. Chow, K. Kamazawa, Y. Doi, and Y. Hinatsu
Frustration and magnetism of the zigzag chain compounds EuL_2O_4 (L = Yb, Lu,Gd, Eu)
Physical Review B **84** 054428 (2011)

91 H. Okabe, M. Isobe, E. Takayama-Muromachi, A. Koda, S. Takeshita, M. Hiraishi, M. Miyazaki, R. Kadono, Y. Miyake, and J. Akimitsu
Ba_2IrO_4: A spin-orbit Mott insulating quasi-two-dimensional antiferromagnet
Physical Review B **83** 155118 (2011)

92 T. Okuda, K. Uto, S. Seki, Y. Onose, Y. Tokura, R. Kajimoto, and M. Matsuda
Effect of spin dilution on the magnetic state of delafossite $CuCrO_2$ with an S = 3/2 antiferromagnetic triangular sublattice
Journal of the Physical Society of Japan **80** 014711-1 (2011)

93 Y. Onodera, K. Mori, T. Otomo, A.C. Hannon, M. Sugiyama, and T. Fukunaga
Reverse Monte Carlo modeling of Li_2S-P_2S_5 superionic conductors
Journal of Physics: Conference Series **340** 012058 (2011)

94 大井元貴、小川弘達、加美山隆、鬼柳善明
Experimental studies of the effect of the ortho/para ratio on the neutronic performance of a liquid hydrogen moderator for a pulsed neutron source
Nuclear Instruments and Methods in Physics Research A **659** 61 (2011)

95 K. Osamura, S. Machiya, Y. Tsuchiya, S. Harjo, H. Suzuki, T. Shobu, K. Kiriyama, and M. Sugano
Unusual Internal Strain Behavior Exerted on YBCO Layer in the Surround Cu Stabilized YBCO Coated Conductor
IEEE Trans. Appl. Supercond. **21** 3090 (2011)

96 大友季哉
高エネルギー加速器研究機構と中性子全散乱装置
触媒技術の動向と展望 2011 235 (2011)

97 T. Otomo
SANS Instruments at Pulsed Neutron Sources
Neutrons in Soft Matter, T. Imae, T. Kanaya, M. Furusaka, N. Torikai, (Eds.) 57 (2011)

98 Y. Sakaguchi, H. Kira, T. Oku, T. Shinohara, J. Suzuki, K. Sakai, M. Nakamura, K. Suzuya, K. Aizawa, M. Arai, M. Takeda, Y. Endoh, L.J. Chang, Y. Arimoto, T. Ino, H.M. Shimizu, T. Kamiyama, K. Ohoyama, H. Hiraka, K. Tsutsumi, K. Yamada, K. Ohara, and K. Kakurai
Structure of glasses for ^{3}He neutron spin filter cells
Journal of Physics: Conference Series **294** 012004 (2011)

99 Y. Sakaguchi, H. Kira, T. Oku, T. Shinohara, J. Suzuki, K. Sakai, M. Nakamura, K. Aizawa, M. Arai, Y. Noda, S. Koizumi, M. Takeda, Y. Endoh, L.J. Chang, Y. Arimoto, T. Ino, H.M. Shimizu, T. Kamiyama, K. Ohoyama, H. Hiraka, K. Tsutsumi, K. Yamada, and K. Kakurai
Applications of ^{3}He neutron spin filters on the small-angle neutron scattering spectrometer SANS-J-II
Journal of Physics: Conference Series **294** 012017 (2011)

100 Y. Sakaguchi, H. Kira, T. Oku, T. Shinohara, J. Suzuki, K. Sakai, M. Nakamura, K. Suzuya, K. Aizawa, M. Arai, M. Takeda, S. Wakimoto, D. Yamazaki, S. Koizumi, Y. Endoh, L.J. Chang, Y. Arimoto, T. Ino, H.M. Shimizu, T. Kamiyama, et al.
Research on glass cells for ^{3}He neutron spin filters
Physica B **406** 2443 (2011)

101 K. Sano, R. Kawamura, T. Tominaga, N. Oda, K. Ijiro, and Y. Osada
Self-Reparing Filamentous Actin Hydrogel with Hierarchical Structure
Biomacromolecules **12** 4173 (2011)

102 K. Sano, R. Kawamura, T. Tominaga, H. Nakagawa, N. Oda, K. Ijiro, and Y. Osada
Thermoresponsive Microtubule Hydrogel with High Hierarchical Structure
Biomacromolecules **12** 1409 (2011)

103 A. Sano-Furukawa, T. Kuribayashi, K. Komatsu, T. Yagi, and E. Ohtani
Investigation of hydrogen sites of wadsleyite: A neutron diffraction study
Physics of the Earth and Planetary Interiors **189** 56 (2011)

104 M. Sato, T. Kawamata, Y. Kobayashi, Y. Yasui, T. Iida, K. Suzuki, M. Itoh, T. Moyoshi, K. Motoya, R. Kajimoto, M. Nakamura, Y. Inamura, and M. Arai
Magnetic Excitation Spectra of Superconducting Ca–Fe–Pt–As System
Journal of the Physical Society of Japan **80** 093709 (2011)

105 瀬戸秀紀
リン脂質膜を中性子で見る
高分子 **60** 804 (2011)

106 瀬戸秀紀、日野正裕、山田悟史
パルス中性子源における NSE ～終わりに代えて
日本中性子科学会誌「波紋」**21** 239 (2011)

107 S. Shamoto, S. Wakimoto, K. Kodama, M. Ishikado, A.D. Christianson, M.D. Lumsden, R. Kajimoto, M. Nakamura, Y. Inamura, M. Arai, K. Kakurai, F. Esaka, A. Iyo, H. Kito, and H. Eisaki
Neutron scattering of iron-based superconductors
Physica C **471** 639 (2011)

108 H. Shigematsu, K. Nomura, K. Nishiyama, T. Tojo, H. Kawaji, T. Atake, Y. Kawamura, T. Miyoshi, Y. Matsushita, M. Tanaka, and H. Mashiyama
Structures and Phase Transitions in Rb_2MoO_4 and Rb_2WO_4
Ferroelecrrics **414** 195 (2011)

109 K. Shimomura
Possibility of precise measurements of muonium HFS at J-PARC MUSE
AIP Conference Proceedings **1382** 245 (2011)

110 S. Shinamura, I. Osaka, E. Miyazaki, A. Nakao, M. Yamagishi, J. Takeya, and K. Takimiya
Linear- and Angular-Shaped Naphthodithiophenes; Selective Synthesis, Properties, and Application to Organic Field-Effect Transistors
Journal of the American Chemical Society **133** 5024 (2011)

111 T. Shinohara, K. Sakai, M. Ohi, T. Kai, M. Harada, K. Oikawa, F. Maekawa, J. Suzuki, T. Oku, S. Takata, K. Aizawa, M. Arai, and Y. Kiyanagi
Quantitative magnetic field imaging by polarized pulsed neutrons at J-PARC
Nuclear Instruments and Methods in Physics Research Section A **651** 121 (2011)

112 篠原武尚
偏極中性子を用いたイメージング
日本中性子科学会誌「波紋」**21** 180 (2011)

113 L. Shu, W. Higemoto, Y. Aoki, A.D. Hillier, K. Ohishi, K. Ishida, R. Kadono, A. Koda, O.O. Bernal, D.E. MacLaughlin, Y. Tunashima, Y. Yonezawa, S. Sanada, D. Kikuchi, H. Sato, H. Sugawara, T.U. Ito, and M.B. Maple
Suppression of time-reversal symmetry breaking superconductivity in $Pr(Os_{1-x}Ru_x)_4Sb_{12}$ and $Pr_{1-y}LayOs_4Sb_{12}$
Physical Review B **83** 100504 (2011)

114 J. Soeda, Y. Hirose, M. Yamagishi, A. Nakao, T. Uemura, K. Nakayama, M. Uno, Y. Nakazawa, K. Takimiya, and J. Takeya
Solution-Crystallized Organic Field-Effect Transistors with Charge-Transfer Layers: High-Mobility, Printable, Air-stable and Low-Threshold-Voltage Operation in Air
Advanced Materials **23** 3309 (2011)

115 J. Soeda, T. Uemura, Y. Mizuno, A. Nakao, Y. Nakazawa, A. Facchetti, and J. Takeya
High Electron Mobility in Air for N,N'-1H,1H-Perfluorobutyldicyanoperylene Carboxydiimide Solution-Crystallized Thin-film Transistors on Hydrophobic Surfaces
Advanced Materials **23** 3681 (2011)

116 Y. Su, Y. Tomota, J. Suzuki, and M. Ohnua
Hydrogen Behavior in an Ultrafine-Grained Electrodeposited Pure Iron
ISIJ International **51** 1534 (2011)

117 J. Sugiyama, H. Nozaki, M. Harada, K. Kamazawa, O. Ofer, M. Månsson, J.H. Brewer, E.J. Ansaldo, K.H. Chow, Y. Ikedo, Y. Miyake, K. Ohishi, I. Watanabe, G. Kobayashi, and R. Kanno
Magnetic and diffusive nature of $LiFePO_4$ investigated by muon spin rotation and relaxation
Physical Review B **84** 054430 (2011)

118 J. Sugiyama, M. Månsson, O. Ofer, K. Kamazawa, M. Harada, D. Andreica, A. Amato, J.H. Brewer, E.J. Ansaldo, H. Ohta, C. Michioka, and K. Yoshimura
Successive magnetic transitions and static magnetic order in RCoAsO (R=La, Ce, Pr, Nd, Sm, Gd) confirmed by muon-spin rotation and relaxation
Physical Review B **84** 184421 (2011)

119 Y. Sumino, H. Kitahata, H. Seto, and K. Yoshikawa
Dynamical blebbing at a droplet interface driven by instability in elastic stress: a novel self-motile system
Soft Matter **7** 3204 (2011)

120 鈴谷賢太郎
中性子回折・全散乱法による液体・非晶質構造解析の基礎
Radioisotopes **60** 63 (2011)

121 N. Takahashi, K. Shibata, Y. Kawakita, K. Nakajima, Y. Inamura, T. Nakatani, H. Nakagawa, S. Fujiwara, T.J. Sato, I. Tsukushi, F. Mezei, D.A. Neumann, H. Mutka, and M. Arai
Repetition Rate Multiplication: RRM, an Advanced Measuring Method Planed for the Backscattering Instrument, DNA at the MLF, J-PARC
Journal of the Physical Society of Japan **80 Suppl. B** SB07 (2011)

122 Y. Takenaka, H. Kitahata, N.L. Yamada, H. Seto, and M. Hara
Growth of gold nanorods in gelled surfactant solutions
Journal of Colloid and Interface Science **356** 111 (2011)

123 K. Taketani, T. Ebisawa, M. Hino, K. Hirota, T. Ino, M. Kitaguchi, K. Mishima, S. Muto, H. Oide, T. Oku, H. Otono, K. Sakai, T. Shima, H.M. Shimizu, S. Yamashita, and T. Yoshioka
A high S/N ratio spin flip chopper system for a pulsed neutron source
Nuclear Instruments and Methods in Physics Research Section A **634** S134 (2011)

124 Y. Tanabe, T. Adachi, K. Suzuki, T. Kawamata, Risdiana, T. Suzuki, I. Watanabe, and Y. Koike
Similarity between Ni and Zn Impurity Effects on the Superconductivity and Cu-Spin Correlation in $La_{2-x}Sr_xCu_{1-y}NiyO_4$ High-T_c Cuprates: A Comparison Based on the Hole Trapping by Ni
Physical Review B **83** 144521 (2011)

125 田中伊知朗、日下勝弘、細谷孝明、大原高志、栗原和男、新村信雄、山田太郎、友寄克亮、横山武司、大西裕季、大隅孝志、内田裕久、鈴木榮一郎、柏木立己、宮本晃男、古川保典、吉村政志、河村貴宏
茨城県生命物質構造解析装置 (iBIX) による水素・水和水の構造研究 / 産業利用
RADIOISOTOPES **60** 89 (2011)

126 I. Tanaka, K. Kusaka, T. Hosoya, N. Niimura, T. Ohhara, K. Kurihara, T. Yamada, Y. Ohnishi, K. Tomoyori, and T. Yokoyama
Neutron structure analysis using the IBARAKI biological crystal diffractometer (iBIX) at J-PARC
Acta Crystallographica Section D **66** 1194 (2010)

127 H. Tatsumoto, T. Aso, T. Kato, K. Ohtsu, F. Maekawa, and M. Futakawa
Design of a high power heater for the cryogenic hydrogen system at J-PARC
Cryogenics **51** 315 (2011)

128 Y. Terayama, H. Arita, T. Ishikawa, M. Kikuchi, K. Mitamura, M. Kobayashi, N.L. Yamada, and A. Takahara
Chain dimensions in free and immobilized brush states of polysulfobetaine in aqueous solution at various salt concentrations
Journal of Physics: Conference Series **272** 012010 (2011)

129 K. Toh, T. Nakamura, K. Sakasai, and K. Soyama
Effects of Gamma-Rays on Polymethylmethacrylate Plastic Optical Fiber under Low Dose-Rate Irradiation
2011 IEEE Nuclesr Scinece Symposium Conference Record, M-149 (2011)

130 K. Tomiyasu, and K. Kamazawa
A spin molecule model for geometrically frustrated spinel $ZnFe_2O_4$
Journal of the Physical Society of Japan **80** SB024 (2011)

131 S. Torii, M. Yonemura, T.Y.S. Panca Putra, J. Zhang, P. Miao, T. Muroya, R. Tomiyasu, T. Morishima, S. Sato, H. Sagehashi, Y. Noda, and T. Kamiyama
Super High Resolution Powder Diffractometer at J-PARC
Journal of the Physical Society of Japan **80** SB20 (2011)

132 N. Torikai, N.L. Yamada, D. Kawaguchi, A. Takano, Y. Matsushita, E. Watkins, and J.P. Majewski
Depth distribution of different solvents in a phase-separated block copolymer thin film
Journal of Physics: Conference Series **272** 012027 (2011)

133 N. Torikai, N.L. Yamada, H. Sagehashi, T. Sugita, M. Furusaka, Y. Higashi, M. Hino, T. Fujiwara, and H. Takahashi
Development of a Physically Bent Cylindroid Mirror for Beam Focusing for a Pulsed Neutron Reflectometer
IOP Conference Series: Materials Science and Engineering **24** 012016 (2011)

134 鳥飼直也、山田悟史、川口大輔
中性子・X 線斜入射散乱法によるブロック共重合体薄膜のその場構造観察
日本中性子科学会誌「波紋」**21** 91 (2011)

135 T. Toriyama, A. Nakao, Y. Yamaki, H. Nakao, Y. Murakami, K. Hasegawa, M. Isobe, Y. Ueda, A.V. Ushakov, D.I. Khomskii, S.V. Streltsov, T. Konishi, and Y. Ohta
Peierls Mechanism of the Metal-Insulator Transition in Ferromagnetic Hollandite $K_2Cr_8O_{16}$
Physical Review Letters **107** 266402-1 (2011)

136 S. Wakimoto, K. Kodama, M. Ishikado, M. Matsuda, R. Kajimoto, M. Arai, K. Kakurai, F. Esaka, A. Iyo, H. Kito, H. Eisaki, and S. Shamoto
Degradation of Superconductivity and Spin Fluctuations by Electron Overdoping in $LaFeAsO_{1-x}F_x$
Journal of the Physical Society of Japan **79** 074715-1 (2010)

137 P.G. Xu, H. Suzuki, S. Harjo, and T. Suzuki
Development and Prospect of Bulk Texture Measurement Technique by Neutron Diffraction
Proceedings of 120th Spring Conference of the Japan Institute of Light Metals 289 (2011)

138 N.L. Yamada, N. Torikai, K. Mitamura, H. Sagehashi, S. Sato, H. Seto, T. Sugita, S. Goko, M. Furusaka, T. Oda, M. Hino, T. Fujiwara, H. Takahashi, and A. Takahara
Design and Performance of Horizontal Type Neutron Reflectometer SOFIA at J-PARC/MLF
The European Physical Journal Plus **126** 108 (2011)

139 H. Yamagishi, K. Toh, T. Nakamura, K. Sakasai, and K. Soyama
Simulation program for multiwire-type two-dimensional neutron detector with individual readout
Journal of Instrumentation **6** C12025 (2011)

140 T. Yamamoto, Y. Nakazawa, M. Tamura, A. Nakao, Y. Ikemoto, T. Moriwaki, A. Fukaya, R. Kato, and K. Yakushi
Intradimer Charge Disproportionation in Triclinic-$EtMe_3P[Pd(dmit)_2]_2$ (dmit: 1,3-Dithiole-2-thione-4,5-dithiolate)
Journal of the Physical Society of Japan **80** 123709-1 (2011)

141 S. Yano, S. Itoh, S. Satoh, T. Yokoo, D. Kawana, and T.J. Sato
Data acquisition system for high resolution chopper spectrometer (HRC) at J-PARC
Nuclear Instruments and Methods in Physics Research Section A **654** 421 (2011)

142 T. Yokoo, N. Kaneko, S. Itoh, T.Otomo, K. Suzuya, Y. Suetsugu, and M. Shirai
Examination of gas desorption by B4C resin for use in neutron scattering experiment
Review of Scientific Instruments **82** 95109 (2011)

143 T. Yui, Y. Kobayashi, Y. Yamada, K. Yano,Y. Fukushima, T. Torimoto, and K. Takagi
Photoinduced Electron Transfer between the AnionicPorphyrins and Viologens in Titania Nanosheetsand Mono-disperse Mesoporous Silica Hybrid Films
ACS Appl. Mater. Interfaces **3** 931 (2011)

144 Y. Zhou, M. Matsuo, Y. Miura, H. Takamura, H. Maekawa, A. Remhof, A. Borgschulte, A. Züttel, T. Otomo, and S.-I. Orimo
Enhanced Electrical Conductivities of Complex Hydrides $Li_2(BH_4)(NH_2)$ and $Li_4(BH_4)(NH_2)_3$ by Melting
Materials Transactions **52** 654 (2011)

145 Muon Science Laboratory, IMSS Muon Section, Materials and Life Science Divison
Presentations for the Muon Science Advisory (and the 9th Muon Science Experimental Facility Advisory Committee) MuSAC
KEK-Proceedings 2011-3 (2011)

Editorial Board - MLF Annual Report 2011

Chief Editor
Mitsutaka Nakamura
Neutron Science Section

Tetsuya Yokoo
Neutron Science Section

Shinichi Takata
Neutron Science Section

Shin-ichiro Meigo
Neutron Source Section

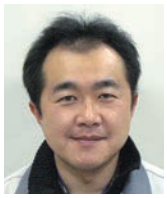

Hiroyuki Kogawa
Neutron Source Section

Hiroki Iwase
CROSS-Tokai

Yoshifumi Sakaguchi
CROSS-Tokai

Kaoru Sakasai
Neutron Instrumentaion Section

Toshinori Asai
CROSS-Tokai

Garry Foran
CROSS-Tokai

Kenji M. Kojima
Muon Science Section